# BASE MATERIAL CHARACTERISATION OF SPOIL PILES AT BMA COAL MINES

**Md Golam Mostofa**
**Bachelor of Science in Civil Engineering**

Principle supervisor: Dr. Chaminda Gallage

Associate supervisor: Dr. Jay Rajapakse

Submitted in fulfilment of the requirements for the degree of
Master of Engineering (Research)

SCHOOL OF CIVIL ENGINEERING
SCIENCE AND ENGINEERING FACULTY
QUEENSLAND UNIVERSITY OF TECHNOLOGY
2015

# Keywords

*Keywords:* coal mine spoil, slaking, overburden pressure, time, slaking chamber, shear strength, permeability.

# Abstract

In open-cut strip mining, waste materials are placed in-pit to minimise the mine operational costs. The slope failures of these spoil piles can cause significant damage to human lives, machinery, and can delay mine operation. It has been observed that most spoil pile failures occur when the pit is filled with water and when it is dewatered. The failures often initiated at the base of spoil piles where material undergoes significant slaking (disintegration) over time due to overburden pressure and water saturation. It is important to understand how the mechanical properties of base spoil material are affected by slaking in order to design safe spoil pile slope and height, and a safe dewatering rate. In this study, fresh spoil material collected from a coal mine in the Bowen Basin in Queensland, Australia was subjected to high overburden pressure (0 – 900kPa) under saturated conditions and maintained over a period of time (0 – 6 months) allowing the material to slake. To create the above conditions, the laboratory designed pressure chambers of 360 mm internal diameter and 400 mm high acrylic tubes having a wall thickness of 20 mm. Once a spoil sample was slaked under a certain overburden pressure over a period of time, it was tested for classification, mineralogy, permeability, and strength properties. Results of this testing program suggested that the slaking of saturated coal mine spoil increased with the overburden pressure and the time duration over which the overburden pressure was maintained. Further, it was observed that slaking had significant influences on particle size distribution that produced more silty particles in spoil. As a result of silt particle increment, liquid limit and shear strength was decreased. But triaxial tests indicated that a decrease in the effective angle of internal friction was about 5˚ after six months of slaking. It was clear from this study that short term slaking was not significant in creating mineralogical changes of strong bonded clay particles, though, minor changes were observed with weak boned clay particles. Permeability decreased rapidly for short term slaking spoils but decreased at a comparatively slower rate for spoils slaked over long term duration. In brief, the changes in chemical and mechanical properties of spoil were confirmed but largely depended on slaking duration rather than overburden pressure.

# Table of Contents

Keywords ..... i
Abstract ..... ii
List of Figures ..... v
List of Tables ..... viii
Statement of Original Authorship ..... ix
Acknowledgements ..... x
**Chapter 1: Introduction ..... 1**
1.1 Background ..... 1
1.2 Aim and objectives ..... 2
1.3 Significance of the study ..... 3
1.4 Scope of research project ..... 3
1.5 Thesis structure ..... 4
**Chapter 2: Literature Review ..... 5**
2.1 Introduction ..... 5
2.2 Influencing factors for spoil pile stability ..... 5
2.2.1 Slope geometry ..... 6
2.2.2 Geotechnical properties of materials ..... 7
2.2.3 Geology ..... 10
2.2.4 Groundwater ..... 13
2.2.5 Climate ..... 15
2.2.6 Mining technique and procedures ..... 15
2.2.7 Drainage ..... 16
2.2.8 Blasting ..... 17
2.3 Mine spoil pile failures and failure mechanisms ..... 17
2.3.1 Surface failure ..... 18
2.3.2 Circular failures ..... 19
2.3.3 Flow failures ..... 20
2.3.4 Wedge failures ..... 20
2.4 Chemical and mechanical properties of mine spoil ..... 21
2.5 Laboratory investigation on properties of mine spoils ..... 26
2.6 Summary ..... 27
**Chapter 3: Methodology ..... 29**
3.1 Introduction ..... 29
3.2 Development of slaking chambers ..... 29
3.3 Field collection of coal mine spoil ..... 29
3.4 Coal mine spoil subjected to slaking in the laboratory ..... 35
3.5 Laboratory testing on spoil ..... 35
3.5.1 Particle size distribution ..... 36
3.5.2 Atterberg limit ..... 36
3.5.3 Mineralogy and soil chemistry ..... 36

3.5.4 Permeability ..... 37
3.5.5 Shearing strength properties ..... 37
3.6 Interpretation of the results of the laboratory testing program ..... 38
**Chapter 4: Testing Apparatus ..... 39**
4.1 Introduction ..... 39
4.2 Design and development of pressure chamber to slake spoil ..... 40
4.3 Basic spoil property testing apparatus ..... 43
4.3.1 Liquid limit ..... 43
4.3.2 Plastic limit ..... 44
4.3.3 Shrinkage limit ..... 45
4.3.4 Sieve analysis ..... 46
4.4 Direct shear machine ..... 46
4.5 Malvern particle size analyser ..... 48
4.6 X-Ray diffraction apparatus ..... 49
4.7 Triaxial testing apparatus ..... 51
4.8 Constant head permeability testing apparatus ..... 54
**Chapter 5: Results and Discussion ..... 57**
5.1 Introduction ..... 57
5.2 Effects of overburden pressure and time on coal mine spoil slaking ..... 57
5.3 Effects of slaking on physical properties of coal mine spoil ..... 61
5.3.1 Particle size distribution ..... 61
5.3.2 Atterberg limits ..... 63
5.4 Effects of slaking on chemical properties of coal mine spoil ..... 67
5.5 Effects of slaking on shear strength properties of coal mine spoil ..... 73
5.5.1 Triaxial tests ..... 73
5.5.2 Direct shear tests ..... 79
5.6 Effects of slaking on the hydraulic conductivity of coal mine spoil ..... 83
**Chapter 6: Conclusions and Recommendations ..... 85**
6.1 Conclusions ..... 85
6.2 Recommendations ..... 87
**References ..... 89**

# List of Figures

Figure 2.1 Showing bench, ramp, overall slope and their respective angles (Hem, November 2012) ..... 6

Figure 2.2 Variation of angle of shearing resistance with median particle diameter (Effects of Particle Size Distribution on Shear Strength of Accumulation Soil, 2013) ..... 8

Figure 2.3 Variation of angle of shearing resistance with total gravel content (Effects of Particle Size Distribution on Shear Strength of Accumulation Soil, 2013) ..... 9

Figure 2.4 Variation of angle of shearing resistance with coefficient of uniformity (Effects of Particle Size Distribution on Shear Strength of Accumulation Soil, 2013) ..... 9

Figure 2.5 Typical seatearth geological fault underneath of coal seam ..... 12

Figure 2.6 Typical Dragfloding upper thrust geological fault (Bruno, 2015) ..... 13

Figure 2.7 Artesian aquifers in Mining pit floor (Sources: Environment Canada) ..... 14

Figure 2.8 Conceptual application of drainage (Rahardjo, et al., 2003) ..... 17

Figure 2.9 Effects of Debris flow in Glenwood Springs (Highland, Ellen, Christian, & Brown III, 1997) ..... 18

Figure 2.10 (a, b, c) Various Circular Failures (Rizkalla, 1983) ..... 19

Figure 2.11 (a, b, c, d) Sequence of Development of Wedge Failure ..... 20

Figure 2.12 Grain size distribution of spoil materials (Ulusay, Arikan, & Yoleri, 1995), where A: recent spoil dumped by dragline, B: samples from upper level of spoil & C: samples from sliding surface ..... 22

Figure 2.13 Relationship between permeability and maximum particle size (Smith, et al., 1999) ..... 25

Figure 3.1 Three conceptual strength modes for spoil (Simmon & McManus, 2004) ..... 31

Figure 3.2 The Bowen Basin mining area and location of projects (Bowen Basin Coal Mines and Coal Projects map with workforce (Quarter 2 2013), 2013) ..... 32

Figure 3.3 Spoil materials type (a) Category 1, (b) Category 2, (c) Category 3, (d) Category 4 ..... 33

Figure 3.4 (a) Sample particle size observed by visual inspection, (b) Sample collection ..... 34

Figure 3.5 (a) Highwall height, (b) Slope of spoil pile ..... 34

Figure 4.1 Schematic diagram of pressure chamber ..... 40

Figure 4.2 Photograph of pressure chambers ..... 41

Figure 4.3 (a) Marking in pressure chamber, (b) Sample compacting weight ..... 42
Figure 4.4 (a) Pressure chambers connected with water, (b) Slaked sample ready for testing ..... 43
Figure 4.5 Cone penetrometer for Liquid limit test ..... 44
Figure 4.6 (a) Rolled sample inside of Palms (b) Rolled on frosted Glass ..... 45
Figure 4.7 Linear shrinkage limit mould ..... 45
Figure 4.8 (a) Slaked sample soaked in water; (b) Sieves shacked mechanically ..... 46
Figure 4.9 (a) Complete Shear Track II apparatus & (b) Placing of direct shear box ..... 48
Figure 4.10 (a) Hydro MV unit for sample automated dispersion & (b) Malvern Mastersizer 3000 ..... 49
Figure 4.11 (a) X'Pert PRO X-ray diffraction system, (b) Samples Under testing for mineralogy ..... 50
Figure 4.12 (a) McCrone micronizing mill & (b) Compressing sample in sample holder ..... 50
Figure 4.13 (a) Computerized system control, (b) Back pressure control & Volume change measuring unit and (c) Confining pressure control unit ..... 51
Figure 4.14 Universal triaxial system ..... 52
Figure 4.15 Constant head permeability testing apparatus (a) Front view (b) Side view (c) Top view (d) Porous disc and Surcharge ..... 56
Figure 5.1 Vertical deformation of spoil in 180 days ..... 58
Figure 5.2 Vertical deformation of spoil under 900kPa overburden pressure ..... 59
Figure 5.3 The maximum vertical deformation of slaked spoil under different overburden pressure and time ..... 60
Figure 5.4 Particle size distributions of spoil samples ..... 62
Figure 5.5 Particle size distribution of spoil samples after 180 days ..... 63
Figure 5.6 Particle size distribution of spoil for 900kPa overburden pressure ..... 63
Figure 5.7 Variation of liquid limit of spoil with overburden pressure and time ..... 64
Figure 5.8 Variation of plastic limit of spoil with overburden pressure and time ..... 65
Figure 5.9 Variation of shrinkage limit of spoil with overburden pressure and time ..... 66
Figure 5.10 X- ray diffraction pattern of spoil samples ..... 69
Figure 5.11 Mineralogical changes of spoil samples ..... 71
Figure 5.12 Typical result of TGA analysis of sample 10 ..... 72
Figure 5.13 Variation of Deviator Stress versus axial strain for Spoil Sample 9 ..... 74
Figure 5.14 Variation of pore pressure versus axial strain for the specimen of spoil sample 9 ..... 75
Figure 5.15 Effective Mhor's circle for sample 9 ..... 76

Figure 5.16 Mhor's circle for total stress of sample 9 ..... 76
Figure 5.17 Graph plotted after direct shear test..... 81
Figure 5.18 The variation coefficient of permeability (*k*) for slaked spoil samples..... 83
Figure 5.19 Influence of overburden pressure and time on spoil slaking ..... 84

# List of Tables

Table 2.1 Mineralogical percentages (wt. % by XRD) of spoil and fresh rock (Ulusay, Arikan, & Yoleri, 1995) ..... 21

Table 2.2 Physical properties of spoil materials (Ulusay, Arikan, & Yoleri, 1995) ..... 22

Table 2.3 Summary of Triaxial test result of spoil Total analysis (Karfakis, et al., 1996) ..... 23

Table 2.4 Shear strength parameters for four categories and mobilisation modes (Simmon & McManus, 2004) ..... 24

Table 2.5 Average falling head permeability for mine spoil sample (Karfakis, et al., 1996)..... 25

Table 3.1 Spoil categories and attributes (Simmon & McManus, 2004)..... 30

Table 3.2 Shear strength parameters for spoil categories and spoil mode (Simmon & McManus, 2004) ..... 31

Table 3.3 Slaking condition of spoil samples ..... 35

Table 5.1 The vertical deformation of spoil under different overburden and time..... 60

Table 5.2 Physical properties of slaked spoil samples ..... 67

Table 5.3 Summary of minerals present in spoil samples (quantitative analysis) ..... 70

Table 5.4 Stresses at failure of all stages of the specimen prepared using sample 9 ..... 75

Table 5.5 Summary of multistage triaxial test data at failure of all 10 specimens .... 77

Table 5.6 Shear strength properties of spoil samples obtained from multi-stage triaxial tests ..... 78

Table 5.7 Summary of direct shear test results ..... 82

# Statement of Original Authorship

The work contained in this thesis has not been previously submitted to meet requirements for an award at this or any other higher education institution. To the best of my knowledge and belief, this thesis contains no material previously published or written by another person except where due reference is made.

Signature: QUT Verified Signature

Date: October 2015

# Acknowledgements

I wish to express my gratitude and appreciation to my supervisor, Dr Chaminda Gallage and associate supervisor, Dr Jay Rajapakse for their constant help and support throughout the course of this study. Their patience, constructive criticism and continuous encouragement have been greatly acknowledged. It would have been impossible to accomplish this task without their persistent guidance and support.

It would not have been possible to conduct this research without the financial and in-kind support provided by BHP-BMA. Therefore, I gratefully acknowledge the management of BHP-MBA. Special thanks goes to Andrew Johnstone, Nicole Tucker, Dominic Mills, and Ross Branch who have been directly involved with the activities of this project.

Special appreciation is extended to the technical and research office staff at the Science and Engineering Faculty at QUT. I am grateful to Glen Barnes, Anthony Morris, Armin Liebhardt, David Page (CARF), and Tony Raftery (CARF) for their constant support and help. Thanks also to David Vosolo and Mario Ferreira De Menezes for their help in the laboratory work for this project.

Finally, I would like to thank my family members and friends for encouraging me in all my pursuits and inspiring me to follow my dreams. I am especially grateful to my parents, who supported me emotionally and believed in me. This journey would not have been possible for me without their love.

# Chapter 1: Introduction

## 1.1 BACKGROUND

The coal mining industry is one of the major and expanding industries which is deeply embedded in the world economy. Around 41 per cent of world electricity generation depends on coal as fuel (Australian Coal, 2015). It benefits the economy through its contribution to exports, tax, wages, jobs, investment and royalties. One of the biggest challenges in this industry is waste disposal during and after the mining operation and associated costs.

Coal mine spoil is overburden waste material which is removed to expose the coal seams in the open-cut mining process. This material is typically placed in piles and it is also called boney pile, gob pile, or pit heap. The spoil materials are typically composed of crushed fragments of mudstone, siltstone and sandstones. The mean particle size of spoil ranges from fine to a size of 0.5 m to 1.0 m depending on in-situ properties of overburden material, blasting technique and equipment used. Within the coal mine industry, spoil materials are categorised into four groups; Category 1 (Cat-1), Category 2 (Cat-2), Category 3 (Cat-3), and Category 4 (Cat-4) (Simmon & McManus, 2004).

In open-cut strip mining, waste materials are placed in-pit to minimise mine operational costs. It is common to observe blasted rock (Cat-3 or Cat-4) being placed by draglines to form the base for spoil piles and the weaker spoil materials such as soil (Cat-1) and highly weathered rock (Cat-2) to be placed by dump trucks on the top of base material to form the final spoil profile. To accommodate increasingly high volumes of spoil within a mine pit, spoil pile heights and slope angles are increased. In the Brown Basin Coalfield of Queensland in Australian, the typical height of spoil piles range from 30 m–70 m and the slope of the spoil pile varies between 26° to 40° (Wilkins, 1970). As spoil pile heights are increased, the foundation material is subjected to a higher stress regime that may increase the rate of disintegration of base spoil material due mechanical breakdown. The slaking of the base material is further increased with time and when this high stress is maintained in saturated conditions. In open cut mining, it is common to observe a

10–15 m height of water in the pit when mining and pumping has stopped temporarily. Therefore, it is assumed that the base spoil material is saturated.

Generally, the foundation spoil materials are subjected to mechanical breakdown over time due to a high overburden pressure, degree of saturation, cyclic drying and wetting caused by de-watering of the mining pit and recharge of water due to internal drainage or infiltration of rain water, and cyclic heating and thawing.

Slaking has been found to transform fresh or slightly weathered Permian (Cat-4 or Cat-3) at the base of spoil pile to weaker and/or weathered Permian (Simmon & McManus, 2004). This mechanical breakdown leads to a decrease in particle sizes, consequently reducing the shear strength and permeability of slake affected materials (Gökceoğlu, Ulusay, & Sönmez, 2000; Wilkins, 1970). This reduction in material properties of spoil base materials have been a root cause for the failures in spoil piles during dumping, and flooding/dewatering events. The failures of spoil piles can cause human casualties, damage to equipment, delay in miming, and an increase in mine operational costs.

In order to determine safe height and slope angles for spoil piles and their appropriate dewatering rates, it is important to understand how the shear strength and permeability of saturated spoil foundation materials decrease with overburden pressure and time. Research has been conducted (Fityus, Hancock, & Wells, 2008; Hendrychová, Šálek, Tajovský, & Řehoř, 2012; Ulusay, Arikan, & Yoleri, 1995) to determine the shear strength and other properties of relatively fresh coal mine spoil under high overburden stress. However, no systematic research has been conducted to investigate the degradation of properties of saturated spoil material due to slaking under overburden pressure and time.

## 1.2 AIM AND OBJECTIVES

This research aims to develop an apparatus to simulate field slaking of mine spoil and demonstrate its application in investigating the effect of slaking on the geotechnical properties of mine spoil. The aim of the research is achieved through the following objectives:

- Design and develop a pressure chamber to simulate field slaking conditions, such as water, overburden pressure, time, cyclic drying and wetting on mine spoil.

- Demonstrate the use of a pressure chamber to simulate slaking of coal mine spoil over time due to overburden pressure and water saturation.
- Investigate the effects of slaking parameters (overburden pressure and time) on the degradation of physical, chemical, mechanical and hydraulic properties of a saturated coal mine spoil.

## 1.3 SIGNIFICANCE OF THE STUDY

The outcomes of this research will establish a systematic approach to investigate the slaking-induced material property degradation in mine spoil materials. Proper understanding of the material properties of mine spoil helps to make mine spoil piles safe against failures (slope failures) during mining and de-watering of mine pits for resuming mine operations. It has been reported that most mine spoil pile failures occur due to slaking-induced degradation of the shear strength of mine spoil base materials. Failures of mine spoil piles in open-cut mining; bring spoil materials into operational areas (bottom of active wall) which area a risk for people working in the mine and for machinery. Furthermore, failures increase operational costs as the failures spoil material has to be removed from the operational area before resuming operations. Therefore, spoil pile design using ultimate properties of mine spoil, creates secure working areas in open-cut mining and as well as reduce mine operational costs.

## 1.4 SCOPE OF RESEARCH PROJECT

This study predominantly focuses on developing a systematic framework for investigating effects of slaking parameters on degradation or change in physical, chemical, mechanical, and hydraulic properties of a mine soil. Due to the available resources and time, the study is subjected to certain limitations mentioned below:

- In this research, the investigation is conducted on only one spoil material collected from a coal mine in Brown Basin Coalfield in Queensland. This material is classified as category-3 and used as the base of spoil piles.
- The effects of overburden pressure on slaking of saturated spoil material over time will be investigated. The effects of cyclic drying-wetting, heating and thawing will not be considered.

- Due to the limitation of a compressed air system at QUT, 900kPa is the maximum overburden pressure under which the spoil is subjected to slaking.
- The spoils are subjected to slaking over a maximum period of 6 months.

## 1.5 THESIS STRUCTURE

This thesis consists of six chapters, a list of references and appendices. Each chapter is summarised below.

Chapter one contains a background to the problem, aim and objectives, significance of the research, and scope of the study.

Chapter two provides a comprehensive literature review relevant to the key areas of this research, such as spoil pile stability, spoil pile failure mechanism, slaking of mine spoil, and laboratory determination of physical, chemical, mechanical, and hydraulic properties of mine spoil.

The third chapter presents the methodology including the testing program and material used in this research. Material collection and its physical properties are also presented in this chapter.

Chapter four discusses the pressure chamber developed in this study to simulate the slaking of mine spoil materials and its testing procedures. Further, other laboratory testing apparatus is used in this research and their testing procedures are also briefed.

Chapter five shows and discusses the experimental results to demonstrate the effects different parameters have on mine spoil slaking and how the physical, mechanical, chemical, and hydraulic properties are affected by mine soil slaking parameters.

The major findings of the research are summarised and concluded in chapter six. Further, recommendations for future research are suggested. A list of references is provided at the end of the main text.

# Chapter 2: Literature Review

## 2.1 INTRODUCTION

The primary focus of the literature review is to gain a proper understanding of mechanisms of mine spoil pile failures, factors contributing to the failures, and the method of determination of these factors. Following, is the identification of research gaps in determination of spoil properties and the way in which they are used in design and forms an important part of this literature review.

After the Aberfan disaster in 1966 when a slide involving 107,044 $m^3$ of colliery rubbish resulted in the loss of 144 lives, the miners and public became aware of the drastic effects of spoil failure (Highter & Vallee, 1980). The investigation revealed that the reduction of effective shear strength of foundation spoil materials led to the failure (Ulusay, Arikan, Yoleri, & Çağlan, 1995). This incident initiated research on mine spoils to investigate;

(i) Failure mechanisms of spoil piles;

(ii) Factors affecting the failures of spoil piles;

(iii) Geotechnical properties of mine spoils and factors affecting these properties;

(iv) Laboratory and field determination of geotechnical properties of mine spoils.

## 2.2 INFLUENCING FACTORS FOR SPOIL PILE STABILITY

For a minimum operational cost and environmentally safe spoil pile, the design of maximum slope and height of spoil are some of the important factors for miners and mine engineers. There are so many other factors which need to be taken into consideration in the case of spoil pile stability designs. Those factors can be geological, geomorphological, and hydrological man induced mining techniques and spoil material properties. However, it is weathering that brings rapid change of spoil materials (Gökceoğlu, et al., 2000). A large number of articles, case studies and literature is available concerning the reclamation of spoil pile, vegetation, slope stability, landslides and many other issues related to ground water contamination and water pollution (Kalinski, Karem, & Little, 2010; Shrestha & Lal, 2011; Ulusay, Arikan, & Yoleri, 1995; Ulusay, Arikan, Yoleri, et al., 1995; Ulusay, Çağlan, Arikan,

& Yoleri, 1996; Upadhyay, Sharma, & Singh, 1990). However, these are not directly part of the scope of this study. Much research and case studies have been carried out to understand those factors.

### 2.2.1 Slope geometry

Spoil slope geometry is one the major factors related to spoil stability. Slope angle, height of the spoil pile and the area of failure are major factors affecting spoil stability. The stability of spoil slopes decreases with an increase in height, and an overall spoil slope increases the possible extent of the development of any failure to the rear of the crests. The slope geometry of spoil pile depends on spoil materials' shear strength properties, permeability and climatic conditions of the mining area. In the case of a disturbed slope angle or low surface runoff, spoil pile rainwater infiltration can create multi-wedge failure of spoil piles. It is evident that steeper and higher slopes are less stable. In general practice, spoils are dumped at a rill slope angle of 37° by truck in Bowen Basin area (Leonie Bradfield, 2013; Simmon & McManus, 2004). The slope angle was varied from 37° to 45° in case of dumping by dragline. Conjointly, slope curvature has a fundamental effect on the stability, and as a result convex section slopes are avoided during slope designs. According to research (Zhang, Chen, Zheng, Li, & Zhuang, 2013), concave surfaces can increase the factor of safety up to 11 per cent and concave turning corners can increase the factor of safety up to 20 per cent compared to convex sections. Figure 2.1 shows different sections of slopes including bench, overall slope and their respective angles.

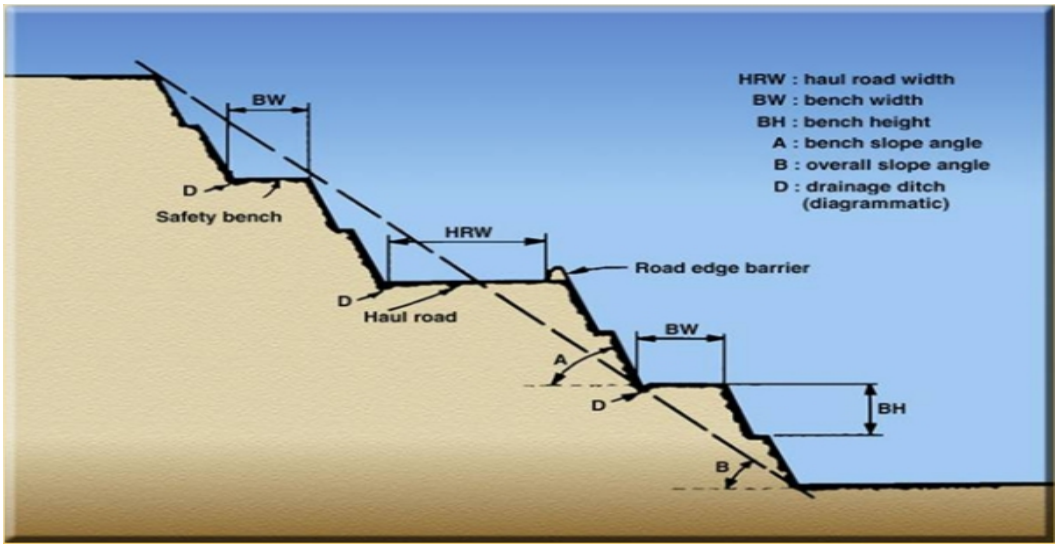


Figure 2.1 Showing bench, ramp, overall slope and their respective angles (Hem, November 2012)

### 2.2.2 Geotechnical properties of materials

The important geotechnical properties that influence the stability of spoil pile are shear strength properties of spoil materials, particle size distribution, density, permeability (k), moisture content as well as plasticity (Leonie Bradfield, 2013; Simmon & McManus, 2004). The stability design of any spoil pile and slope stability analysis requires accurate consideration of shearing strength parameters; hence angle of internal friction and cohesion is essential. Generally, the slope of spoil pile increases with increases of angle of internal friction. Previously constant shearing strength parameters angle of internal friction was utilised for stability calculation. But the angle of internal friction or shearing strength properties decreases with increasing of confining stress (Indraratna, 1994; Wilkins, 1970). In the case of spoil pile, the apparent friction angle decreases with increasing pile height and exhibits higher value close to the surface or base (Indraratna, 1994). In the case of spoil pile stability analysis and design considerations, the use of apparent friction angle provides a higher safety factor.

Shearing strength properties of any slope are closely related to its particle mineralogy, size, roundness and surface properties. The mineralogical study indicated that illite, mixed layer clay, kaolinite, cholite, quartz, carbonate and organic carbon are the regular minerals contained in coal spoil (Kusuma et al., 2012; Taylor, 1975). From those, quartz content has significant influence on the angle of internal friction. Sand with high quartz content can experience higher weathering action. Clay has a lower friction angle in comparison to sand with less quartz content and a higher percentage of potassium-feldspar, plagioclase, and calcite, while dolomite generally has a higher friction angle (Bareither, Edil, Benson, & Mickelson, 2008). The other component of shear strength properties is cohesion, which is caused by electrostatic forces and cementation by mainly $Fe_2O_3$, CaO, NaCl. Cohesion resists soil or rock materials from deforming or breaking because of forces like gravity. Less cohesion of rocks and soil particles tends to make unstable slope. However, the apparent cohesion is caused by negative capillary pressure, and pore pressure response during undrained loading.

The distribution of particle size also affects shear strength properties of spoil. The effect of particle size on shear strength was analysed by various researchers in relation to three parameters of particles, namely the median particle diameter, coefficient of uniformity and gravel content. It was found that the angle of internal friction increases with mean particle sizes ($D_{50}$) and gravel content of spoil. Likewise, the angle of shearing resistance decreases with an increase of coefficient of uniformity (Kim & Ha, 2014; Li, 2013; Tordesillas, Shi, & Tshaikiwsky, 2011). Figure 2.2, 2.3 and 2.4 present the relationship between angles of shearing resistance with median particle diameter, gravel content and coefficient of uniformity.

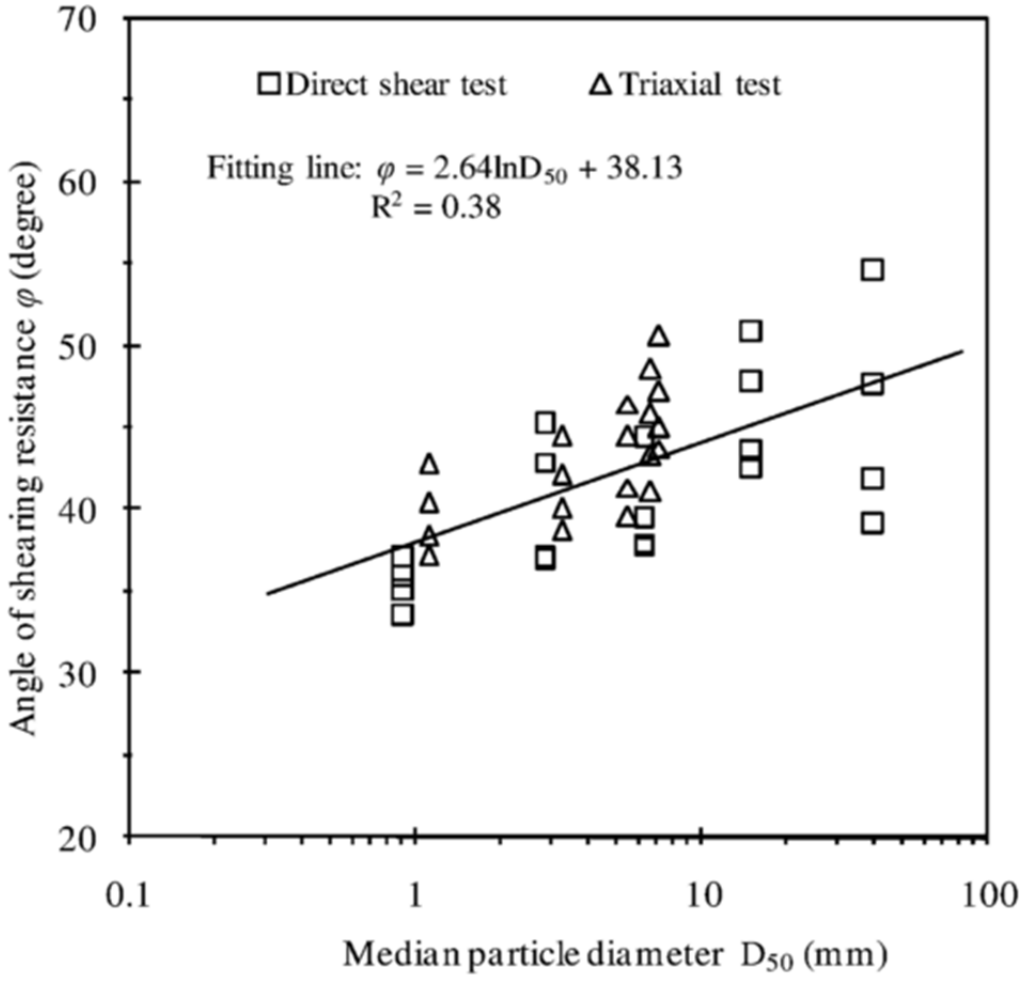


Figure 2.2 Variation of angle of shearing resistance with median particle diameter (Effects of Particle Size Distribution on Shear Strength of Accumulation Soil, 2013)

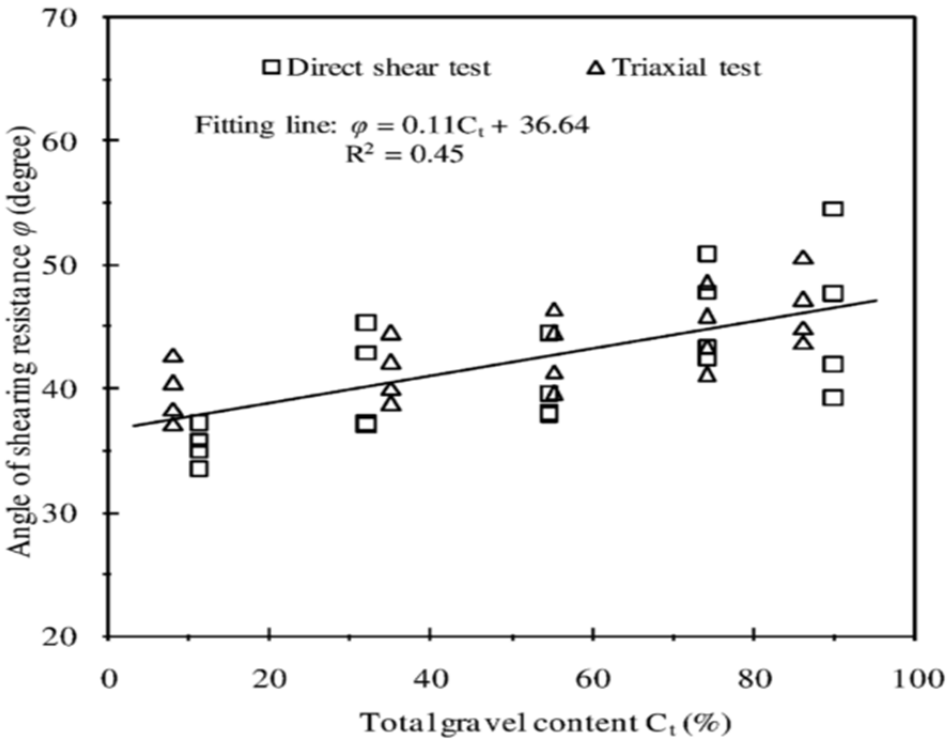


Figure 2.3 Variation of angle of shearing resistance with total gravel content (Effects of Particle Size Distribution on Shear Strength of Accumulation Soil, 2013)

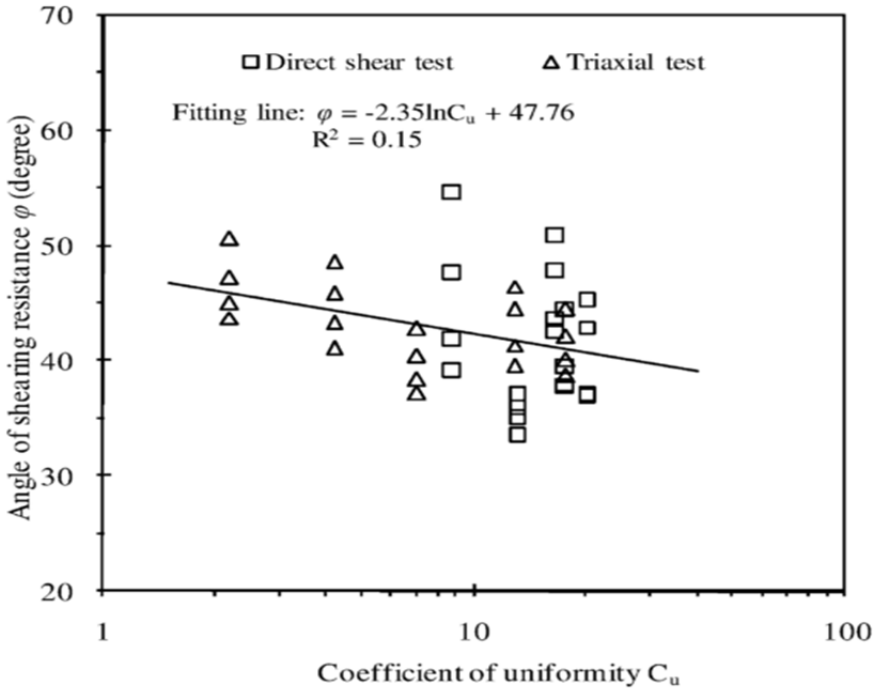


Figure 2.4 Variation of angle of shearing resistance with coefficient of uniformity (Effects of Particle Size Distribution on Shear Strength of Accumulation Soil, 2013)

Density is also an important factor in spoil slope stability analysis and design. The density of materials depends on mining methods and equipment used in mining, gradation and loading history. With relatively small increases in density, shear strength and stress increase for any kind of spoil. The density of spoil materials fall between 13kN/$m^3$ and 15 kN/$m^3$ depending on the moisture content and void ratio of spoil (Ulusay, Arikan, & Yoleri, 1995).

Permeability of soil or rock largely affects the stability of a spoil. The seepage pattern, water level of infiltrate at the time of rain and moisture content in spoil materials all affect the permeability of materials. With the increase in water content in spoil pile the shear strength reduces and the rate of degradation of spoil materials increases (Smith, Cripps, & Wymer, 1999). According to the Kozeny–Carman equation, the coefficient of permeability is a function of effective particle size, placement or compaction technique, unit weight and viscosity of flowing water and void ratio of materials (Kalinski, et al., 2010; Karem, Kalinski, & Hancher, 2007).

### 2.2.3 Geology

Mine spoil pile material, includes various kinds of excavated rocks, (Upadhyay, et al., 1990) soils and process materials. The nature of these materials primarily depend on the geological condition of the mine sites (Kayabasi & Gokceoglu, 2012). The related geological conditions include the nature and thickness of soil or rock present in spoil pile or highwall, and the presence of underclay or expansive clay and any other kind of adverse geological structures (Jiang et al., 2013). Swelling behaviour of expansive clay is closely related to water. For loosely compacted spoil materials, rain water infiltrates into the pile and forms internal drainage in wet spoil materials, changing the field moisture content (Jiang, et al., 2013; Seedsman & Emerson, 1985b). Excess moisture in spoil pile causes a swell of materials and the quantity of volume changes, which depends predominantly on the mineralogy and clay content of the mine sites. It is evident that rainfall (amount and flow direction) and height of spoil pile largely depends on the topography of the mining area.

The nature of rock or soil of overburden, spoil influence, and spoil stability affects the slaking properties of spoil materials. The slaking process has been defined in literature extensively in terms of external environmental parameters. One particular definition was provided by Morgenstern and Eigenbrod, (1974) as ‘the

disintegration of mudstones upon alternate drying and wetting'. For engineering structures carrying clay bearing rocks, slacking is a common and complex problem. The American society of Testing and Materials (ASTM) and the International Society for Rock Mechanics (ISRM) developed standardised methods to quantify the slaking properties of clay bearing rocks which involved cyclic drying and wetting of rock samples.

In a natural environment, the degree of slaking and rate of disintegration varies with the natural climatic conditions of a region and their geological and engineering properties (Erguler & Shakoor, 2009; Gökceoğlu, et al., 2000; Santi, 2006). In field conditions, rocks are exposed to natural climatic conditions of heating and cooling, wetting and drying and freezing and thawing. It is evident in literature (Erguler & Shakoor, 2009) that freezing and thawing is more responsible for causing slaking and disintegration of clay bearing rocks. But slaking behaviour in the laboratory is quite different from field conditions because several external factors influence the slacking process under field conditions.

Slaking is a contributory factor to the alternation of physical properties of spoil because of one or more of the following factors (Erguler & Ulusay, 2009). Slaking or disintegration has been considered as the key mechanism in the degradation of the physical and mechanical properties of mine spoils. The finer the grain of the parent rock, the quicker the degradation. Although, a fine grained rock from one region or horizon may be more resistant than a coarser grained rock from another region due to the mineralogy of rocks. Particles of coal and sandstone do not degrade noticeably compared to siltstones and mudstones. A decrease in particle size distribution, permeability, shear strength and an increase in compressibility are the major physical and mechanical property changes induced by slaking in weak rock.

Such alternation of the physical properties of spoil materials can impact on the stability of spoil piles at the surface and depth of spoil piles. However, it must be noted that practical degradation of spoil material, is not only the result of slaking, but may also be caused by the mechanical breakdown due to the mining procedures and physio-chemical processes (Erguler & Ulusay, 2009; Ghose & Kundu, 2004; Highter & Tobin, 1980; Shrestha & Lal, 2011; Ulusay, Arikan, Yoleri, et al., 1995).

The existence of weak rock and underclay underneath coal seams is another geological function influencing slope stability of spoil in a particular area. Although generally, the underneath layer of coal seam should be able to resist bearing failure (Coggan, Gao, Stead, & Elmo, 2012; Zuo, Wang, Zhou, Pei, & Liu, 2013). This geological weak formation frequently occurs due to glacial drag and sometimes the folding of layers containing low strength materials. A presence of this kind of geological structure affects slope stability of spoils. The existence of this sort of adverse geological fault or structure is possibly one of the top most geological factors affecting stability of spoil pile and highwall. Figure 2.5 presents typical seatearth geological fault under coal seam.

Figure 2.5 Typical seatearth geological fault underneath of coal seam

In case of highwall and spoil pile design, the location of geological structure is taken into consideration to achieve the maximum factor of safety and slope stability of spoil pile and highwall. Drag folding deformation is another common weak geological structure. Normally, drag folding is complicated in feature and subjected to compression force. This may act as a weak plane for slope failure. The faults can be various in types depending upon the folding orientation, reverse faults, upthrusts, and over-thrusts. Figure 2.6 shows typical drag folding upper thrust geological fault in Portugal.

Figure 2.6 Typical Dragfloding upper thrust geological fault (Bruno, 2015)

### 2.2.4 Groundwater

The volume and location of ground water depends on the mining area's regional climate, spoil material permeability, surface runoff factor and topography of that region. Rainwater that infiltrates due to a low surface runoff coefficient, generates ground water rising. The ground water influences the stability of spoil pile

by imposing moisture content and by introducing slaking or hydrocompression (compaction or settlement due to wetting) in spoil pile heap. Furthermore, groundwater influences spoil stability by governing pore pressure in the materials and as a result shear strength properties change (Mohammed, 1997).

Groundwater movement may be instigated due to the opening of external fractures or faults in the pit floor as a consequence of the removal of coal seam and earlier from spoil dumping in heaps in height (Kaiser & Hewitt, 1983; Simpson & Walker, 1975). The water moves from a high pressure area to a low pressure area and can induce hydrostatic pressure leading to failure or stability problems in the spoil pile. The development of artesian aquifers is one of the examples. Due to the presence of an impervious coal layer, the geological fracture works as an opening of aquifers. Figure 2.7 shows one example of artesian aquifers in the pit floor.

Figure 2.7 Artesian aquifers in Mining pit floor (Sources: Environment Canada)

### 2.2.5 Climate

Climatic conditions, particularly variations, the amount of rainfall and temperature changes, are considered to have the greatest effect on spoil stability (Clarke & Smethurst, 2010; Gautam & Shakoor, 2013; Paranunzio, Laio, Nigrelli, & Chiarle, 2015; Rouainia, Davies, O'Brien, & Glendinning, 2009; Schmidt & Dikau, 2004). The recharge of groundwater of any area depends on the amount of precipitation and frequency affecting the slaking properties, permeability, shear strength reduction and internal drainage. The stability of any spoils pile decreases with the increase of the amount and frequency of precipitation. Precipitation can cause local increases in pore pressure and erosion (Gasmo, Rahardjo, & Leong, 2000).

The heating and cooling & freezing and thawing cycle also affects the stability of spoil pile. Melting of frozen ground surfaces and underground can increase the pore pressure of spoil materials. That can lead to changes in apparent cohesion and the friction angle and as a result, failure could occur in spoil pile. These are the kinds of climatic changes that accelerate the slaking of spoil materials. In addition, the freezing of near-surface materials may block drainage and cause pore pressure build-up within the spoil (Clarke & Smethurst, 2010; Dehn, Bürger, Buma, & Gasparetto, 2000; Rouainia, et al., 2009) which causes unstable slope.

### 2.2.6 Mining technique and procedures

The influences of mining techniques are often disregarded in stability calculation of spoil piles. Data for mining techniques is not easy to incorporate in stability designs as it is hard to generalise with growing technology. The main effect of mining technology is related to mining equipment and the procedures used to remove the overburden crust and its compacting. Generally, haul truck and drag bulldozer are efficient methods of better compaction. Yet unlike site conditions, mining conditions may vary within a mine or during the life time of the mine.

Mining equipment used in excavation and the removal of spoil can affect the strength, stability, compaction and density of spoil pile. In surface mining operation, popular equipment used to removal spoils from overburden and excavated pit floors are haul trucks, draglines and bucket wheel excavators (Molotilov, Cheskidov, Norri, Botvinnik, & Ils'buls'din, 2010). The selection of equipment depends upon highwall

condition and types of spoil material. Some equipment is suitable for removal of thicker deposits of overburden of weak rock like Bucket Wheel Excavators (BWE). This can reduce the overall slope angles but increase the segregation of spoil and lead to spoil material failure and pit flooding (Crespo Marquez, 2005). On the other hand, draglines are very efficient in considering spoil pile safety and it able to deal with the poor stability of spoil materials. The stripping shovel that is efficient in handling tougher materials, resulting from blasting problems is responsible for spoil failures and the damaging of coal seams (Aksoy, 2005; Ulusay & Aksoy, 1994). Shovels are efficient in producing immediate compaction of spoils whereas draglines can provide compaction in a wide range of spoil (Molotilov, et al., 2010).

### 2.2.7 Drainage

The main purpose of mine drainage is to collect and remove surface water and groundwater from the mine pit floor. The water present in spoil materials, in highwall or the infiltration of water can cause the failure of spoil pile by increasing the groundwater table. The result of the increasing groundwater table height softens the spoil material and decreases strength properties. That could lead to potential slope failure. Any drainage in the pit influences the spoil material property by lowering the height of the groundwater table (Lau & Kenney, 1984; Rahardjo, Hritzuk, Leong, & Rezaur, 2003) to the level of drainage. The drainage can be provided in various methods such as with ditches, channels and dewatering programs (Mokhov, 2011; Rahardjo, et al., 2003). The selection of a particular drainage type for any particular mining site depends on experience. Any inadequate drainage makes spoil unstable by building up pore water pressure and reducing apparent effective angle of spoil material (Cai, Ugai, Wakai, & Li, 1998; Eckersley, 1985; Gasmo, et al., 2000; Howladar, 2013; Kayabasi & Gokceoglu, 2012; Mokhov, 2011; Rahardjo, et al., 2003). Figure 2.8 presents a conceptual application of drainage in terms of lowering the groundwater table. In case of strip mining, the dip of the pit floor is maintained towards the drain near the highwall to collect the water.

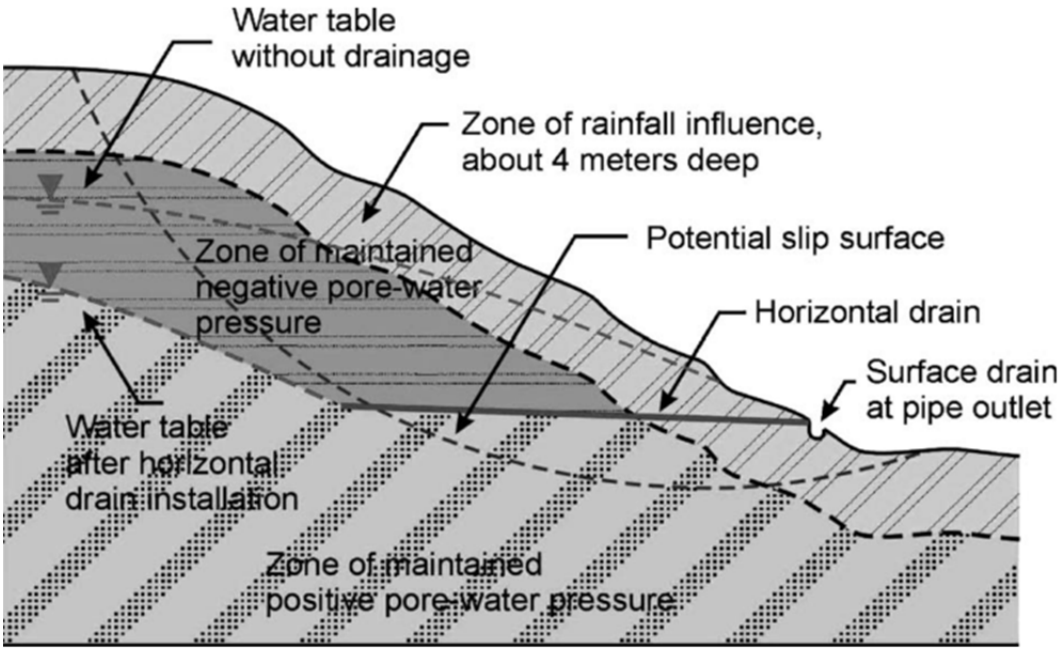


Figure 2.8 Conceptual application of drainage (Rahardjo, et al., 2003)

### 2.2.8 Blasting

The fragmentation of rock mass hinges on the type of rock present in overburden, the amount of explosive used for blasting and distance between explosive locations. The shear strength properties such as the angle of internal friction depends on particle size (Effects of Particle Size Distribution on Shear Strength of Accumulation Soil, 2013; Kim & Ha, 2014; Li, 2013), density and compaction whih also relies on the gradation of fragmented rock mass. Comparatively, weaker rock mass creates smaller fragment due to blasting whereas rocks like limestone or sandstone provides larger and angular fragments from blasting (García Bastante, Alejano, & González-Cao, 2012; Hamdi, Bouden Romdhane, du Mouza, & Le Cleac'h, 2008; M Mohammadnejad, 2011). Seismic reaction due to blasting influences groundwater levels which could lead to failure of spoil slope (Donzé, Bouchez, & Magnier, 1997; Monjezi, Amiri, Farrokhi, & Goshtasbi, 2010).

## 2.3 MINE SPOIL PILE FAILURES AND FAILURE MECHANISMS

The failure of spoil pile can be divided into four groups: surface failure, circular failure, flow failure and wedge failure (Nguyen & Chowdhury, 1984;

Okagbue, 1986; Ulusay & Aksoy, 1994). The reasons and mechanisms involved in those failures are given below.

### 2.3.1 Surface failure

The main reason for surface failure is the presence of fine particles on the pile surface and loose compaction of the spoil surface. In addition, low permeability of spoil materials and a higher runoff coefficient also contributes. Debris flow is one example of surface failure. Debris flow takes place when poorly deposited surface materials are washed away by water after saturation due to gravitational forces (Iverson, 1997). Debris flow starts within a few metres of spoil pile top and as a result, fine surface materials are deposited at the bottom of pile. The result of the debris flow could be catastrophic by up to a quarter of a kilometre (Pernichele & Kahle, 1971) is shown in Figure 2.9.

Figure 2.9 Effects of Debris flow in Glenwood Springs (Highland, Ellen, Christian, & Brown III, 1997)

In addition, edge slump type surface failure occurs when steep slopes take place in spoil pile. The surface materials from pile slope moves downwards to the

bottom of the pile dump. Sheet type failure also termed, plane shear failure occurs because of the loose dumping of granular spoil materials by a dragline or shovel.

### 2.3.2 Circular failures

Generally, because of the shape of failure it is termed as a circular failure. This type of failure is noticed in spoil pile when materials have low shearing strength properties like soil with high cohesion. Also, when the particle size is comparatively smaller or joint rock mass is weak (Prakash, 2009; Rizkalla, 1983). Failure takes place with this sort of spoil pile by building up pore pressure or an increase of ground water table. Circular failure could be classified in three different categories slope, toe and base failure.

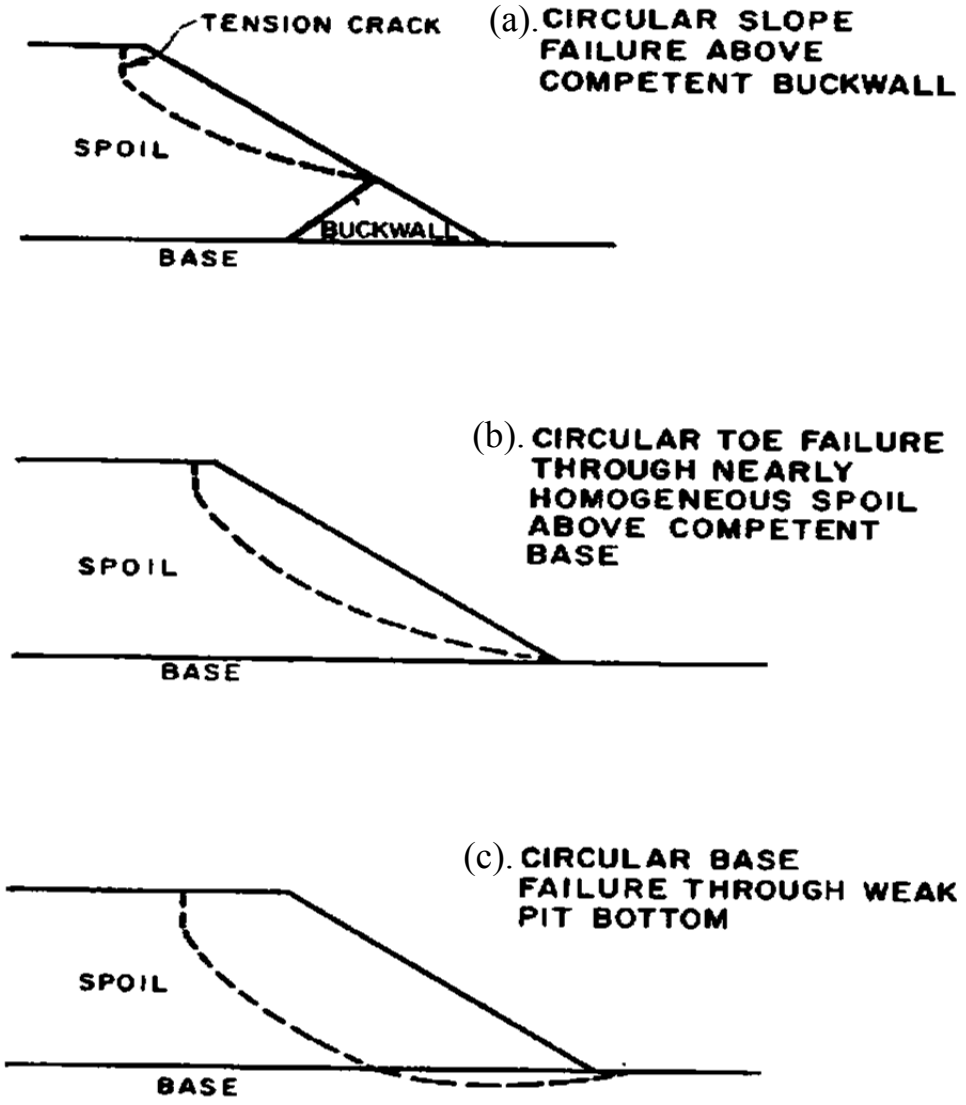


Figure 2.10 (a, b, c) Various Circular Failures (Rizkalla, 1983)

### 2.3.3 Flow failures

This category of failure in spoil pile occurs because of the application of dynamic forces of seismic action or blast induced dynamic forces. In case of loosely compacted fine grained spoil pile, the groundwater table fluctuates due to a dynamic reaction and then increases the pore pressure. That results in more reduction in shear strength parameters. As a result, shear strength parameters reduce and instability develops in the spoil pile causing a failure of spoil pile (Blight & Fourie, 2005).

### 2.3.4 Wedge failures

Wedge failure takes place when low shear strength and soft, saturated spoil materials are placed on top of the spoil pile. Saturated spoil materials soften the contact layer and produce a slip plane towards the horizontal plane. Consequently, the slip surface of soft spoil blocks the movement towards the ground surface attributable to gravitational forces and the front block of spoil moving towards the mining pit. The general mechanism of wedge failure is shear displacement (Nguyen & Chowdhury, 1984). From the back analysis of failure regarding case studies of various spoil piles, it is observed that wedge failure is the major reason for foundation failure (Jhanwar & Thote, 2011; Poulsen, Khanal, Rao, Adhikary, & Balusu, 2014; Seedsman & Emerson, 1985b; Seedsman, Richards, & Williams). Figure 2.11 presents the four phases of wedge failure.

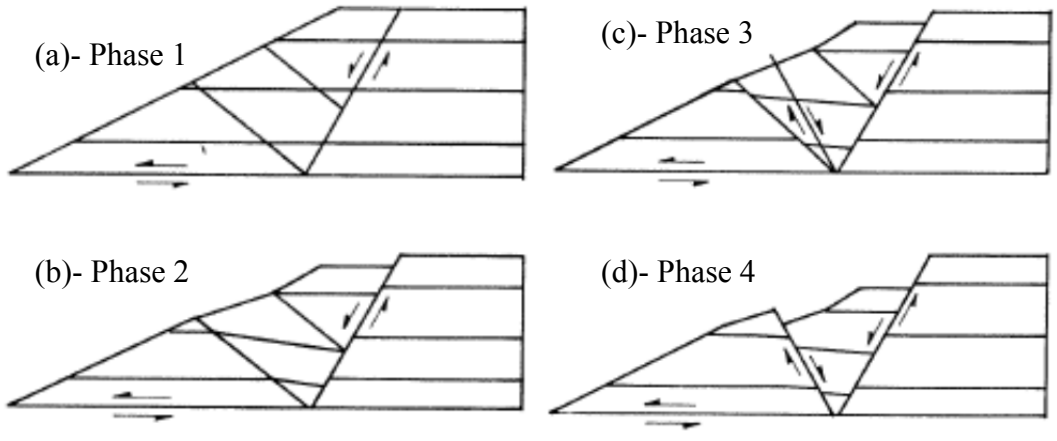


Figure 2.11 (a, b, c, d) Sequence of Development of Wedge Failure

## 2.4 CHEMICAL AND MECHANICAL PROPERTIES OF MINE SPOIL

Coal mine soil is a heterogeneous material. Countless research and case studies have been carried out, characterising spoil properties. In this section chemical and mechanical properties of spoil will be discussed. Chemical properties of spoil materials are important considering ecological influences, especially acid mine drainage characteristics and the mineralogy of spoil. Diverse techniques were used to determine the mineralogy of coal mine spoil, but X-ray diffraction test (Ward, Corcoran, Saxby, & Read, 1996; Ward, Nunt-jaruwong, & Swanson, 2005) presents the most accurate results compared to other testing methods. Table 2.1 presents the mineralogy of typical coal mine spoil and fresh rock of southwest Turkey. From the table it is clear that kalonite, illite, montmorillonte, quartz, feldspar, calcite, aragonite and dolomite are some of the common minerals present in spoil materials. Pyrite is another common mineral ($FeS_2$) found sometimes with coal mine spoil. The sulphur mixed with leaching water from spoil after oxidizing in the air, normally creates acid mine drainage. According to (Campbell, 2005), spoil with a sulphide concentration of more than 0.3% exhibits the possibility of acid mine drainage. Most of the Bowen Basin area had a sulphide concentration of less than 0.1% (BMA) which was clearly referred to as non-acid forming (NAF) spoil. In addition, hazardous phosphorus concentration was less than 0.05% (Ward, et al., 1996) in the Bowen Basin area.

Table 2.1 Mineralogical percentages (wt. % by XRD) of spoil and fresh rock (Ulusay, Arikan, & Yoleri, 1995)

| Material type | No. of Samples | Clay minerals (%) | | | | Other minerals (%) | | | |
|---|---|---|---|---|---|---|---|---|---|
| | | Kaolinite | Illite | Montmorillonite | Quartz | Feldspar | Calcite | Aragonite | Dolomite |
| Spoil material | 9 | 5–10 (5.0) | 10–30 (17.8) | 0–10 (4.4) | 0–10 (1.7) | 0–3 (0.3) | 5–25 (1.33) | 5–77 (50.2) | 0–17 (5.2) |
| [a]Fresh rock | 5 | 5–10 (6.4) | 10–20 (14.0) | - | 0–5 (1.6) | 0–5 (1.6) | 5–20 (12) | 30–65 (53) | 0–30 (11) |

[a]Laminated and compact marl samples; numbers in the parenthesis indicate mean values.

The physical properties of spoil material were observed from various studies conducted in different parts of the world. Generally, from grain size distribution of spoil properties it was observed that spoil is moderately well graded material (Ulusay, Arikan, & Yoleri, 1995). The quantity of fine particles is less in fresh

sample which gradually increases with the slaking of spoil. Table 2.2 and Figure 2.12 presents the physical properties of typical spoil in southwest Turkey. According to the study the amount of gravel content in different spoil varied from 10 to 67 per cent and the fine content ranged from 15 to 69 per cent. Silt was the dominant finer part of the spoil sample. In addition, the liquid limit of spoil generally varied from 20 to 70 per cent (Ulusay, Arikan, & Yoleri, 1995). From the study carried out on spoil from the Bowen Basin, spoil category three contained low plastic materials with a liquid limit from 25 to 35 per cent (Leonie Bradfield, 2013; Simmon & McManus, 2004).

Table 2.2 Physical properties of spoil materials (Ulusay, Arikan, & Yoleri, 1995)

| Grain size distribution | | | | [a]Atterberg Limits | | | Moisture Content | | Slake Durability Index | |
|---|---|---|---|---|---|---|---|---|---|---|
| Gravel (%) | Sand (%) | Silt (%) | Clay (%) | Liquid limit (%) | Plastic limit (%) | Plasticity index (%) | All samples (%) | Samples from trenches (%) | $I_{d2}$ (%) | [b]$I_d$ (%) |
| 10–67 (37.2) | 8–41 (19.1) | 11–48 (33.3) | 0–30 (10.4) | 40–73 (59.4) | 30–54 (40.9) | 9–27 (18.5) | 26–52 (39.2) | 28–49 (37.2) | 17.9–96.4 (85.8) | 13.0–92.7 (74.8) |

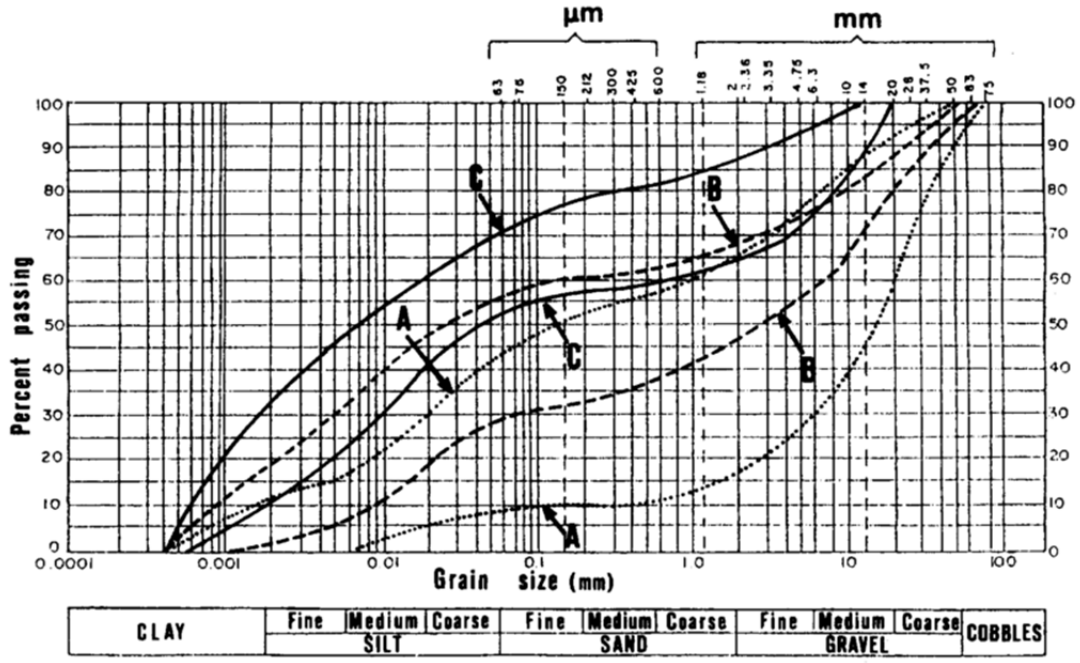


Figure 2.12 Grain size distribution of spoil materials (Ulusay, Arikan, & Yoleri, 1995), where A: recent spoil dumped by dragline, B: samples from upper level of spoil & C: samples from sliding surface

A great deal of research (Fu & Liao, 2010; Kim & Ha, 2014; Li, 2013; Nakao & Fityus, 2008; Simmon & McManus, 2004) has been carried out to investigate the behaviour of granular spoil heaps. According to this research, coal mine spoil behaves like a frictional material. The results were obtained from two types of shear testing; the direct shear test and the triaxial compression test. The difference between peak and residual shear strength was low (Ulusay, Arikan, & Yoleri, 1995). The peak and residual frictional angles were 34.3° and 33° with negligible cohesion ($C_p$= 12kPa & $C_r$=8.9kPa). On the other hand, the friction angle obtained from triaxial varied from 16° to 35° and cohesion from 0 to 34 kPa. Undrained triaxial tests were performed on spoil materials comparatively smaller than 12.7mm (Karfakis, Bowman, & Topuz, 1996). The angle of internal friction varied from 13.9° to 17.8° (total analysis) and cohesion varied from 97 to 234 kPa for dry samples. The angle of friction decreased with increasing moisture content of sample (Table 2.3).

Table 2.3 Summary of Triaxial test result of spoil Total analysis (Karfakis, et al., 1996)

| Sample number | Cohesion (kPa) | | | Angle of internal friction (degrees) | | |
|---|---|---|---|---|---|---|
| | Dry | w = 10% | w = 15% | Dry | w = 10% | w = 15% |
| 1 | 138 | 296 | 234 | 16.8 | 11.2 | 7.0 |
| 2 | 124 | 269 | 200 | 17.4 | 9.5 | 5.6 |
| 3 | 234 | 276 | 372 | 17.1 | 14.0 | 9.4 |
| 4 | 97 | 338 | 324 | 17.8 | 9.7 | 7.0 |
| 5 | 165 | 303 | 283 | 14.8 | 10.0 | 7.2 |
| 6 | 172 | 290 | 296 | 14.8 | 11.9 | 7.4 |
| 7 | 124 | 317 | 221 | 15.4 | 8.8 | 6.4 |
| 8 | 110 | 228 | 359 | 17.2 | 14.6 | 8.7 |
| 9 | 159 | 352 | 165 | 13.9 | 11.5 | 5.6 |

The result obtained from the direct shear test and triaxial test (Simmon & McManus, 2004) on spoil samples from the Bowen Basin area indicated that remoulded spoil of that area was comparatively compiled of low strength materials with negligible cohesion. A shear strength framework was proposed from rigorous direct shear tests, triaxial test results and field visual properties of four available types spoil of samples. The effective shear strength parameter was verified from back analysis of failure of spoil by using GLENA software.

Table 2.4 Shear strength parameters for four categories and mobilisation modes (Simmon & McManus, 2004)

*(Parameter standard deviations in italicised parentheses)*

| Category | Unsaturated | | | Saturated | | | Remoulded |
|---|---|---|---|---|---|---|---|
| | γ (kN/m$^3$) | c' (kPa) | ϕ' (deg) | γ (kN/m$^3$) | c' (kPa) | ϕ' (deg) | c'=0 kPa, ϕ' (deg) |
| 1 | 18 *(1)* | 20 *(10)* | 25 *(2.5)* | 20 *(1)* | 0 *(0)* | 18 *(3)* | 18 *(1.5)* |
| 2 | 18 *(1)* | 30 *(15)* | 28 *(3)* | 20 *(1)* | 15 *(7.5)* | 23 *(2.5)* | 18 *(1.5)* |
| 3 | 18 *(1)* | 50 *(15)* | 30 *(2)* | 20 *(1)* | 20 *(10)* | 25 *(2.5)* | 18 *(1.5)* |
| 4 | 18 *(1)* | 50 *(15)* | 35 *(2.5)* | 20 *(1)* | 0 *(0)* | 30 *(1.5)* | 28 *(2)* |

Another study was carried out by a large scale direct shear test on spoil material, and smaller than 19mm was from the Hunter Valley, Australia (Fityus, et al., 2008). The test results drew similar conclusions (Ulusay, Arikan, & Yoleri, 1995) for peak and residual friction angles of spoil materials of the Hunter Valley. The peak and residual friction angles were obtained at 33.4° and 32.4° respectively. That shear strength value was higher than the Bowen Basin (Richards, 1998). The peak and residual angle of internal friction obtained from the Hunter Valley was higher than the peak and residual friction angle of 28° and 18°.

The permeability of any material is the function of the effective diameter of particles ($D_{10}$). According to particle size distribution, spoil is a gravel type material and moderately permeable. The falling head permeability tests of southwest Turkey indicated that it ranged between 8.4 x$10^{-03}$ and 8.7 x$10^{-03}$ cm/sec (Ulusay, Arikan, & Yoleri, 1995). Again, Karfakis, et al. (1996) studied permeability of spoil samples which were used as backfill material. The falling head permeability test result (Table 2.5) suggested a similar conclusion. The permeability properties of nine spoil samples ranged from 1.19x$10^{-06}$ to 7.92x$10^{-06}$ m/sec and an average result was 4.55x$10^{-06}$ m/sec.

It was observed that with increasing overburden pressure, the void ratio changed due to particle crushing which lead to changes in particle size (Smith, et al., 1999). As a result, permeability property changes decreased with the increasing of

overburden pressure. The relationship between maximum particle size and permeability properties of spoil were studied by Smith et al. (1999). According to the study, permeability of spoil material escalates with increasing the maximum particle size, Figure 2.13. Particle size effects became less significant with the increasing moisture content of materials. The excess moisture content in spoil material increases the void ratio by replacing clusters of smaller particles.

Table 2.5 Average falling head permeability for mine spoil sample (Karfakis, et al., 1996)

| Sample no. | Coefficient of permeability (m/s) |
|---|---|
| 1 | $3.78 \times 10^{-6}$ |
| 2 | $4.74 \times 10^{-6}$ |
| 3 | $1.59 \times 10^{-6}$ |
| 4 | $3.75 \times 10^{-6}$ |
| 5 | $3.69 \times 10^{-6}$ |
| 6 | $1.70 \times 10^{-5}$ |
| 7 | $7.92 \times 10^{-6}$ |
| 8 | $1.19 \times 10^{-6}$ |
| 9 | $7.73 \times 10^{-6}$ |

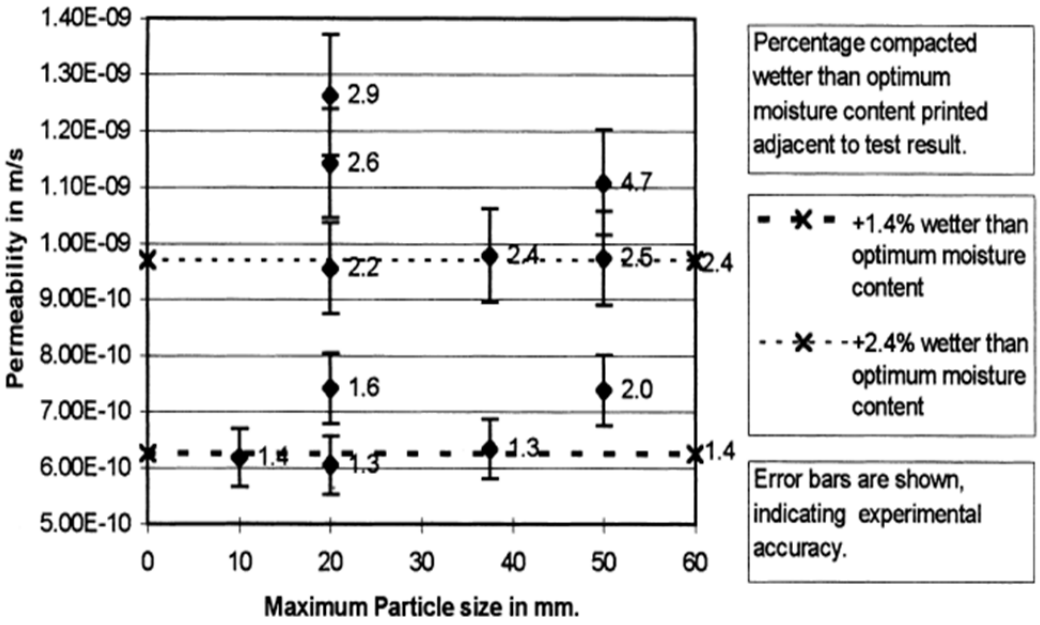


Figure 2.13 Relationship between permeability and maximum particle size (Smith, et al., 1999)

## 2.5 LABORATORY INVESTIGATION ON PROPERTIES OF MINE SPOILS

For earthwork excavation and rehabilitation design, it is essential to understand the properties of spoil materials which include classifying it by assessing permeability, compressibility and shear strength. Due to weathering behaviour and slaking, spoil materials change in their physical and chemical characteristics. The laboratory test included grain size distribution, Atterberg limits, specific gravity, compaction, permeability, compressibility, shear strength, for mineralogy analysis and x-ray diffraction. Field tests are performed to determine the effect of construction methods on dry unit weight and field moisture content at the site.

Several case studies (Jhanwar & Thote, 2011; Jiang, et al., 2013; Kayabasi & Gokceoglu, 2012; Seedsman & Emerson, 1985a; Ulusay, Arikan, Yoleri, et al., 1995) and analysis are available on failure in mines (Gökceoğlu, et al., 2000; Jiang, et al., 2013; Nguyen & Chowdhury, 1984; Ulusay & Aksoy, 1994; Ulusay, Arikan, Yoleri, et al., 1995). The aforementioned studies suggest that reduction in strength of materials in spoil; high steep slope and changes in moisture content are the major influential parameters of spoil pile failure. According to available literature related to spoil materials, sieve analysis was used to determine particle size of spoil (Spears & Taylor, 1972; Ulusay, Arikan, & Yoleri, 1995) in combination with hydrometer analysis for finer clay particles. In some cases, the Malvern apparatus was chosen to analyse finer clay particles (Fityus, et al., 2008). For plasticity and moisture content of spoil materials, the standard atterberg limit test and oven dried tests were applied. In case of chemical property investigation, most efficient X-ray diffraction techniques were used to analyse mineralogical content of spoil (Kusuma, et al., 2012; Ulusay, Arikan, Yoleri, et al., 1995).

The mechanical properties of spoil shear strength was investigated using mostly two different methods, direct shear and the triaxial compression test depending on the scope of study (Karfakis, et al., 1996; Okagbue, 1984; Ulusay, Arikan, Yoleri, et al., 1995). Since spoil material is a combination of gravel, silt and clay types of particles, any type of screening of spoil particle size will not reflect true condition. As a result of that, now a days large scale direct shear test and triaxial test was preferred by some researchers (Fityus, et al., 2008; Nakao & Fityus, 2008; Ulusay, Arikan, & Yoleri, 1995). In order to investigate the permeability properties

of spoil materials, a falling head permeability test was used by different researchers (Smith, et al., 1999; Ulusay, Arikan, Yoleri, et al., 1995) depending on the scope of research study.

## 2.6 SUMMARY

Throughout this chapter the factors that influence the stability of spoil piles and slope failure types, chemical and mechanical properties of spoil and its testing procedures were introduced and discussed. It was shown that with an understanding of the relative effects of mine spoil materials slaking on spoil stability, knowledge about spoil materials geotechnical and geochemical can help to analyse efficiently the safety of spoil slope. Mine operators can make rational choices of remedial actions of unstable slopes and its failure. A comprehensive study on changes of spoil property due to slaking will help to provide cost effective solutions in ever changing mining environment.

# Chapter 3: Methodology

## 3.1 INTRODUCTION

The critical literature review presented in chapter 2 revealed a lack of a systematic approach in the investigation of slaking induced material property variation of mine spoil. Therefore, this study aims to develop a systematic laboratory approach to slake spoil material and investigate the properties of slaked spoil. The aim of the study is achieved through a number of objectives stated in section 1.2 in Chapter 1. The methodology designed to achieve the objectives of this research consists of the following activities:

- development of shaking chambers
- field collection of coal mine spoil
- slaking of collected spoil in the laboratory
- laboratory testing on slaked coal mine spoil
- interpretation of laboratory test results

## 3.2 DEVELOPMENT OF SLAKING CHAMBERS

To slake spoil under controlled parameters (overburden pressure, water, and time) in the laboratory, a slaking chamber was designed and four such chambers were manufactured at the Queensland University of Technology (QUT) workshop.

Each chamber (360 mm internal diameter and 400 mm filling height) can accommodate 0.05 $m^3$ of material. Though the chamber has been designed to apply maximum 5 MPa vertical overburden pressure, in this study, it was limited to 900 kPa due to the capacity of the compressed air system in the QUT laboratory. In these chambers, material can be slaked over time with or without water. A detail of the slaking chamber is discussed in Chapter 4.

## 3.3 FIELD COLLECTION OF COAL MINE SPOIL

The spoil sample for this research study was collected from a mine in the Bowen Basin area in Central Queensland (Figure 3.2). The coal seam in the Bowen

basin extends to cover a distance of around 200km (Simmon & McManus, 2004) and it is the largest cooking and thermal coal reserve area in the world (Coffin, 2013). This bituminous coal was formed in the Triassic period which is also known as Permian. This is mainly used as coking coal for electricity generation and the steel manufacturing industry. The coal seam dips are flat in this mining area which resulted in increased interest in long strips mining with disposing achieved by walking draglines and shovel and truck methods (Simmon & McManus, 2004).

Spoil materials of the Bowen Basin were classified into four groups with consideration of the relationship between strength control mechanism and particle fabrication. In this classification system, larger particles are called 'framework' and fine particles are called 'matrix' depending on overall particle size distribution (Simmon & McManus, 2004). The spoil groups were, Category 1 (Figure 3.3a), Category 2 – (Figure 3.3b), Category 3 – (Figure 3.3c), Category 4 – (Figure 3.3d).

Table 3.1 presents attributing property descriptions with their weighting of the four spoil categories where predominant particle size and consistency of materials were inspected visually. Plasticity was determined by the liquid limit test and by the term age, referred to the slaking duration until the materials decreased to a constant old spoil state.

Table 3.1 Spoil categories and attributes (Simmon & McManus, 2004)

| **CATEGORY** | | **1** | **2** | **3** | **4** |
|---|---|---|---|---|---|
| **Description Attributes** | **Weighting** *(excl. Age)* | Fine-grained clay-rich high plasticity | Fine-grained low plasticity with larger clasts | Larger clasts with fine matrix, low plasticity | Large blocks, minor fines, minor slaking |
| **Predominant Particle Size** | 3/31=**9.7%** *(11.6%)* | Clay | Sand | Gravel | Cobbles |
| **Consistency: cohesive cohesionless** | 7/31=**22.6%** *(26.9%)* | Soft to Firm Loose | Stiff Med. Dense | Hard Dense | XLS+ rock Very Dense |
| **Structure** | 7/31=**22.6%** *(26.9%)* | Matrix only | Matrix supported | Framework supported | Framework only |
| **Liquid Limit** | 9/31=**29.0%** *(34.6%)* | High (>50) | Intermediate (35 – 50) | Low (20 – 35) | Not Plastic (<20) |
| **Age** | 5/31=**16.1%** | 0 - 2y | 2 - 10y | 10 - 30y | >30y |

*( Note: XLS+ rock refers to rock of extremely low strength, or higher)*

The shear strength properties of each spoil were different in the three different conditions of spoil. The shear strength parameters were high in the fresh unsaturated condition, which continued to decrease in saturation when it came into contact with water and was subjected to stress, shown in Figure 3.1. Finally, the spoil materials came in a lower strength parameter stage after a certain degree of slaking and crushing, called remoulded. Three conceptual strength modes were plotted in Figure 3.1 and the shear strength test result of 150 spoil's samples were presented in Table 3.2.

Table 3.2 Shear strength parameters for spoil categories and spoil mode (Simmon & McManus, 2004)

*(Parameter standard deviations in italicised parentheses)*

| Category | Unsaturated | | | Saturated | | | Remoulded |
|---|---|---|---|---|---|---|---|
| | $\gamma$ (kN/m$^3$) | c' (kPa) | $\phi'$ (deg) | $\gamma$ (kN/m$^3$) | c' (kPa) | $\phi'$ (deg) | c'=0 kPa, $\phi'$ (deg) |
| 1 | 18 *(1)* | 20 *(10)* | 25 *(2.5)* | 20 *(1)* | 0 *(0)* | 18 *(3)* | 18 *(1.5)* |
| 2 | 18 *(1)* | 30 *(15)* | 28 *(3)* | 20 *(1)* | 15 *(7.5)* | 23 *(2.5)* | 18 *(1.5)* |
| 3 | 18 *(1)* | 50 *(15)* | 30 *(2)* | 20 *(1)* | 20 *(10)* | 25 *(2.5)* | 18 *(1.5)* |
| 4 | 18 *(1)* | 50 *(15)* | 35 *(2.5)* | 20 *(1)* | 0 *(0)* | 30 *(1.5)* | 28 *(2)* |

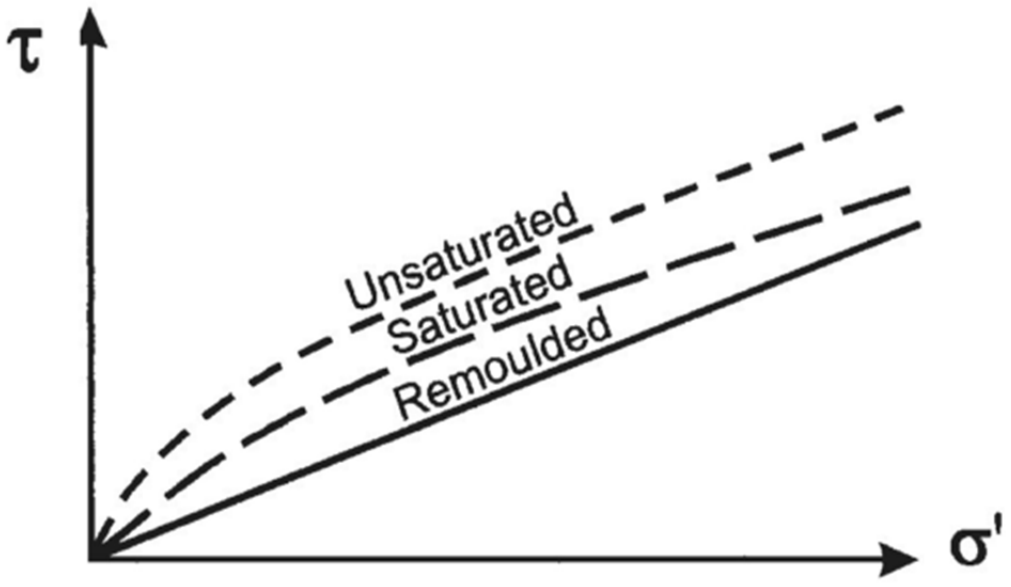


Figure 3.1 Three conceptual strength modes for spoil (Simmon & McManus, 2004)

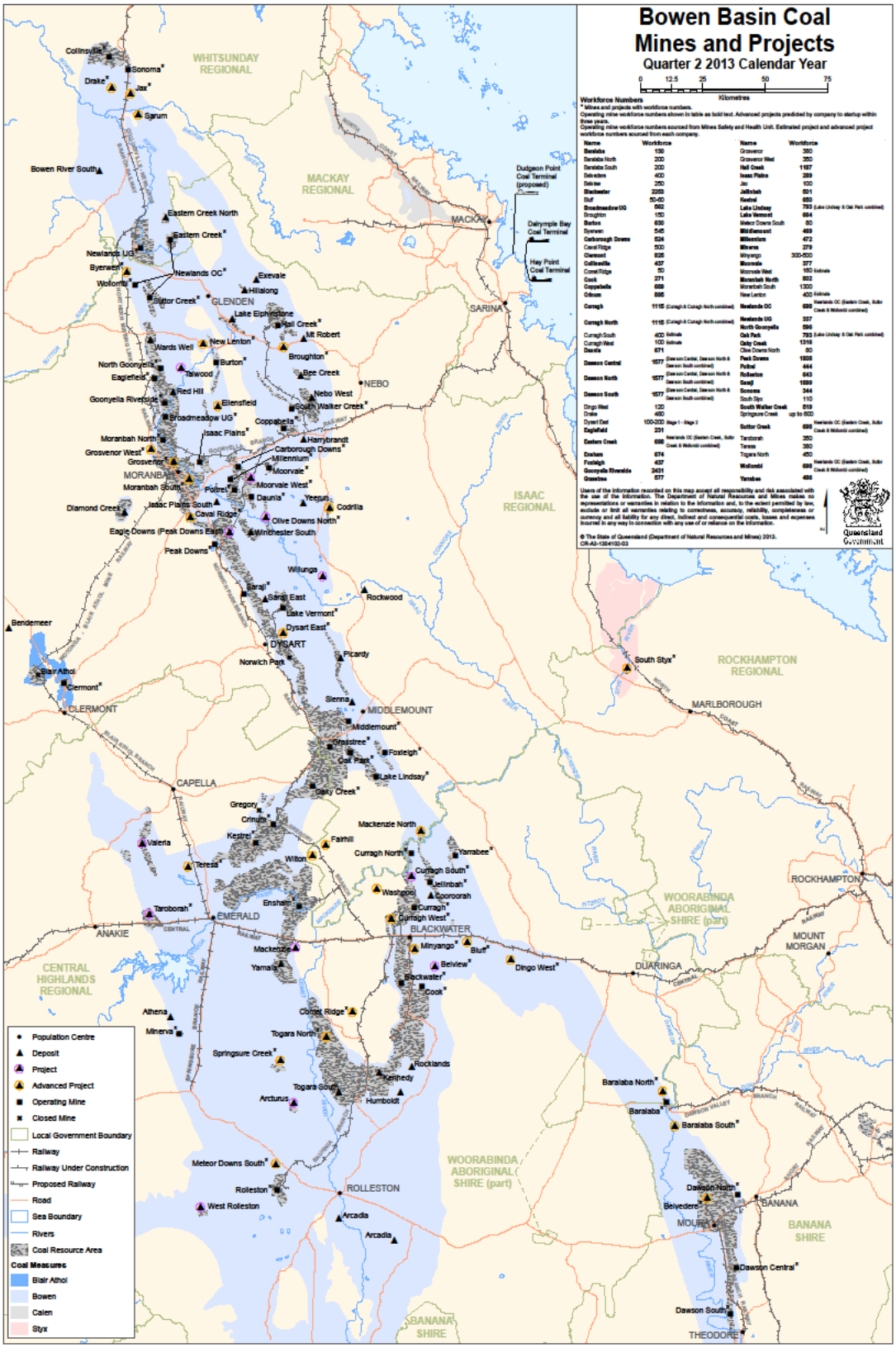


Figure 3.2 The Bowen Basin mining area and location of projects (Bowen Basin Coal Mines and Coal Projects map with workforce (Quarter 2 2013), 2013)

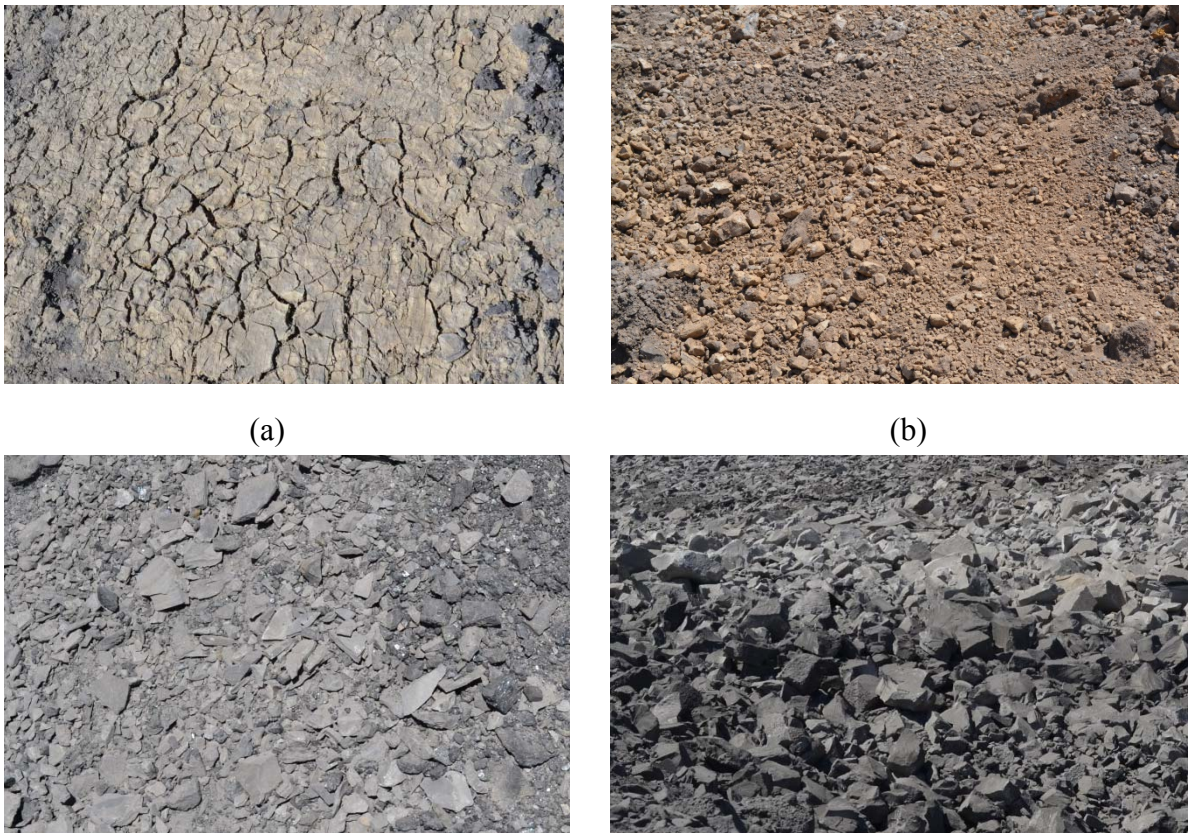

(a) (b)

(c) (d)

Figure 3.3 Spoil materials type (a) Category 1, (b) Category 2, (c) Category 3, (d) Category 4

Category 3 and 4 are commonly placed as the base of spoil pile and can undergo slaking over time due to high overburden stress and water saturation. Since category 3 is weaker than category 4 and the selected coal mine has only category 3 to use as base spoil material, it was decided to use category 3 as the testing material of this research study.

Figure 3.5 depicts the highwall and slope of the soil pile in the mine pit where test material was collected. The height of the highwall was approximately 120 m (Figure 3.5a) and spoil pile height was about 120 m at the location from where spoil samples were collected. The spoil materials were dumped at a sloping angle of about 37 ° (Figure 3.5 b).

Spoil samples were collected along the spoil pile edge by selecting the sampling locations using the judgement sampling method which is also known as purposive sampling (de Rooij, 2004). The spoil was collected in September 2013 from the toe of the spoil pile shown in Figure 3.5a. The collected spoil material had

been produced by blasting and dragging the bottom part of the highwall in August 2013. Therefore, it was reasonable to assume the collected spoil was 'fresh' (not subjected to overburden pressure nor wetting). Though the spoil sample category type 3 collected from same pile but four different locations and due to heterogeneous nature of materials the properties were slightly varied.

As shown in Figure 3.4, spoil was collected into 200L drums using shovels. Every effort was made in the field, not to collect particles greater than 30 mm. Four drums (each 200L) of category 3 coal mine spoil were delivered to QUT for this research program. Before subjecting slaking in spoil materials, the spoil materials of each drum was mixed properly to minimise heterogeneity of spoil.

(a) (b)

Figure 3.4 (a) Sample particle size observed by visual inspection, (b) Sample collection


(a) (b)

Figure 3.5 (a) Highwall height, (b) Slope of spoil pile

## 3.4 COAL MINE SPOIL SUBJECTED TO SLAKING IN THE LABORATORY

The freshly collected spoil was subjected to slaking in the shaking chambers under different conditions given in Table 3.3. The time and overburden pressure was selected for slaking in laboratory based on the field condition. Generally in mining field sometimes are closed for seasonal change especially in rainy season and on that particular mining area some of the mining pit are closed for one year. Each sample shown in Table 3.3 was compacted into a slaking chamber with an initial water content of 1.65 per cent to achieve the initial dry density of 18kN/m3.

Table 3.3 Slaking condition of spoil samples

| Eff. Overburden Pressure / Period over which Pressure was maintained | 300 kPa (about 15-17 m spoil height) | 600 kPa (about 35-40 m spoil height) | 900 kPa (about 50-60 m spoil height) |
|---|---|---|---|
| Zero months ( 2 days) | Sample 2 (300kPa-2days) | Sample 3 (600kPa-2days) | Sample 4 (800kPa-2days) |
| 3 months | Sample 5 (300kPa-90days) | Sample 6 (600kPa-90days) | Sample 7 (800kPa-90days) |
| 6 months | Sample 8 (300kPa-180days) | Sample 9 (600kPa-180days) | Sample 10 (800kPa-180days) |

Note: Sample 1 is considered as the reference sample which is fresh spoil collected from the mine.

## 3.5 LABORATORY TESTING ON SPOIL

Fresh coal mine spoil (sample 1) and another nine samples of slaked spoil (Table 3.1) were subjected to a series of laboratory tests to determine the effect of slaking on physical, chemical, and mechanical properties of coal mine spoil. The following tests were conducted on each spoil sample given in section 3.4:

- particle size distribution (Sieve analysis and Laser analysis)

- Atterberg limit tests (liquid limit, plastic limit and shrinkage limit tests)
- mineralogy analysis (X-ray Diffraction)
- constant head permeability tests
- shear strength tests ( shear test/ Triaxial)

### 3.5.1 Particle size distribution

The grain size distribution of each sample was obtained from a sieve and laser analysis by Malvern Mastersizer 3000. The wet sieve analysis was conducted according to Australian standard (AS 1289.3.6.1-2009) to diminish the particle distribution down to 0.075 mm. The particles passing through the 0.075 mm sieve were analysed using the Malvern apparatus to obtain the fragment size distribution of particles smaller than 0.075 mm. The apparatus and testing procedures adapted in reaching this particle size distribution are briefed in Chapter 4.

### 3.5.2 Atterberg limit

Atterberg limits (consistency limits) are important in classifying fine grained geo-materials. In this study, liquid limit, plastic limit and linear shrinkage were determined for each sample. The liquid limit (LL) of spoil was determined using the cone penetration method according to AS 1289.3.9.2-2006. Plastic limit (PL) and linear shrinkage (LS) samples were determined according to AS 1289.3.2.1-2009 and AS 1289.3.4.1-2008, respectively. Test apparatus and procedures adopted in determination of LL, PL, and LS are briefly described in Chapter 4.

### 3.5.3 Mineralogy and soil chemistry

The characteristic of mineralogy and geochemistry of spoil samples are important to investigate the influence of slaking. In this research, samples were analysed by x-ray diffraction using a diffract metre instrument (model X'Pert PRO). To analyse changes, mineralogy of the spoil samples were diffracted in cobalt monochrome using the Alumina standard. The qualitative and quantitative analysis was performed to determine mineralogy of spoil materials. From the quantitative analysis of spoil sample it was observed, that each sample contained a certain amount of non-diffracting amorphous content. For that reason, thermal gravimetric analysis (TGA) was performed and spoil samples were burned in a furnace to

determine the clay and coal content in each sample. The test apparatus, sample preparation and test procedure are discussed in Chapter 4.

### 3.5.4 Permeability

Permeability is one of key properties required when designing a spoil pile in terms of safety during filling and drawing down of water from the mine pit. As spoil is slaked, particle sizes and void ratio will change. These changes will have a direct effect on the material's permeability. Therefore, it is important to investigate the effects of slaking of mine spoil on its permeability. In this research study, a constant head permeability test was performed on material from each sample and the test was performed according to the Australian standard (AS 1289.6.7.1-2001). The constant head permeability apparatus and its test procedure are briefed in Chapter 4.

### 3.5.5 Shearing strength properties

Shear strength parameters are the most important material properties needed in design and analyses of stability of spoil piles. It has been hypothesised that slaking of base spoil pile material leads to strength degradation causing failures of spoil piles. In this study, shear strength parameters of each soil sample were determined using triaxial and direct shear apparatus to investigate the effect of slaking on shear strength properties of coal mine spoil.

Spoil from each sample was subjected to consolidate undrained triaxial testing with pore-water pressure measurement. Each test was conducted under multi-stage testing conditions (3 stages). Different initial effective confining pressure values (e.g.: 200, 300, 400 kPa) were used in a test to determine both effective and total shear strength parameters. The initial effective confining pressures were selected for series of triaxial test based on capacity of available triaxial apparatus used for this study and maximum available pressure in QUT garden point. A specimen with a diameter of 100 mm and height of 200 mm was re-compacted with an initial water content of ten per cent to achieve the dry density of 18kN/m3 was used in this study.

Direct shear tests were carried out on spoil material that had passed through a 6.7 mm sieve due to the limitation of the size of the shear box used. A square shear box of 100 mm and a specimen depth of 40 mm was used in the study. Slaked spoil with an initial water content of ten per cent was directly compacted into a direct shear box to achieve the initial unit weight of 18kN/m3. Specimens of each sample

were sheared under four different normal stresses (100kPa, 200kPa, 300kPa and 400kPa) to calculate the shear strength.

The apparatus and testing procedure of triaxial and direct shear apparatus will be briefly discussed in Chapter 4.

## 3.6 INTERPRETATION OF THE RESULTS OF THE LABORATORY TESTING PROGRAM

In Chapter 5, the results of the laboratory tests on all spoil samples (10 samples) were analysed and discussed to emphasise the use of the newly developed slaking chamber for systematic investigation of slaking induced material property changes in mine spoil. Furthermore, effects of different parameters (pressure, time) on the slaking of selected coal mine spoil (Category 3) were discussed. Finally, effects of slaking on physical, chemical, and mechanical properties of tested mine soil were presented. Based on the overall testing program, spoil properties to be used in spoil pile design were recommended.

# Chapter 4: Testing Apparatus

## 4.1 INTRODUCTION

The list of tests and standards were mentioned under methodology in chapter three and this chapter demonstrates steps involved in testing. The first section of this chapter presents detailed description of the pressure chamber design and development. In the second section of this chapter a brief overview is provided about the basic soil testing apparatus used in this research study. In the next four sections Malvern mastersizer 3000, X-ray diffraction, Triaxial and constant head permeability apparatus are described. A brief summary of this chapter is presented in the last section.

The saturated spoil material was subjected to slaking under different overburden pressures, which represent the height of the spoil pile, and time over which the overburden pressures were maintained in the laboratory using specially designed pressure chambers. Figure 4.1 shows a schematic diagram and a photo of a pressure chambers used. Four such chambers were employed in this experimental program.

The chamber consists of an acrylic cylinder of 20 mm wall thickness with internal diameter and height of 360 mm and 400 mm, respectively. The top and the bottom plates (Aluminium) are fastened by six bolts to seal the chamber. The chamber can accommodate about 60 kg of spoil allowing space for the piston plate. The initial unit weight of 18 $kN/m^3$ was assumed based on average dry unit weight spoil in Bowen Basin area as described by (Simmon & McManus, 2004).

This mass could be enough for different tests such as classification, shear strength, and permeability to be conducted on the slaked spoil material. The pressure is applied to spoil by applying air pressure to compartment above the piston which then compresses the spoil in the lower compartment with the applied pressure. A special type of rubber seal is attached to the piston to prevent air leak through the space between the piston and the inner wall of the acrylic cylinder. A pressure of 20kPa was needed to overcome the friction between the piston and the inner wall of the cylinder.

## 4.2 DESIGN AND DEVELOPMENT OF PRESSURE CHAMBER TO SLAKE SPOIL

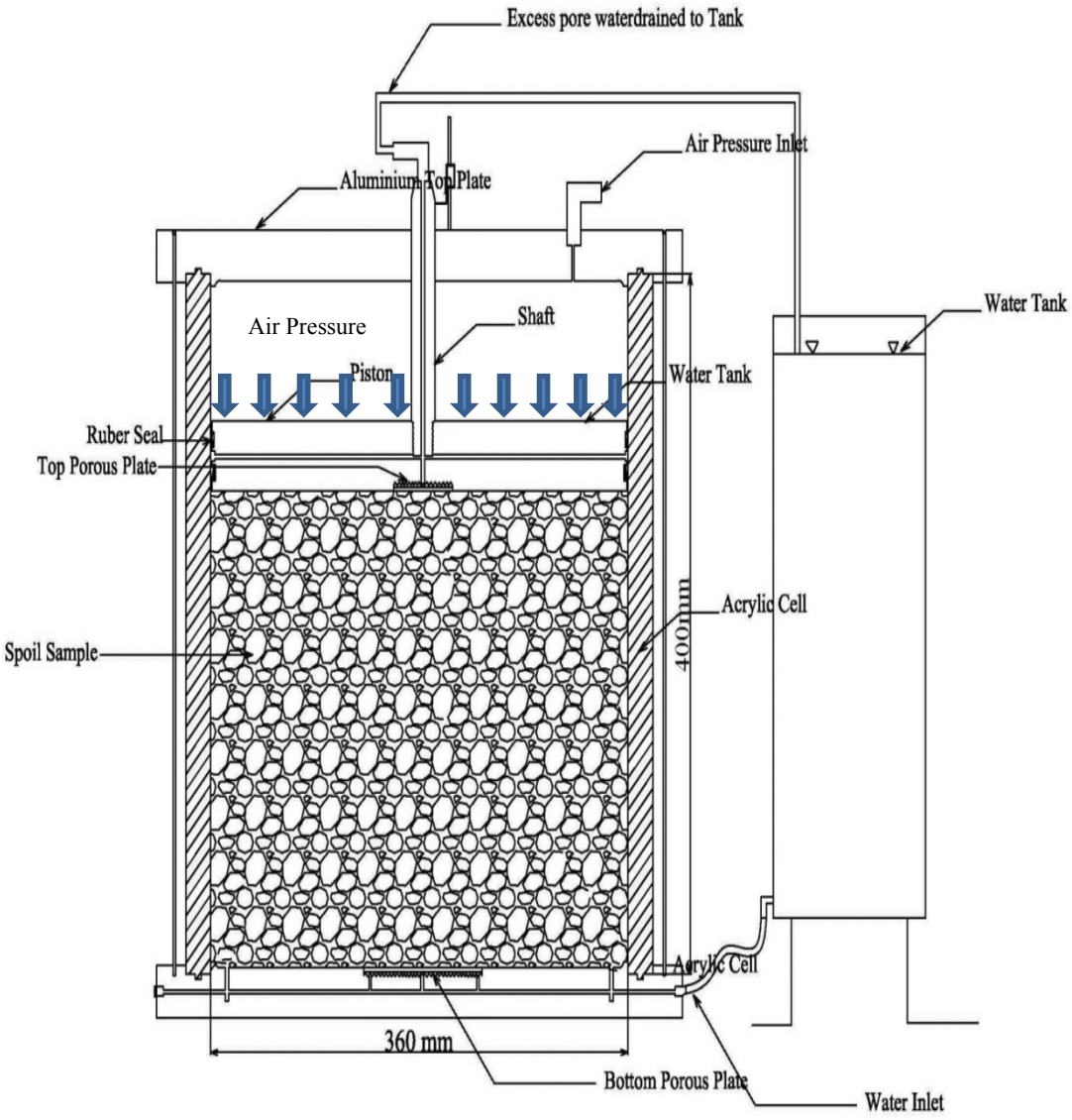


Figure 4.1 Schematic diagram of pressure chamber

Two porous stones (Bronze) are embedded in the base plate and in the piston where the material is in contact. The sample can be saturated by sending water from the bottom and allowing water to freely flow through the sample and to exit from the top. Water pressure in the sample is maintained at atmospheric conditions. It is important to make sure that the water in the chamber is under atmospheric conditions so that the applied pressure on the spoil from the piston is equal to the effective stress.

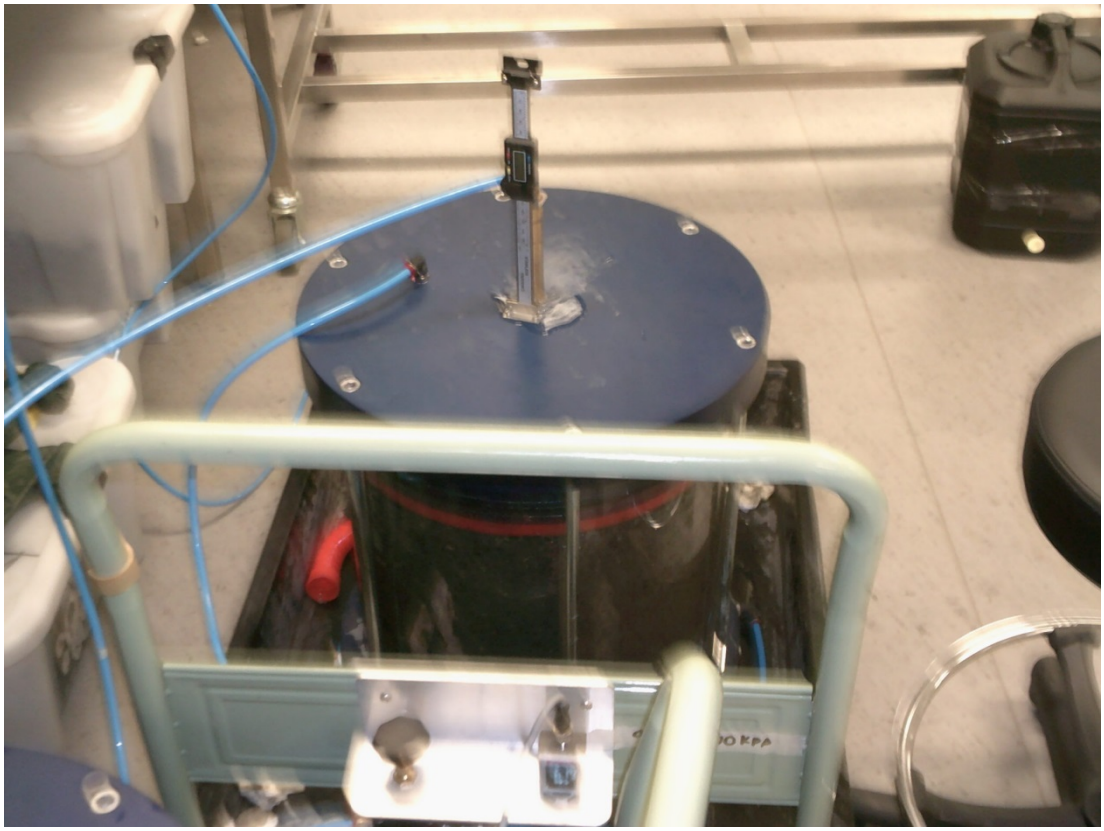

Figure 4.2 Photograph of pressure chambers

The consolidation of the spoil over the period of time under the applied constant overburden pressure can be measured directly from the linear variable differential transformer (LVDT) attached to the piston shaft. Below mentioned methodology were followed for preparing samples in pressure chamber to get the slaked spoil:

- The pressure chamber, of height 320 mm from the bottom plate, was divided into 10 equal layers as shown in Figure 4.3.The water content of the fresh spoil sample was measured. Bulk mass of spoil required for each layer to achieve dry unit weight of 18kN/m3.
- Bulk mass of spoil required for each layer to achieve the dry unit weight of 18kN/m3 was poured into the chamber and compacted by using the weight shown in Figure 4.3(b) until required height was achieved. The procedure was repeated for next nine (09) layers and the height was compared with marked line in chamber.

- The piston and top plate were mounted by using small lifting arrangement and LVDT set to measure the vertical displacement of the piston. A vacuum pump was connected to the top port through the shaft and air in the compacted spoil was pulled on for about 2 hours before applying water to start slaking.

(a) (b)

Figure 4.3 (a) Marking in pressure chamber, (b) Sample compacting weight

- As shown in Figure 4.4 (a) a plastic container was then connected to the bottom of the chamber and system was left for 24 hours (1 day) for complete saturation, with overburden pressure set to 20kPa.
- After saturation, air pressure equivalent to overburden pressure of 300, 600, 900kPa was applied in to the upper part of chamber in between top plate and piston and maintained for periods of 2 days, 3 months and 6 months.
- After the saturated spoil sample subjected to slaking over a time period under a certain overburden pressure, the spoil in Figure 4.4 (b) was taken out from the chamber after releasing pressure and removing top plate and piston.
- Then each slaked spoil sample, kept under different pressures over a different time periods, was tested according to Australian standard or ASTM standard.

(a) (b)

Figure 4.4 (a) Pressure chambers connected with water, (b) Slaked sample ready for testing

## 4.3 BASIC SPOIL PROPERTY TESTING APPARATUS

This section describes detailed overview about basic soil testing apparatus used in this research study. For instance, liquid limit, plastic limit, shrinkage limit, sieve analysis, direct shear testing and specific gravity of spoil samples are those that performed to determine samples basic properties. A brief discussion is provided below:

### 4.3.1 Liquid limit

Liquid limit of slaked spoil samples were determined by cone penetration method (Standard, 2006). The instrument used for this test is shown in Figure 4.5 and methodology for this test is given below:

- The air dried sample grinded by using a mortar and rubber pestle and sieved the ground sample on a 425μm sieve to obtain about 400gms sample.
- About 200gms of sieved sample was taken and water was added to just wet the sample. The wetted sample left for 24 hours to soak and evenly distributed water to sample.

The cup was filled with wetted sample and struck off level by using spatula. The cone point was lowered close to the surface. The digital gauge reading was reset to zero. The cone was released for 5 seconds

- Cleaned the cone and cup and samples from cup with bulk sample and repeated the test. The penetration readings were recorded as two readings were within 1.0mm.
- The sample was removed from cup and mixed with bulk sample in mixing bowl. About 10-15gms of sample was taken for moisture content analysis.
- The procedure was repeated four times with higher moisture content within penetration range of 10-25mm. The moisture content value for penetration reading of 20mm was taken from the plotting moisture content vs penetration.

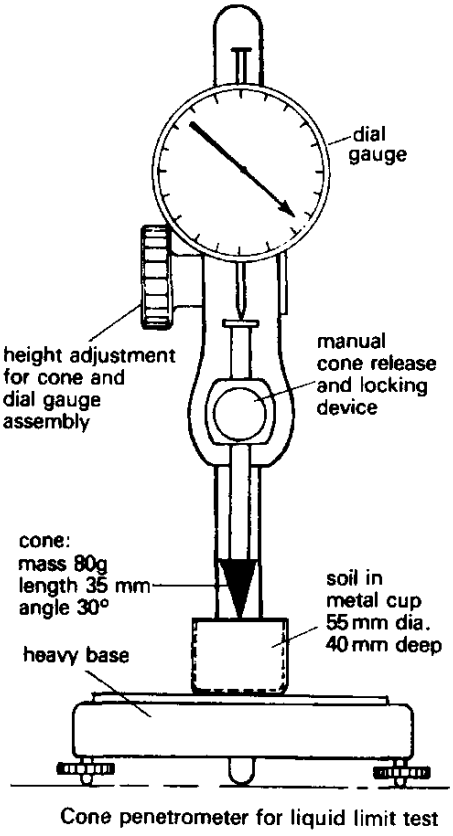


Figure 4.5 Cone penetrometer for Liquid limit test

### 4.3.2 Plastic limit

The plastic limit of slaked sample was determined by standard method (Standard, 2009a). The test methodology followed is given below:

- Small amount of wetted sample was taken to from a small ball approximately of 10mm diameter. The ball was rolled between the palms of two hands as shown in Figure 4.6 (a) until cracks appeared on the sample, and then it rolled on a frosted glass paper gently with a constant rate by one hand.
- The diameter was gradually reduced and the process was continued as shown in Figure 4.6 (b) until the thread just crumbled at 3mm diameter. The moisture content was determined for that crumbled sample and expressed as the plastic limit value.

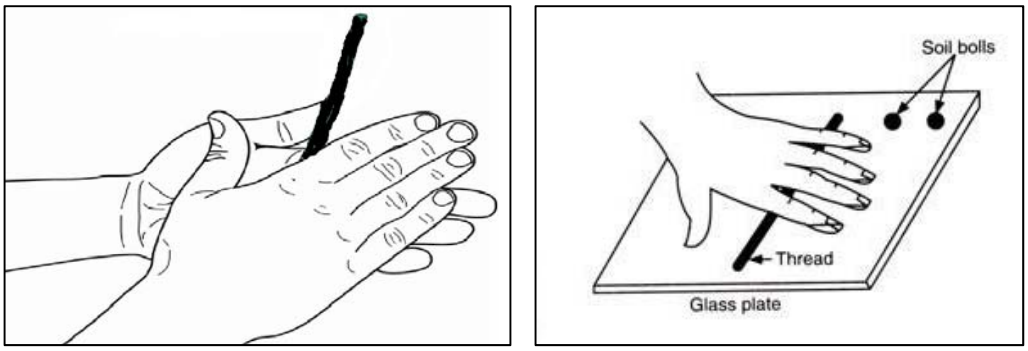


(a) (b)

Figure 4.6 (a) Rolled sample inside of Palms (b) Rolled on frosted Glass

### 4.3.3 Shrinkage limit

The shrinkage limit of slaked samples was determined by standard method (Standard, 2008) using a linear shrinkage mould made of semicircular brass as shown in Figure 4.7 . The methodology used to determine shrinkage limit is given below:

- Small amount of sieved sample was taken and exactly same amount water equal to liquid limit of sample was added. In this regard liquid of that samples were determined earlier.
- The properly mixed sample was placed in cleaned and lightly greasy mould and sample squeezed down with a spatula.
- The mould was lightly tapped to remove air void and level was stroked off after sightly over filling the mould.
- The mould was left for slow drying and then put in the oven for complete drying. The length was measured after drying and then percentage of deformation was calculated which is the shrinkage limit of that sample.

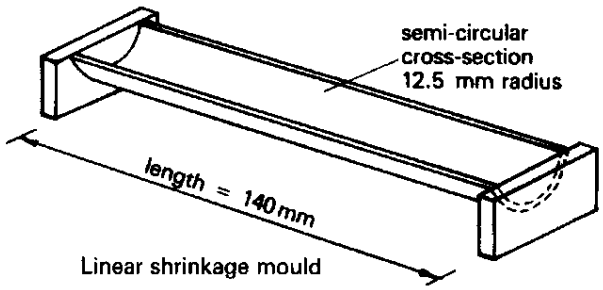


Figure 4.7 Linear shrinkage limit mould

### 4.3.4 Sieve analysis

Sieve analysis of this research study was performed by wet sieving method. According to Australian standard (Standard, 2009b) of wet sieving total 12 sieves of different sizes were selected for that analysis. One mechanical shaker was used to shake all sieves for 15 minutes at the time of testing. The methodology used in sieve analysis is described below:

- About two and half kilogram oven dried spoil samples were soaked in water for one hour before washing through 75 μm sieve as shown in Figure 4.8 (a). Washed water and washed samples were collected in different trays and dried in oven.
- After 24 hours of oven dry, the samples were sieved through a set of sieve of size 26mm, 19mm, 16mm, 13.2mm, 9.5mm, 6.7mm 4.75mm, 2.36mm, 1.18mm, 600μm, 300μm, 150μm & 75μm and fine samples from water were tested using Malvern Mastersizer 3000.

(a) (b)

Figure 4.8 (a) Slaked sample soaked in water; (b) Sieves shacked mechanically

## 4.4 DIRECT SHEAR MACHINE

Shear strength of slaked spoil materials is an important factor for the stability of design and analysis of spoil pile or highwall. Therefore in this research study direct shear tests were also performed to investigate shear strength properties of spoil samples beside of triaxial testing. In current research "Shear Track II" as shown in Figure 4.9(a) was used as a direct shear apparatus. It can also measure residual shear, direct simple shear, cyclic direct, simple shear, and incremental consolidation testing (ShearTrac-II, 2015). It has two force transducers and two displacement transducers

with feedback and real time control system. Shear track II is capable of generating up to 4.4 kN vertical load with transducers measuring capability +/-12.5mm in horizontal and 25.54mm in vertical. In this research strain control shear tests were performed on spoil samples. For each spoil sample four specimen were tested under four different normal loading conditions of 100kPa, 200kPa, 300kPa & 400kPa and shearing strain of 0.002mm/sec was applied for a maximum displacement limit of 12mm. Below mentioned methodology was followed for preparing samples in direct shear test to identify shear strength properties :

- At the beginning of direct shear test, oven dried spoil sample were sieved thorough 6.7 mm sieve to get materials smaller than 6.7 mm and added ten percent of water to it.
- Then, the moist sample was kept for 24 hours to soak water properly. Bulk mass of moist spoil sample required to get dry density 18 $kN/m^3$ was calculated earlier and compacted in shear box in three layers.
- Water was added up to top of shearing chamber after placing the compacted shear box. Vertical loading frame was attached in such a condition that no vertical load was applied at initial condition. Horizontal loading shaft was kept open as shown in Figure 4.9 (b).
- For first specimen, all information of consolidation and shearing stage were provided and test was begun with maximum normal loading condition 100kPa. The horizontal shearing loading shaft was tightened after consolidation stage finished and shearing stage of testing was started.
- The process was repeated for other three specimens of same spoil sample with normal loading conditions of 200kPa, 300kPa & 400kPa. The resultant shear stresses and respective loads were plotted in a plain graph paper to get shearing properties of spoil samples.

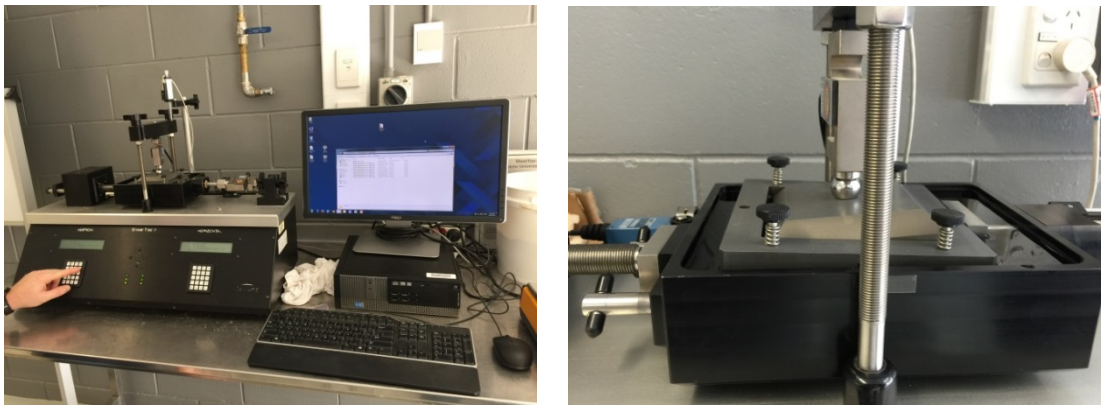

Figure 4.9 (a) Complete Shear Track II apparatus & (b) Placing of direct shear box

## 4.5 MALVERN PARTICLE SIZE ANALYSER

The Malvern Mastersizer 3000 was used in this research to analysis particles size distribution of materials with size below 75μm. Mastersizer 3000 is a laser diffraction particles size analyser which can determine particles sizes from 0.0001 to 3.5 mm rapidly with effective wet dispersion. It also can measure the particle sizes for fragile materials and cohesive dry powers. Mastersizer 3000 instrument (shown in Figure 4.10b) comprises three elements which are optical bench, sample dispersion unit, instrumented software. Generally, it works with the technique of measuring intensity of light scattered as a laser beam passes through a dispersive sample which is poured in sample dispersion unit as shown in Figure 4.10(a). The optical bench works as measurement area for the dispersed sample. Prior to test, the dispersion unit was cleaned after starting the Mastersizer 3000 software in computer and waited until the dispersion unit was fresh filled with water. Then, computerised system was automatically standardised for clean water and notified to add sample in dispersion system. About 0.5 g of dry powder sample (oven dried sample collected from washed water of sieving) was added in dispersion unit and preceded to measuring the sample particles size distribution. For each sample three tests were performed without the application of ultrasonic sound and three tests were performed with the application of ultrasonic sound. And finally, the average result of three tests with the application of ultrasonic sound was taken to combine with sieve analysis result.

(a) (b)

Figure 4.10 (a) Hydro MV unit for sample automated dispersion & (b) Malvern Mastersizer 3000

## 4.6 X-RAY DIFFRACTION APPARATUS

The X-ray diffraction apparatus used in this research was model type X'Pert Pro (Figure 4.11) available at the CARF laboratory in QUT Gardens Point campus. This instrument was designed based on CRISP technology and the application of pneumatic shutters & beam attenuators made that instrument ultimate reliable and smooth in operation. X'Pert Pro can analyse powder samples in a wide range of tilts of +/- 90° with in plane rotation 360°. It has translations capacity in-plane X and Y of 100mm, and vertical Z displacement of 11mm. It operates by 1.8 kW sealed ceramic copper tube and generate four selectable monochromes in a usable range -40°< 2θ <220° (X'Pert³Powder, 2015). In order to determine mineralogy of the spoil samples, cobalt monochrome was used for X-ray diffraction for both qualitative and quantitative analysis. For qualitative mineralogical analysis, small amount of fine part of each sample were collected after sieving through 75μm sieve. Then sample was analysed after mixing glycol standard and oven dried at 40° c.


(a) (b)

Figure 4.11 (a) X'Pert PRO X-ray diffraction system, (b) Samples Under testing for mineralogy

For quantitative mineralogical analysis below mention methodology was followed:

- To prepare test suitable powered sample less than 10μm was used. Oven dried slaked sample was crushed in stone crusher available at R- block in QUT Gardens point campus to prepare powdered sample.
- About 0.3g of Alumina (corundum) was added as a standard with 2.7g of each spoil sample and mixed it properly by using ethyl alcohol in McCrone micronizing mill.
- After mixing in micronizing mill, the wet sample was dried in oven at 40° temperature in a glass tray. Sample was tested after compressing in sample holder shown in Figure 4.12.

(a) (b)

Figure 4.12 (a) McCrone micronizing mill & (b) Compressing sample in sample holder

## 4.7 TRIAXIAL TESTING APPARATUS

The triaxial testing apparatus used for this study was named as Universal cyclic triaxial system. This triaxial testing apparatus comprises of two column load frame, advanced triaxial testing software along with pc, computerised system with 13 channels, 15 kN actuator with 50mm stroke, computerized confining pressure control unit, computerized back pressure control & volume change measuring unit, vacuum pump and air receiver (System, 2015) as shown in Figure 4.13. This computerized system can control back pressure, cell pressure and axial load. It can perform monotonic and cyclic shear test for three different sample sizes of 50mm, 100mm and 150mm with pore pressure, volume and others properties measurement as shown in Figure 4.14.

(a) (b) (c)

Figure 4.13 (a) Computerized system control, (b) Back pressure control & Volume change measuring unit and (c) Confining pressure control unit

As mentioned earlier in chapter three that monotonic multistage triaxial test was performed in this research study. In each stage of triaxial test, the back pressure was kept constant at 300kPa and the effective testing pressure were 200kPa, 300kPa, 400kPa. The testing procedure followed in this study is given below:

- The oven dried samples were sieved through 19mm sieve and mixed with ten percent of water. The water mixed samples were then kept for 24 hours to soak and evenly distribute water in the sample.
- Known bulk mass of moist spoil sample required to fill 100 mm diameter and 200 mm height triaxial testing sample mould were calculated earlier and the moulds were filled in five equal layers (40mm height).

Figure 4.14 Universal triaxial system

- Before pouring the spoil samples inside triaxial sample preparation mould, one thin player of soft plastic sheet were attached in the wall and the bottom of the mould. It prevented samples from sticking on wall or bottom plate. Sidewalls and bottom plate of that were attached firmly and horizontal tilt and diameter was checked
- For each layer, the samples were compacted until the height of layer matched with height of layer to achieve dry unit weight of 18kN/m$^3$. The surface scratched by a fork after compacting one layer and this step were repeated for four layers.

- Triaxial samples were placed on the bottom plate of triaxial cell after placing the porous disk and filter paper. Measurements of those moulded triaxial samples were taken before the start of the test.
- About 50kPa vacuum pressure was applied from top of triaxial sample for about one hour when the setup of triaxial apparatus cell was completed The apparatus cell was then filled with water in zero confining pressure and water was allowed to flow from bottom of triaxial sample.
- The sample was left in that status until no air bubble was noticed in bottom water reserve tank. Then, top water tank was disconnected and started saturation phase.
- Saturation phase was began with initial condition of zero back pressure and 100kPa confining pressure and it were manually increased with a 50kPa increment up to 300kPa back pressure and 400kPa cell confining pressure. Next increment was done for cell confining pressure up to 500kPa by keeping back pressure 300kPa in constant.
- Before the start of consolidation, the pressure condition of triaxial sample was changed to back pressure zero and confining cell pressure 500kPa. Consolidation process was continued until the plotting of time verse consolidation graph appeared to a flat slope.
- The first stage of triaxial test was begun after consolidation phase pressure condition back pressure 300kPa & cell confining pressure 500kPa, loading rate 0.05mm/ min, and maximum vertical deformation was 4 mm.

  At end of first stage, the loading was stopped automatically and the test was progressed to the second stage by using pressure conditions back pressure 300kPa & cell confining pressure 600kPa. This process was repeated for third stage with pressure condition back pressure 300kPa and cell confining pressure 700kPa. In both second and third stages the loading and maximum vertical deformation was kept same as that of first stage.

## 4.8 CONSTANT HEAD PERMEABILITY TESTING APPARATUS

The slaked spoil samples were tested by constant head permeability test. The apparatus was designed and supplied by Geo-Con Products Pty Ltd according to Australian standard AS 1289.6.7.1-2001 (Standard, 2001) The experimental setup consists of an electroplated metallic cylinder with internal diameter and height of 150 mm and 200 mm, respectively and the wall thickness is 10 mm. It consists of one bottom plate, two porous discs and two surcharge loadings. It also contains a constant head water supply unit. The constant head water supply unit is connected with a valve at the bottom plate.

Bottom plate (made by Aluminium) is fastened with permeability cell by two GI bolts and contains two valves. The bottom porous plate is placed at the middle grove of bottom plate and an O- ring is placed in the joint of bottom plate and cylinder to prevent water leak. Out of two valves installed at bottom plate, one valve is used for water supply and other one is to drain out air and water. The cylinder can accommodate about 170 mm sample in between two porous disc made by sand stones. Both porous discs are circular of diameter and height of 148 mm and 8 mm respectively but top plate contains a duct of 20 mm diameter. The two surcharge loads are placed at the top of porous disc at the time of saturation and testing. The sample can be saturated by sending water through bottom valve and can exit from the top in barometric pressure.

The constant head water supply unit contains a small water submersible pump along with a regulator to control water flow. At the time of test, laminar water flows to top water tank which drains excess water when system reaches required specified head as well as water flows from that constant head tank to cylinder. In order to maintain proper height difference for laminar flow, one adjustable hydraulic trolley was used and a digital thermometer to record water temperature. Below mentioned procedure was followed to perform the test

- The oven dried samples were sieved through 19mm sieve and mixed with ten percent of water and kept for 24 hours to soak.
- Two porous discs of permeability testing apparatus was soaked for 24 hours before use and small amount of petroleum jelly was applied along the wall of permeability testing mould.

- The permeability mould was placed in upside down position on the top of plastic board with clearance for placing porous disc and surcharge load in future.
- Known bulk mass of moist spoil sample required to fill triaxial testing sample mould of 150 mm in diameter and 170 mm in height were calculated earlier and the mould were filled in five equal layers.
- The bottom porous disc and O-ring were placed at bottom plate and the mould filled with sample was flipped over bottom plate. The mould was attached firmly with bottom plate.
- After placing the porous disc and surcharge the mould was connected with constant head water source and was kept for 24 hours for saturation. The difference of height was adjusted to keep laminar flow from the top of mould. The difference height between free water level head and top outlet of mould was measured. Water flow and temperature was measured when those was constant. Permeability of slaked spoil was calculated (Standard, 2001).

(a)

(b)

(c)


(d)

Figure 4.15 Constant head permeability testing apparatus (a) Front view (b) Side view (c) Top view (d) Porous disc and Surcharge

# Chapter 5: Results and Discussion

## 5.1 INTRODUCTION

This chapter presents results of geotechnical and mineralogical investigations performed on fresh and slaked spoil materials. This will contribute to the evaluation around the use of the newly designed pressure chambers to slake spoil material under controlled parameters and to investigate the influence of slaking on spoil properties. As described in chapter 3, nine spoil samples were compacted into pressure chambers to achieve a dry unit weight of 18 kN/m$^3$at a water content of 10%. After saturation, the samples were subjected to different overburden pressures (e.g. 300, 600, 900 kPa) and maintained over different time periods (e.g. 2, 90, 180 days). The vertical deformation of each sample was monitored over time and results will be discussed in this chapter. A section of this chapter will present physical properties, such as particles size distribution and Atterberg limits of 10 spoil samples (e.g. fresh spoil and nine slaked soil samples). The results are discussed, emphasising the effects of overburden pressure and time on the slaking of saturated spoil. Following this, the results of the chemical analysis conducted on all 10 spoil samples are presented and discussed. Finally, shear strength and saturated permeability properties of 10 spoil samples are presented and considered in relation to spoil slaking induced by overburden pressure and time under saturated conditions.

## 5.2 EFFECTS OF OVERBURDEN PRESSURE AND TIME ON COAL MINE SPOIL SLAKING

As discussed in both the introduction of this chapter and chapter three, nine samples of saturated spoil were subjected to different overburden pressures (e.g. 300, 600, 900 kPa) in the pressure chambers and vertical displacements of the pistons (compression of spoil) were monitored over different time periods (e.g. 2, 90, 180 days). Figure 5.1 shows the vertical displacement of pistons (compression of spoil) of three of the samples subjected to different overburden pressures (e.g. 300, 600, and 900 kPa) over the period of 180 days. It is evident that the volume of spoil decreases as the overburden pressure increases.

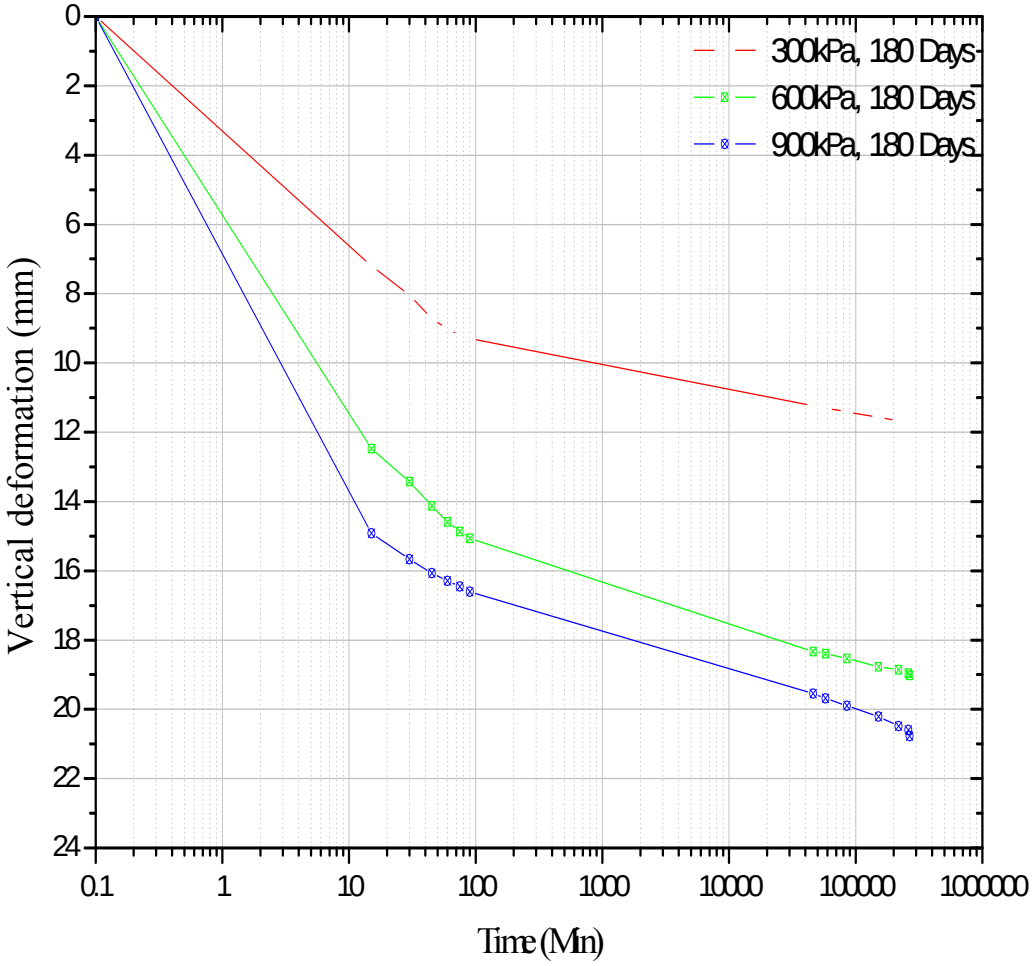


Figure 5.1 Vertical deformation of spoil in 180 days

Figure 5.2 illustrates the vertical deformation of three samples under constant overburden stress (900 kPa) over different time periods (e.g. 2 days, 90 days, 180 days). As shown in the figure, the sample was compressed by a mere 3 mm (about 1% of the initial height of 320 mm) over a period of 2 days to 180 days under the overburden pressure of 900 kPa. After that, the deformation rate reduced to a steady rate with a logarithm of time during a six month duration.

For samples shown in Figures 5.1 and 5.2, irrespective of the applied overburden pressure, 60-80% of total vertical occurred within 20 minutes after application of overburden pressure. Furthermore, after the first 100 minutes deformation continued at approximately the same constant rate (when time is in logarithmic scale).

The vertical settlement of the spoil sample shown in these figures consists of initial compression, elastic settlement, consolidation settlement, and settlement due

to particle breakage (slaking). Each sample's particle size analysis is discussed in section 5.2 of this chapter and confirms the slaking of spoil material.

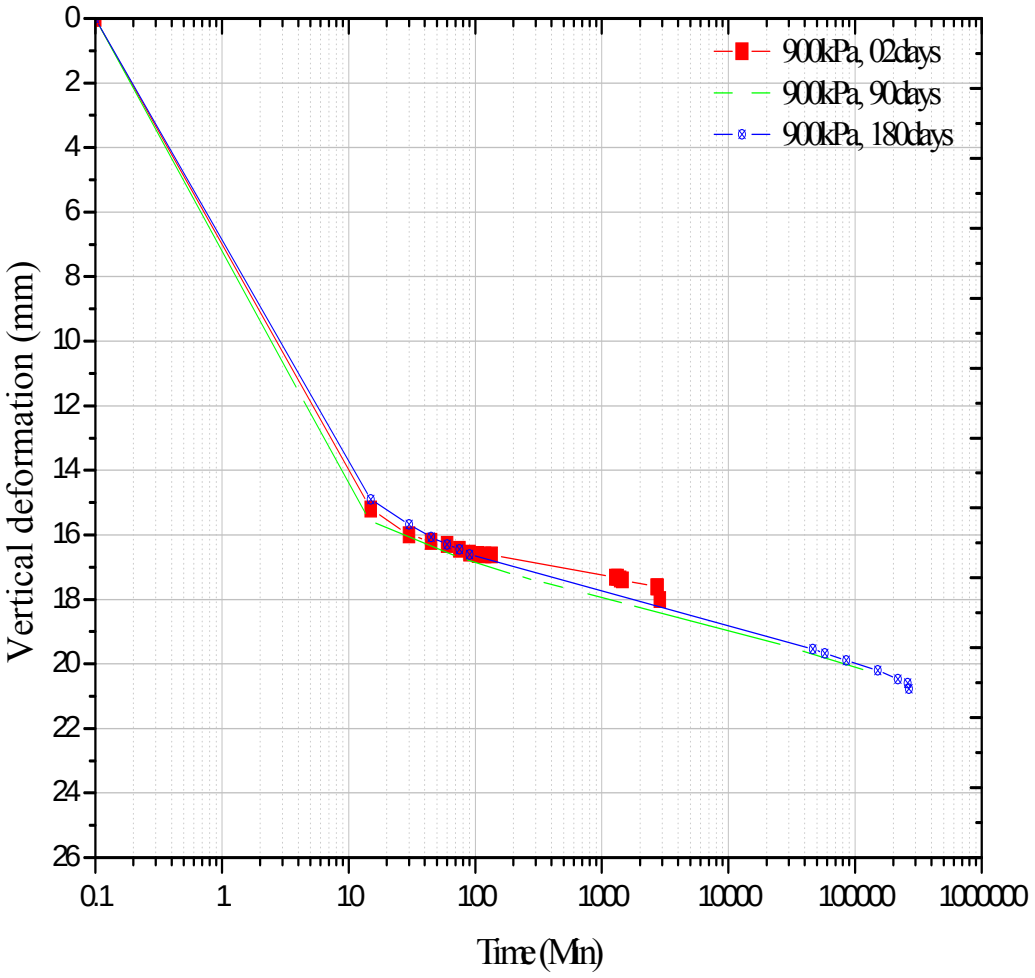


Figure 5.2 Vertical deformation of spoil under 900kPa overburden pressure

The vertical settlement of samples observed at the end of a period over which the overburden pressure was maintained, are summarised in Table 5.1 and Figure 5.3. It is indisputable that the amount of total settlement elevated with the increasing of overburden pressure and time. These observations are consistent with (Kalinski, et al., 2010). The effect of overburden pressure on the settlement of spoil is more significant than the time over which the pressure is maintained. Just after application of stress on statured spoil, it deforms rapidly because of elastic deformation, crushing and slaking (Brandon, Duncan, & Gardner, 1990; Cheeks, 1996; Karem, et al., 2007). With time, sample continues to settle at a slower rate due to slaking or hydrocompression (Kalinski, et al., 2010). The deformation (volume decrease) of

spoil sample due to particle breakage (slaking) could lead to a decrease in void ratio, permeability, and shear strength of spoil (Kalinski, et al., 2010; Mohamad Nor, Abbiss, Mohd. Raihan, & Khairul Anuar Mohd, 2011; Wunsch, Dinger, Taylor, Carey, & Graham, 1996).

Table 5.1 The vertical deformation of spoil under different overburden and time

| Overburden pressure/ Time | 300kPa | 600kPa | 900kPa |
|---|---|---|---|
| 02 Days | 11.42 | 17.32 | 18.01 |
| 90 Days | 10.31 | 18.90 | 20.23 |
| 180 Days | 11.80 | 19.01 | 20.77 |

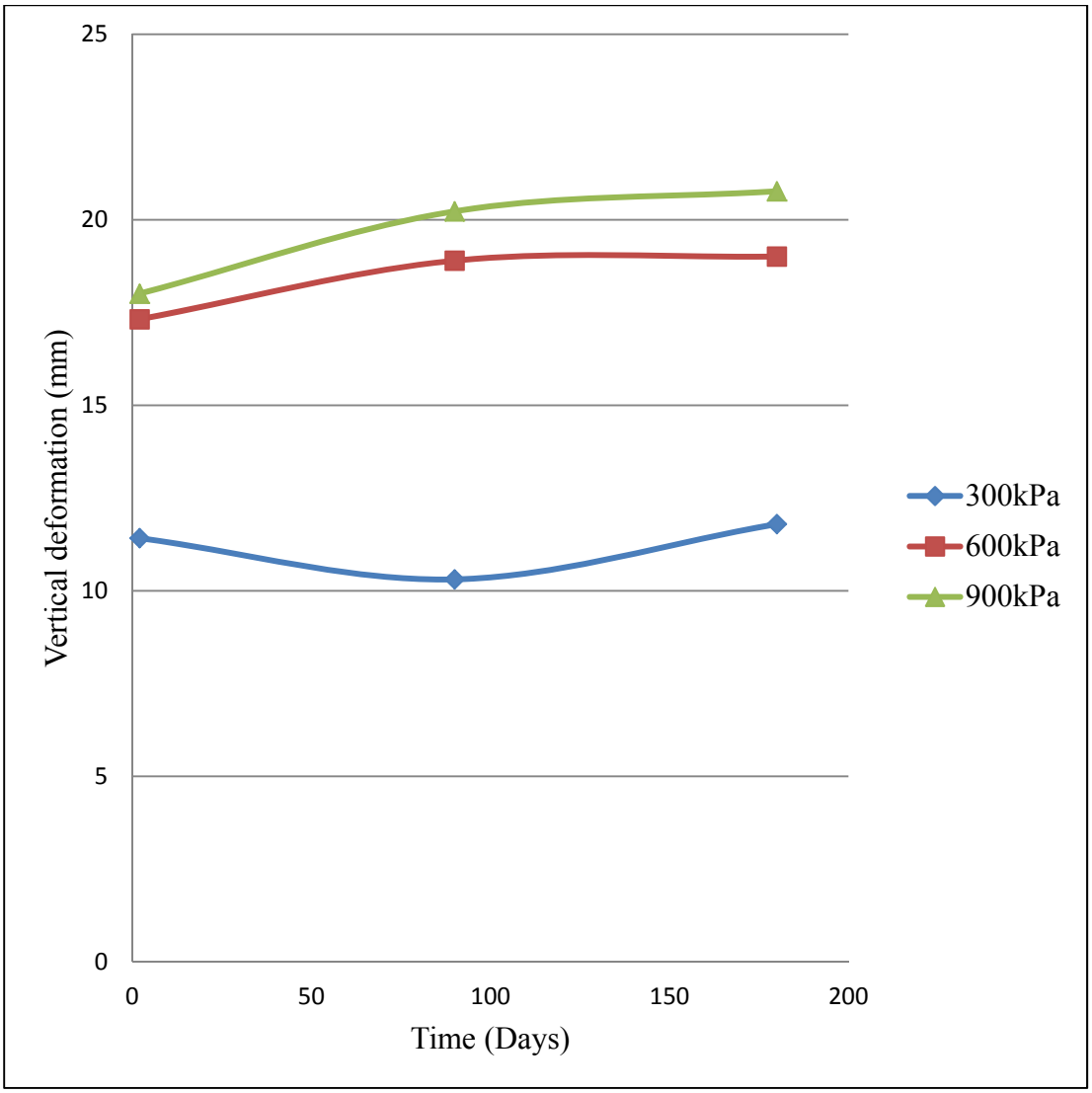


Figure 5.3 The maximum vertical deformation of slaked spoil under different overburden pressure and time

## 5.3 EFFECTS OF SLAKING ON PHYSICAL PROPERTIES OF COAL MINE SPOIL

### 5.3.1 Particle size distribution

The influence pressure and time on slaking of coal mine spoil was first determined by conducting particle size distribution for each sample. Figure 5.4 presents the results of particle size distribution of 10 spoil samples which were obtained from the combined results of wet sieve analysis and laser diffraction analysis.

It can be seen in Figure 5.4 and Table 5.2, the amount of fine particles increased with the increment of slaking time and overburden pressure. For spoil sample one, the amount of material finer than 75μm was approximately 8% which grew with increasing time and pressure to about 25% for spoil sample 10. However, there was no significant increment of clay particles (particle size less than 0.002mm) due to slaking but had a significant increment of silt particles. The increase in the amount of fine particles in spoil samples with saturation time and pressure is an indication of more material disintegration or slaking. Similar findings have been reported by some other researchers (Gautam & Shakoor, 2013; Gökceoğlu, et al., 2000; Sadisun, Shimada, Ichinose, & Matsui, 2005; Stavridakis, 1999; Ulusay, Arikan, & Yoleri, 1995).

Figure 5.5 presents particle size distribution of three slaked spoil samples for 180 days with reference to the original spoil sample. It is perceptible from the graphs, that due to slaking over 180 days, spoil particles have disintegrated in a similar pattern under three different overburden stresses. The median diameter of fresh spoil samples were 6.00mm which decreased to 1.9mm, 2mm, 2.7mm for slaking under 300, 600 and 900kPa overburden pressure. On the other hand, significant particle size reduction is observed from the graph presented in Figure 5.6 for particle size distribution with 900kPa overburden pressure with time. The change in particle size was nearly the same after two and 90 days slaked. The median diameter of spoil particles decreased by 2mm after 90 days of slaking, then further deceased to 1.9mm after 180 days of slaking. Examining Figure 5.5, 5.6 and Table 5.2, it is clear that slaking duration played a more dominant role in spoil slaking than overburden pressure. Initially spoil samples were taken to soften the particles and after that spoil slaking increased with time and overburden pressure.

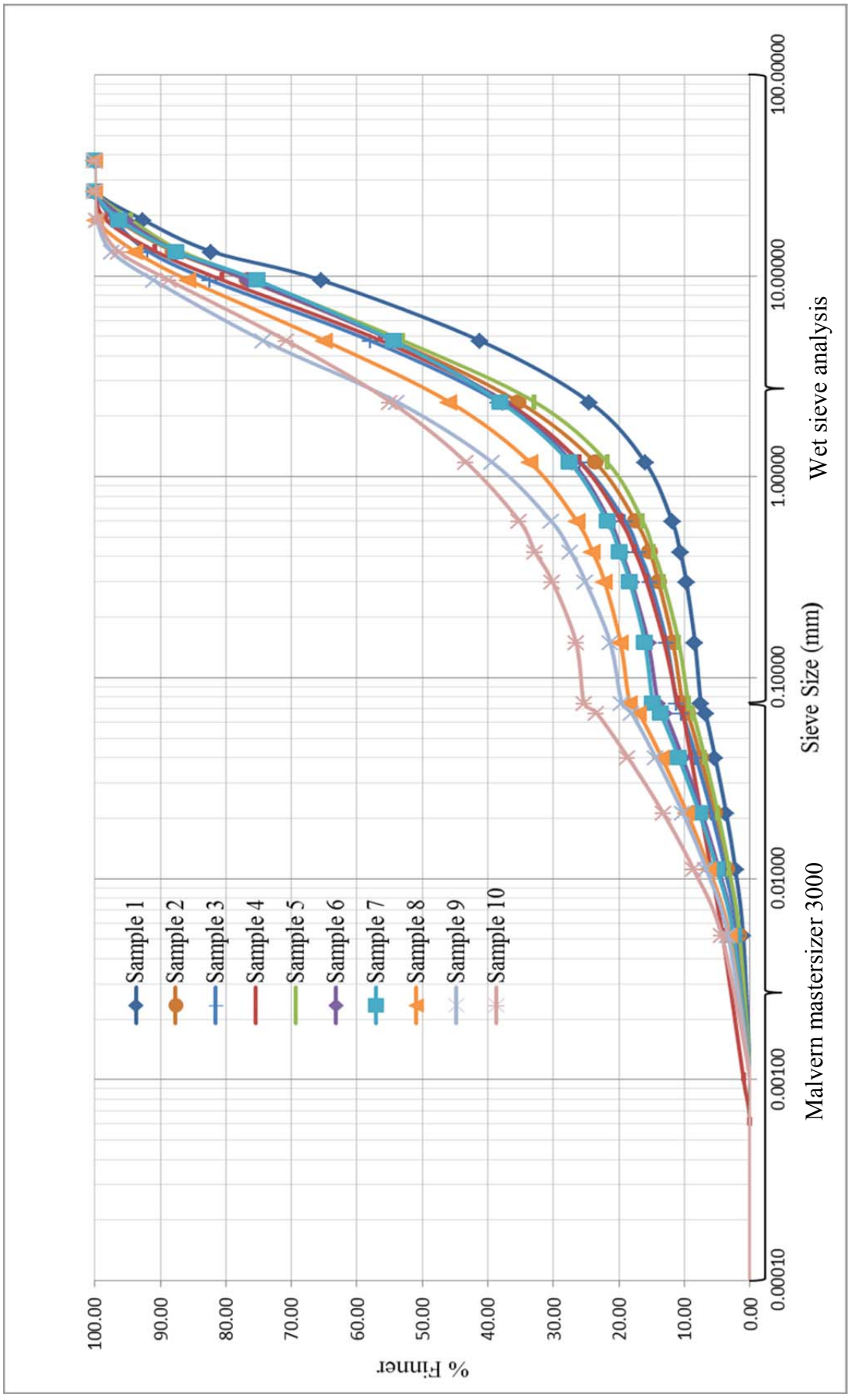


Figure 5.4 Particle size distributions of spoil samples

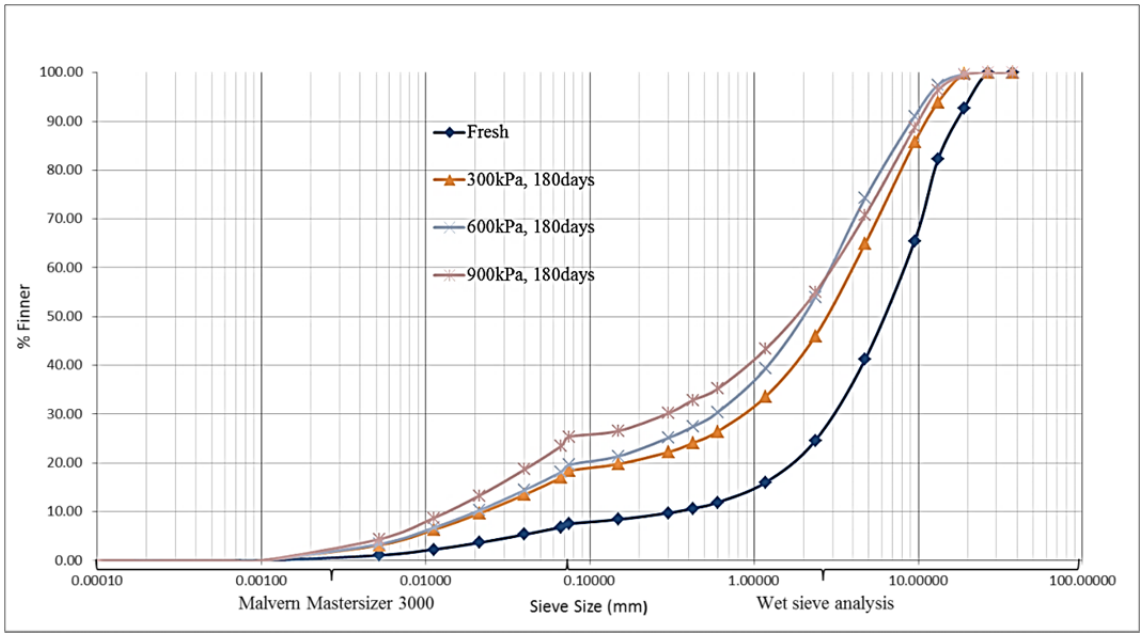


Figure 5.5 Particle size distribution of spoil samples after 180 days

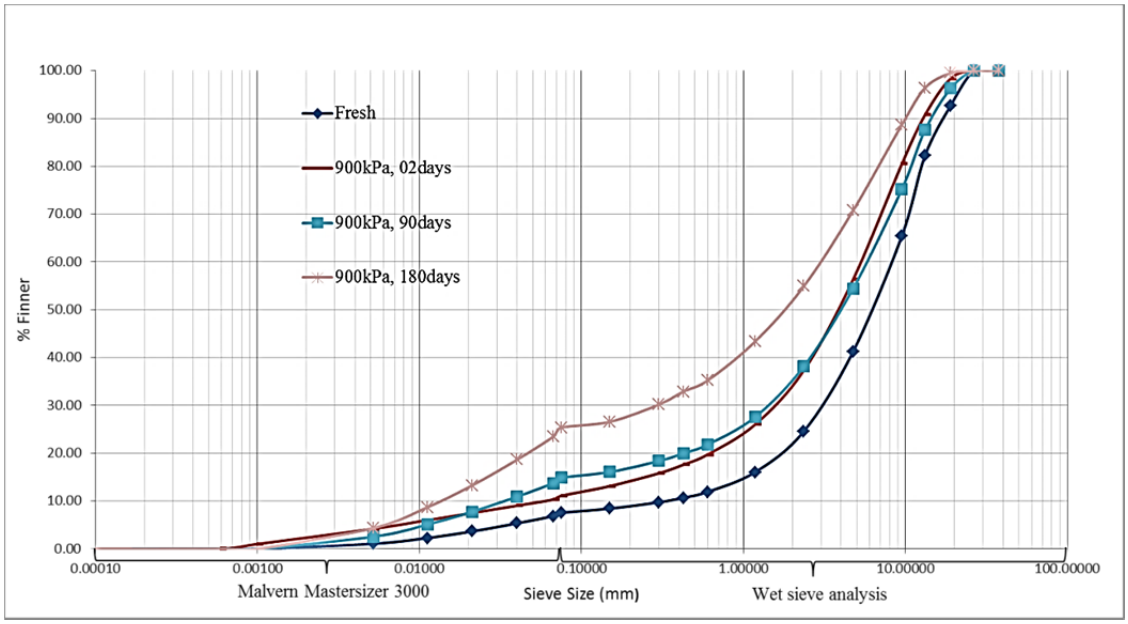


Figure 5.6 Particle size distribution of spoil for 900kPa overburden pressure

### 5.3.2 Atterberg limits

In addition to grain size distribution analysis, all spoil samples were tested for Liquid Limit (LL), Plastic Limit (PL) and Linear Shrinkage (LS) and the results are shown in Figures 5.6 – 5.10 and in Table 5.2. Initially, the liquid limit, plastic limit and shrinkage limit of fresh spoil sample (Sample 1) was found 34.08 %, 22.04 %

and 4.85 % respectively. Figure 5.7 illustrates the variation of liquid limit in spoil samples with overburden pressure and logarithm scale of time. It can be seen that the liquid limit of fresh sample or slaked sample for two days under different overburden pressures were between 33 and 34 percent. With the increase in overburden pressure and time, liquid limit slightly decreased hyperbolically to approximately 32 percent.

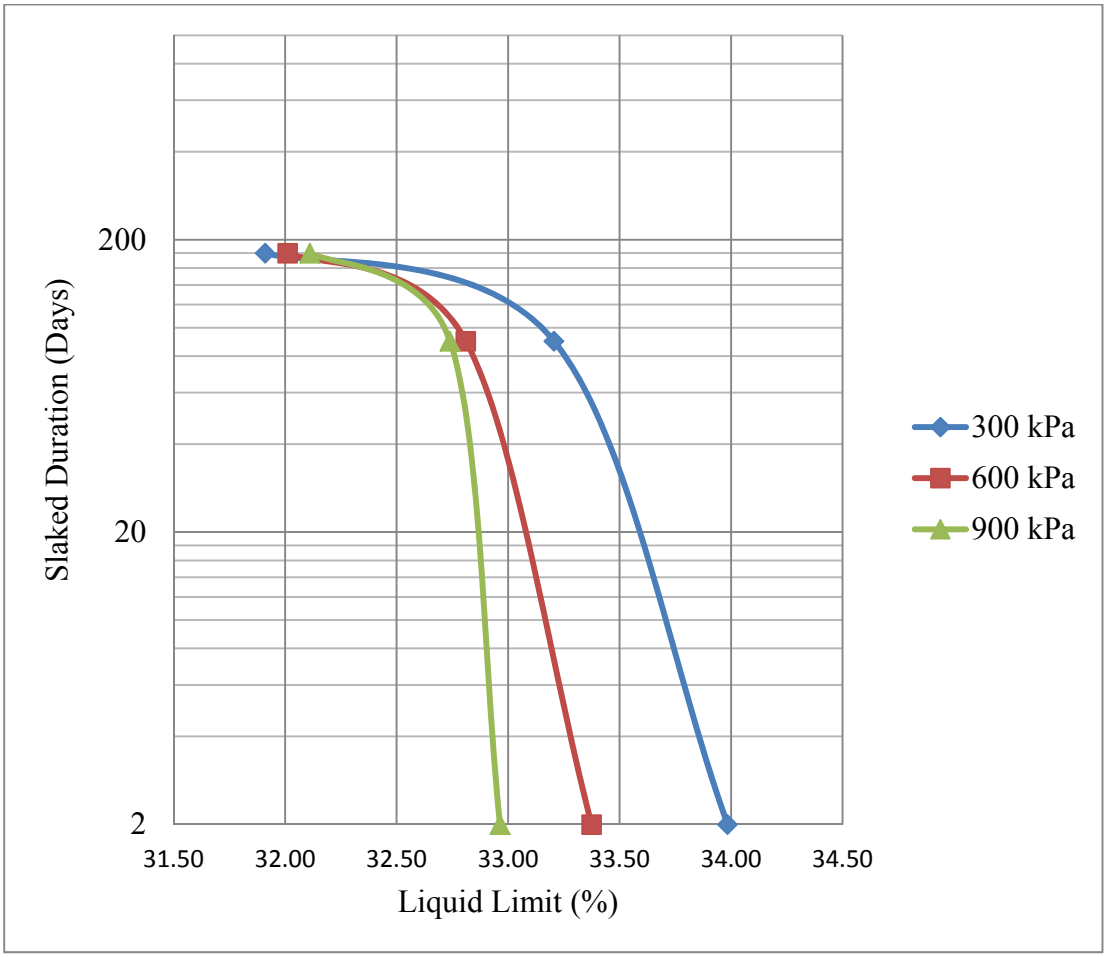


Figure 5.7 Variation of liquid limit of spoil with overburden pressure and time

Figure 5.8 illustrates the variation of plastic limit for slaked spoil samples collected from the Bowen Basin area. The plastic limit of slaked spoil samples under different overburden pressures (300, 600, 900 kPa) over 2 days was between 20.7% and 23.4%. During three months of slaking, the plastic limit gradually decreased to about 18.5 -19.5% and it further decreases at a slower rate to 17.0 – 17.7% by the end of 6 months of slaking.

It is clear from both Figure 5.7 and 5.8 that the influence of overburden pressure on LL and PL is noticeable at low slaking time (e.g. two days) and becomes insignificant as the slaking period increases. Furthermore, both LL and PL decreases as the slaking of material increases. This observation can be due to the increase of non-cohesive fine particles ( 0.425 mm – 0.002 mm) which is much greater than the increase in clay particles (particles smaller than 0.002 mm) (Figure 5.4) as the slaking increases. This is consistent with the finding of (Fityus, et al., 2008; Simmon & McManus, 2004).

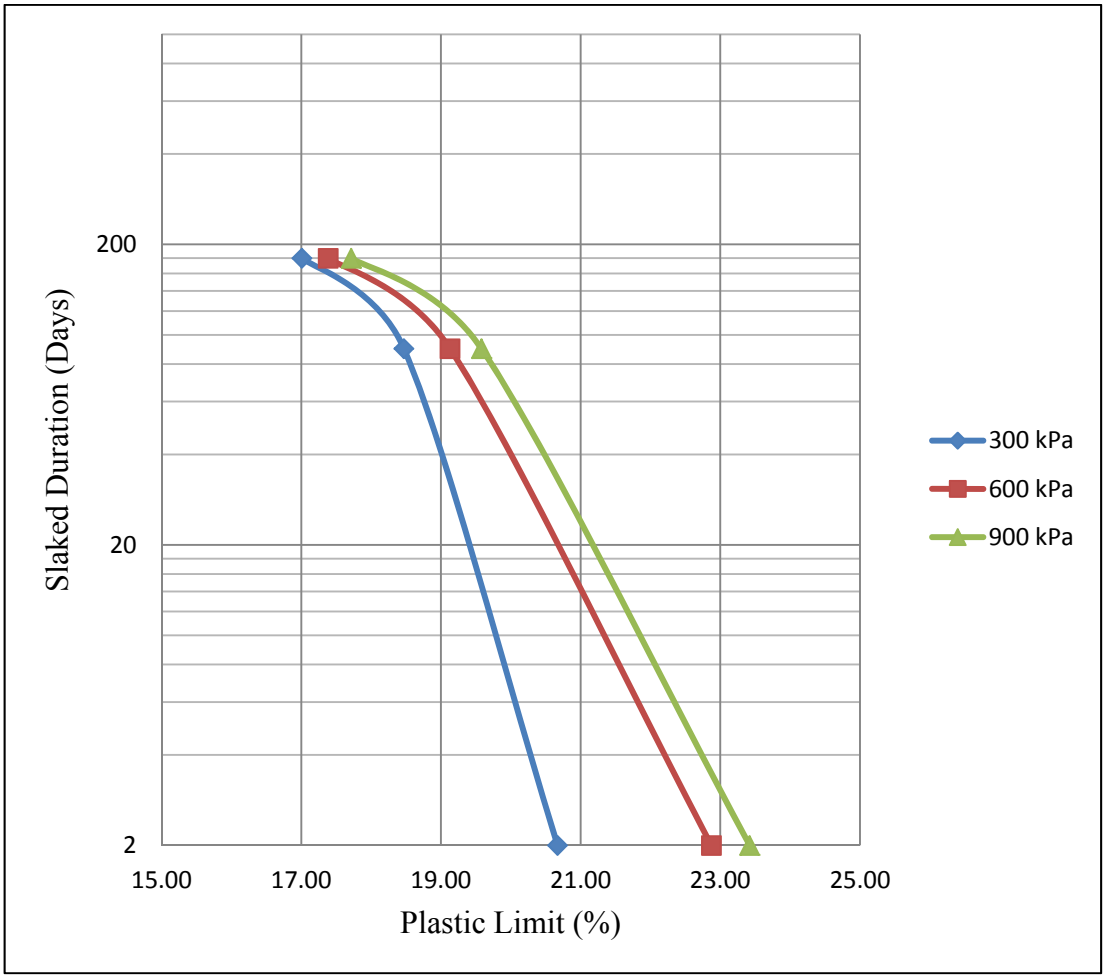


Figure 5.8 Variation of plastic limit of spoil with overburden pressure and time

Figure 5.9 shows the shrinkage limits (SL) of spoil samples. It can be noted that the SL of the material is about 4.5% and is not affected by slaking. SL informs the swelling/shrinking potential of material due to an increase/decrease in water content. SL is affected by the amount of clay and type of clay minerals. The results in Figure 5.9 suggest that the slaking of material has not caused any increase in either

amount of clay or the type of clay minerals significantly. Figure 5.4 clearly demonstrates that the amount of clay increased only by 1-2% during the slaking process and it could be insignificant in terms of affecting SL and other Atterberg limits (LL and PL).

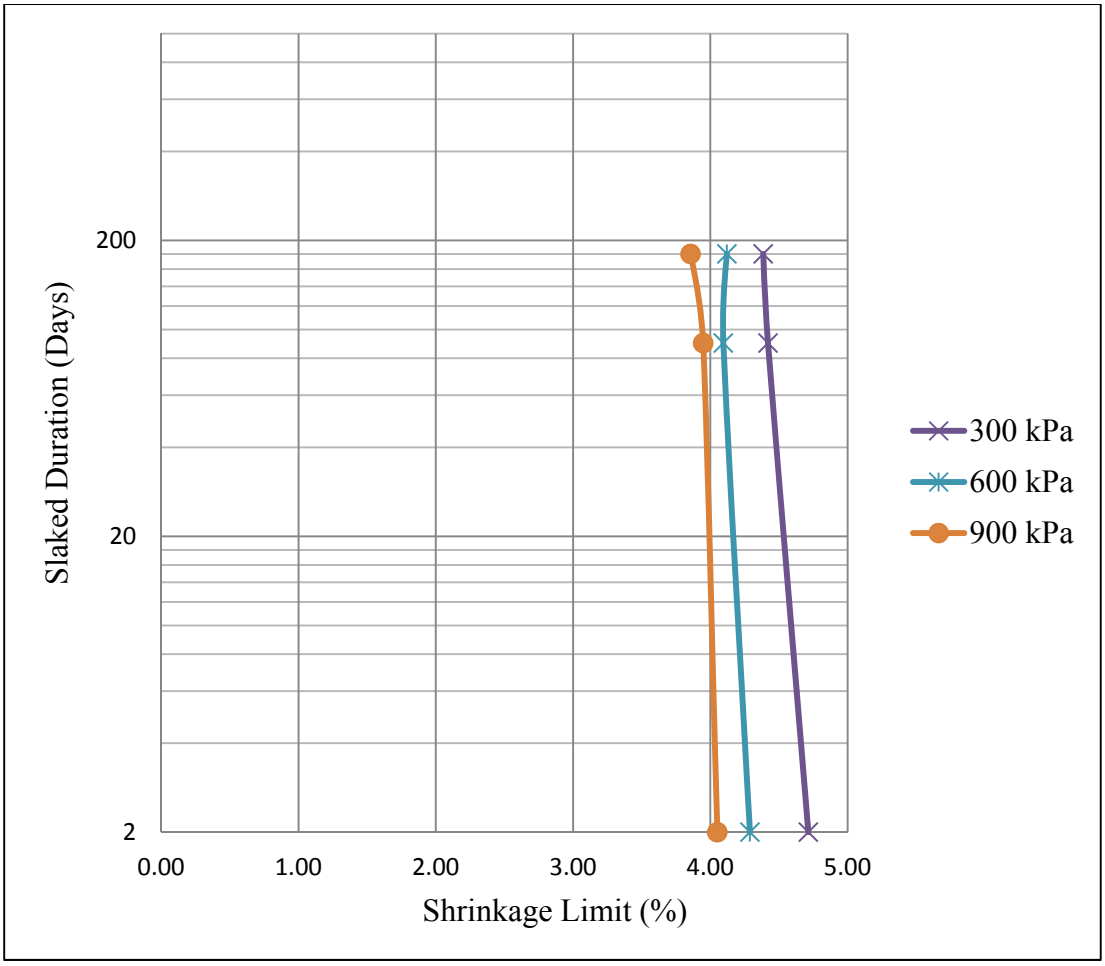


Figure 5.9 Variation of shrinkage limit of spoil with overburden pressure and time

In summary, the results obtained from the Atterberg limit tests and particle size distributions of ten spoil samples are encapsulated in table 5.2. The slaked spoil was classified according to the Australian unified soil classification system (Standard). From table 5.2, spoil sample 1 to 5 contained more than 50 per cent of coarse particles at a size of > 2.36mm and finer particles of less than 12 per cent at a size of < 0.075mm. In addition, table 5.2 demonstrates the plasticity index of spoil samples 1 to 5, more than four per cent. In that case, samples 1 to 5 were classified as Poorly Graded Gravels to Clayey Gravel (GP-GC). On the other hand, samples 6 to 10 contained approximately fifty per cent of coarse particles (bigger than 2.36mm) and

the plasticity index was more than 4% but fine particles increased more than 12 per cent. Therefore, sample 6 to 10 was classified as Clayey Gravel (GC), which is a mixture of gravel and a high proportion of fine sand and clay.

Table 5.2 Physical properties of slaked spoil samples

| Spoil Samples/ Properties | Sample 1 | Sample 2 | Sample 3 | Sample 4 | Sample 5 | Sample 6 | Sample 7 | Sample 8 | Sample 9 | Sample 10 |
|---|---|---|---|---|---|---|---|---|---|---|
| 0.075mm>(%) | 7.53 | 10.33 | 11.24 | 11.09 | 9.44 | 14.09 | 14.86 | 18.40 | 19.62 | 25.37 |
| (%)<2.36mm | 75.39 | 64.54 | 61.58 | 62.65 | 67.02 | 62.20 | 61.79 | 53.99 | 46.00 | 45.04 |
| D10 (mm) | 0.3 | 0.1 | 0.09 | 0.08 | 0.07 | 0.06 | .05 | 0.04 | 0.03 | 0.02 |
| D30 (mm) | 3 | 2 | 1.9 | 1.8 | 1.8 | 1.6 | 1.5 | 0.90 | 0.60 | 0.30 |
| D60 (mm) | 8 | 6.0 | 5.8 | 5.6 | 5.4 | 5.2 | 5.0 | 4.0 | 3.0 | 3.0 |
| Cc | 3.75 | 6.67 | 6.92 | 7.23 | 8.57 | 8.21 | 9.00 | 5.06 | 4.00 | 1.50 |
| Cu | 26.67 | 60.0 | 64.4 | 70.0 | 77.1 | 86.6 | 100 | 100 | 100 | 150 |
| Liquid Limit (%) | 34.09 | 33.98 | 33.37 | 32.96 | 33.21 | 32.81 | 32.74 | 31.91 | 32.01 | 32.11 |
| Plastic Limit (%) | 22.04 | 20.67 | 22.87 | 23.42 | 18.47 | 19.13 | 19.58 | 17.01 | 17.39 | 17.72 |
| Shrinkage Limit (%) | 4.86 | 4.71 | 4.29 | 4.05 | 4.42 | 4.10 | 3.95 | 4.39 | 4.12 | 3.86 |
| Plasticity Index (%) | 12.04 | 13.31 | 10.50 | 9.54 | 14.74 | 13.68 | 13.16 | 14.90 | 14.63 | 14.40 |
| USCS Classification | GP-GC | GP-GC | GP-GC | GP-GC | GP-GC | GC | GC | GC | GC | GC |

Where, $C_c$ = Coefficient curvature, $C_c = (D_{30})^2/(D_{10})(D_{60})$; $C_u$ = Coefficient Uniformity, $C_u = D_{60}/D_{10}$

## 5.4 EFFECTS OF SLAKING ON CHEMICAL PROPERTIES OF COAL MINE SPOIL

The influences of slaking on spoil minerals were determined by x-ray analysis of nine slaked and one fresh spoil sample.

Figure 5.10 presents combined XRD spectra of ten samples. The x-ray diffraction summarised result in table 5.3, indicated that quartz (SiO2) dominates

over all other minerals present in the spoils in the Bowen basin area. Other minerals present in the spoils of this area are:

- Albite ((Na,Ca)Al(Si,Al)3O8);
- Kaolin (Kaolinnite Al2Si25(OH)4);
- Muscovite (KAl2Si3AlO10(OH)2);
- Mixed layer illite;
- Anatase (TiO2);
- Siderite (FeCO3);
- Ankerite (Ca(Fe+2,Mg)(CO3)2);
- Coal and other organic carbon with non-diffracting amorphous content.

Kaolin, muscovite, and mixed layer Illite are common clay minerals. Albite, anatase, siderite, and ankerite are heavy metal minerals which are usually found as by-products in coal mines. From figure 5.10 and table 5.3 it is clear that there is no systematic change in clay minerals, quartz or other minerals content with overburden pressure and time. The quartz content in ten samples was a fairly constant after slaking, between 28.5 and 32 per cent. It made spoil materials chemically less reactive when in contact with water and when physically stable (Cadierno et al., 2014). Generally, samples with higher quartz content behave like sand and have no or low plasticity (Gotze, 2009). It is also verified by the result of the plastic limit of spoil samples. Moreover, it can be seen in Figure 5.11 that the other four crystalline rock minerals albite, ankerite, anatase and siderite exhibit small unsteady fluctuations which indicate experimental and sampling errors. There are no substantial changes in rock minerals due to slaking over the six month period.

It can be seen from figure 5.12 and table 5.3 that clay minerals, mixed layer Illite and muscovite changed due to slaking whereas kaoline (kaolinite) remained unchanged during six months of slaking. Generally, kaoline which is also termed as china clay has a stable structure and therefore, exhibits good crystalline morphology and is less reactive due to slaking (Chen et al., 2013; Murray, 1999; Murray, 2006). In the fresh spoil sample, the total amount of mixed layer illite was 21.71% by weight which gradually decreased with the increase in slaking time and overburden

pressure to 11.6% with some minor exemptions. Whereas, for muscovite, it was approximately 4.5% for the fresh sample (sample 1) and increased unsteadily with time and pressure. As can be seen in figure 5.12, the amount of kaoline was fairly constant and no significant change was observed. These changes in mineralogy indicate alteration of clay mineralogy structure due to hydrothermal reaction (Krinari, Khramchenkov, & Rakhmatulina, 2014).

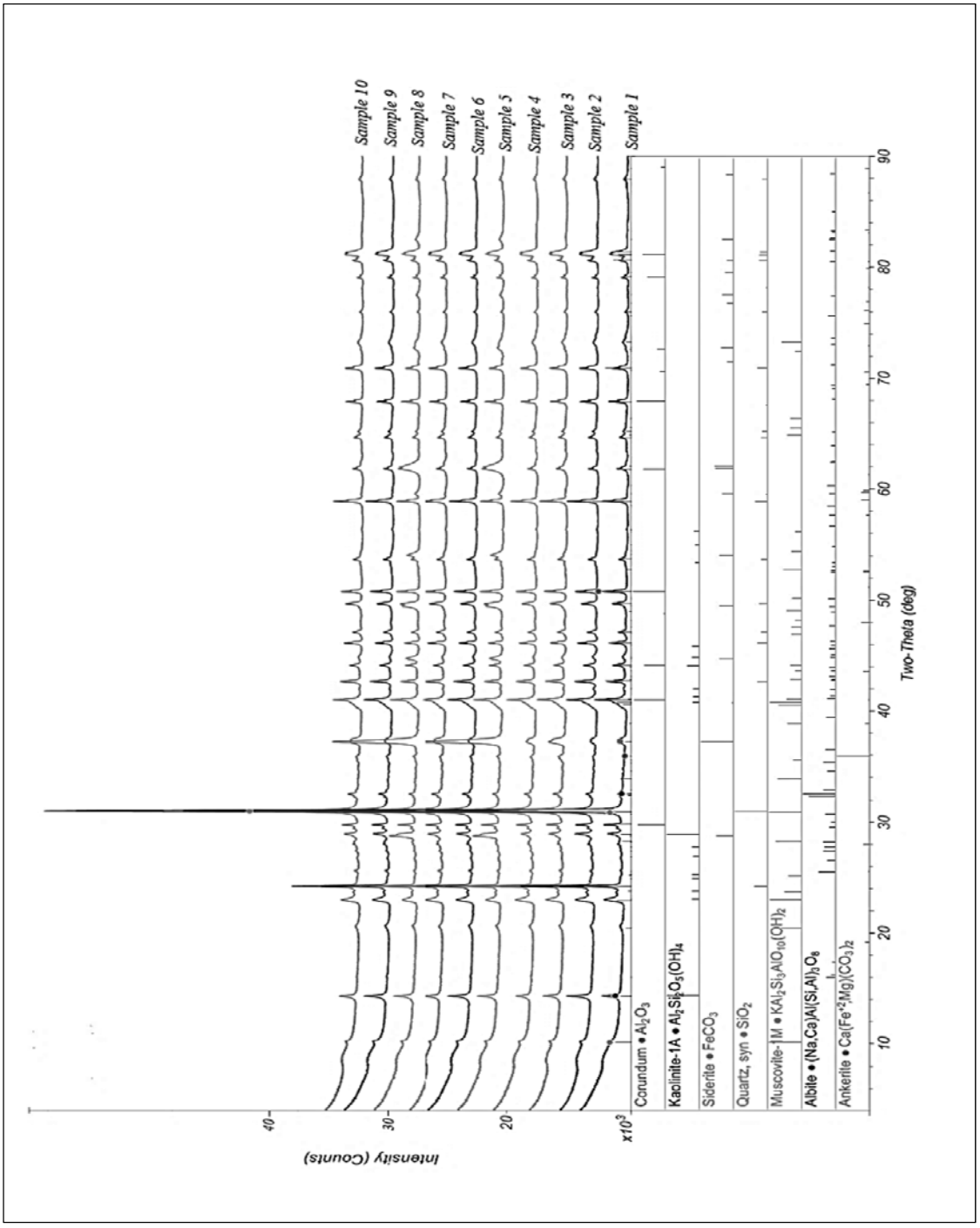


Figure 5.10 X- ray diffraction pattern of spoil samples

Table 5.3 Summary of minerals present in spoil samples (quantitative analysis)

| Spoil sample/ Minerals | Sample 1 | Sample 2 | Sample 3 | Sample 4 | Sample 5 | Sample 6 | Sample 7 | Sample 8 | Sample 9 | Sample 10 |
|---|---|---|---|---|---|---|---|---|---|---|
| Amorphous Clay Crystal | 18.50 | 22.85 | 26.91 | 26.48 | 27.72 | 29.56 | 31.77 | 32.51 | 26.49 | 25.57 |
| Quartz | 31.81 | 31.18 | 30.00 | 29.65 | 28.72 | 30.29 | 29.30 | 28.94 | 29.70 | 29.60 |
| Albite | 3.50 | 2.80 | 2.81 | 2.81 | 3.00 | 2.81 | 1.79 | 2.40 | 3.40 | 2.00 |
| Kaolin | 5.20 | 6.50 | 4.60 | 4.71 | 5.20 | 5.31 | 5.37 | 5.89 | 5.10 | 8.00 |
| Muscovite | 4.50 | 4.90 | 6.56 | 7.61 | 6.70 | 8.62 | 8.12 | 7.58 | 8.10 | 7.70 |
| Mixed layer Illite | 21.71 | 20.08 | 16.01 | 15.23 | 14.51 | 12.00 | 11.50 | 10.98 | 12.20 | 11.60 |
| Anatase | 0.20 | 0.30 | 0.00 | 0.20 | 0.20 | 0.40 | 0.42 | 0.20 | 0.40 | 0.40 |
| Siderite | 5.90 | 3.40 | 5.10 | 4.41 | 5.40 | 2.71 | 4.10 | 3.99 | 5.10 | 5.40 |
| Total Organic Carbon Content | 7.37 | 6.90 | 7.10 | 7.70 | 7.40 | 7.30 | 6.90 | 6.52 | 7.50 | 8.03 |
| Ankerite | 1.30 | 1.10 | 0.90 | 1.20 | 1.15 | 1.00 | 0.74 | 1.00 | 2.00 | 1.70 |

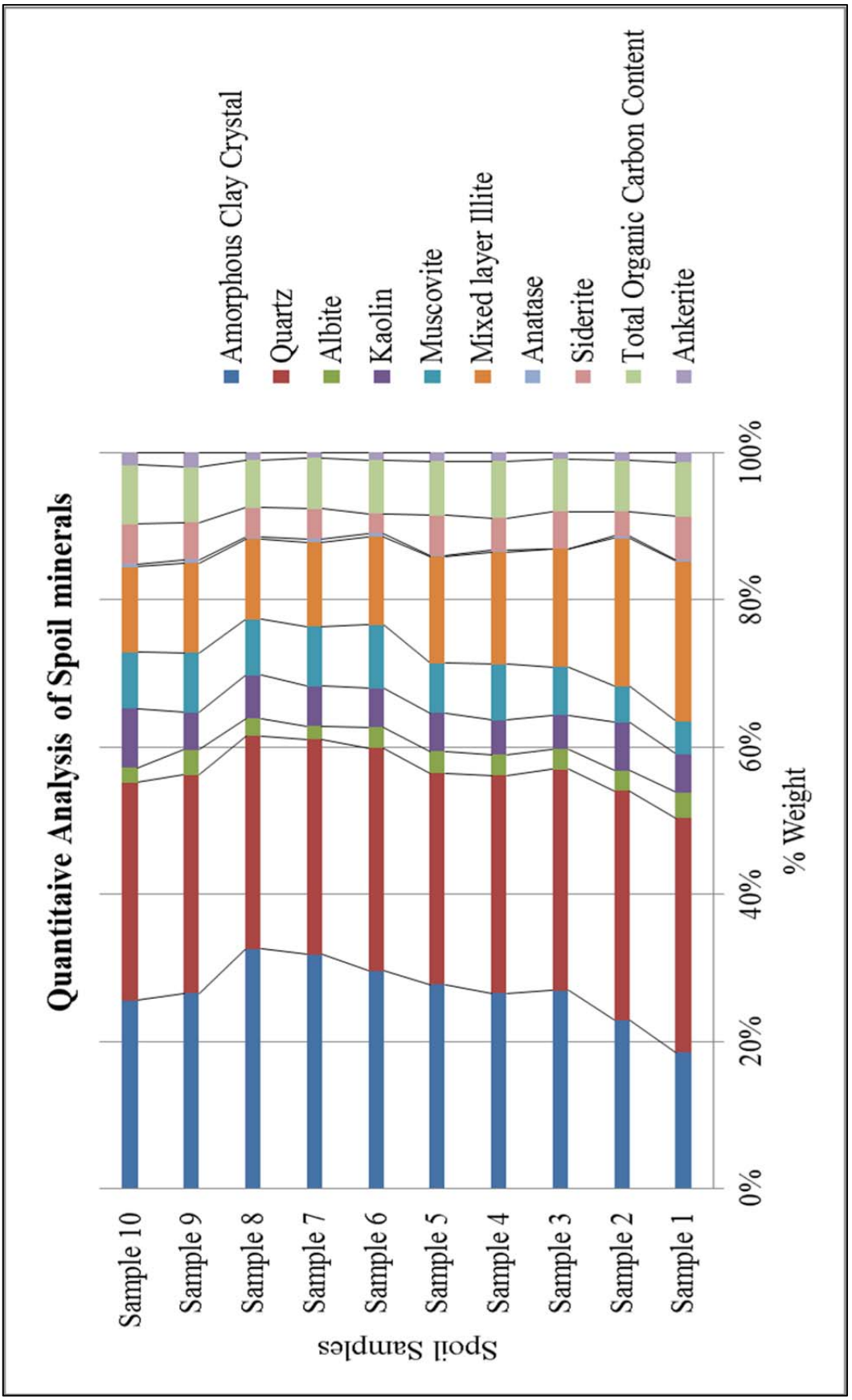


Figure 5.11 Mineralogical changes of spoil samples

In the XRD report, it was observed that every sample contained a substantial amount of amorphous content. The amount of amorphous content present in spoil samples was increased unsteadily due to slaking over time under different overburden pressures. Thermogravimetric analysis (TGA) was performed up to 1000°C for some spoil samples in order to investigate organic (Camby & Van Deventer, 1987) and inorganic carbon contents in samples. The graph shown in Figure 5.12 presents the typical result of TGA analysis for spoil sample 10. As can be observed from figure 5.13, the sample contained about 0.4 % moisture and other volatile impurities which evaporated slowly up to a temperature of 298.73˚ C. After that, organic carbon (including coal) was burnt rapidly between the temperature of 298.73˚ C and 703.28˚ C (Li, Whitely, Xu, & Pan, 2005). Total organic carbon including coal was about 8% for spoil sample 10 and a nearly similar result was obtained from randomly performed TGA of others samples. As a result, the changes in amorphous content shown in figure 5.12 are an indication of change in clays crystalline structure. Initially, the amount of non-diffracting content was about 18.5% increasing unsteadily to 32.51% over six months. In general, no significant change was observed in clay and minerals due to slaking spoils up to six months under different overburden pressures.

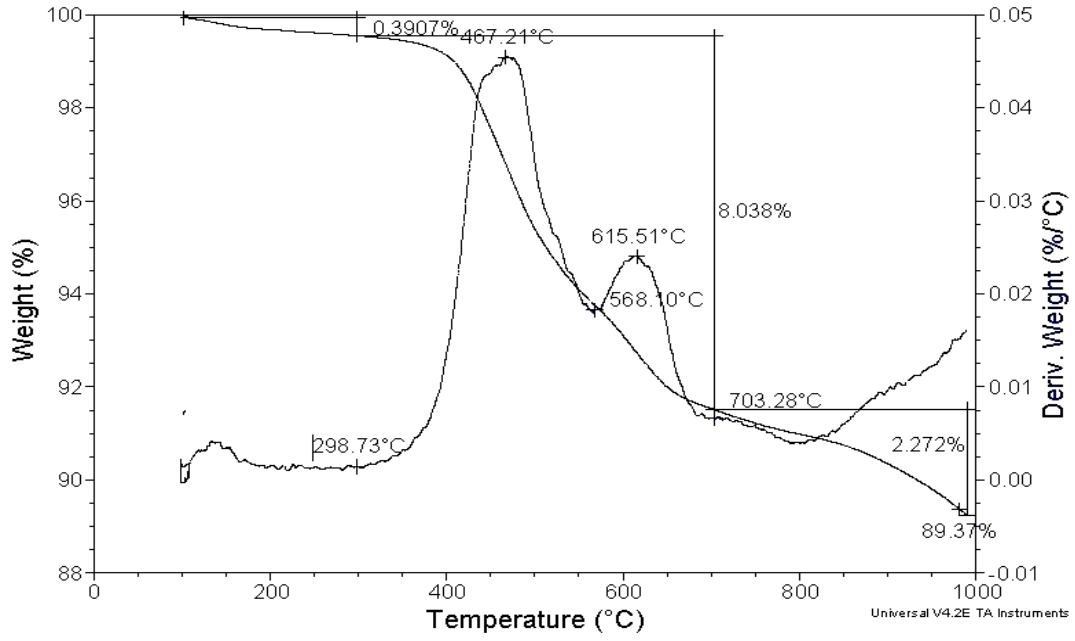


Figure 5.12 Typical result of TGA analysis of sample 10

## 5.5 EFFECTS OF SLAKING ON SHEAR STRENGTH PROPERTIES OF COAL MINE SPOIL

The influence of slaking on shear strength properties is important to investigate as they are directly related to spoil stability. In this study, both drained and undrained shear strength properties of 10 spoil samples (one fresh and nine slaked samples) were obtained by performing multi-stage consolidated undrained (with pore-water pressure measurement) triaxial tests as outlined in chapters three and four. In addition to the series of triaxial tests, a series of saturated direct shear tests were also conducted on spoil samples using particles smaller than 6.7 mm at a depth of 100mm x 100mm shear box was 45 mm.

### 5.5.1 Triaxial tests

The multistage consolidated undrained triaxial tests were performed on cylindrical spoil samples. Each test specimen of 100mm diameter and 200mm height was prepared to achieve a dry density of 18kN/m3 by wet compaction with initial moisture content of 10%. Once a specimen was enclosed in a 0.8 mm thick latex membrane, it was saturated to achieve B-value of above 0.95. Multistage triaxial tests were conducted in three stages with three different cell confining pressures of 500kPa, 600kPa and 700kPa and at the beginning of each stage back pressure was maintained at 300kPa. The effective confining pressures at the beginning of each stage were 200, 300 and 400kPa.

After consolidating the specimen for about two hours under drained conditions and stage one stress conditions (cell pressure ($\sigma_3$) = 500kPa and backpressure = 300kPa), it was sheared by applying monotonic vertical stress with a vertical strain rate of 0.05% per minute. The failure for each stage was assumed when maximum deviator stress ($\sigma_d$) was reached or 2% vertical strain (from the beginning of each loading stage) was achieved. Once the failure was reached for stage one, the applied vertical stress (deviator stress) was released and stage two stress conditions were applied (cell pressure, $\sigma_3$ = 700 kPa and backpressure = 300 kPa). The specimen was then consolidated under drained conditions for about two hours before shearing it under undrained conditions until above mentioned failure criteria was achieved. Then, following the same steps, stage three of the test was completed. Figure 5.13 illustrates the observed axial strain ($\varepsilon_a$) versus deviator stress

behaviour of a multi-stage triaxial testing of the spoil specimen prepared using Sample 9.

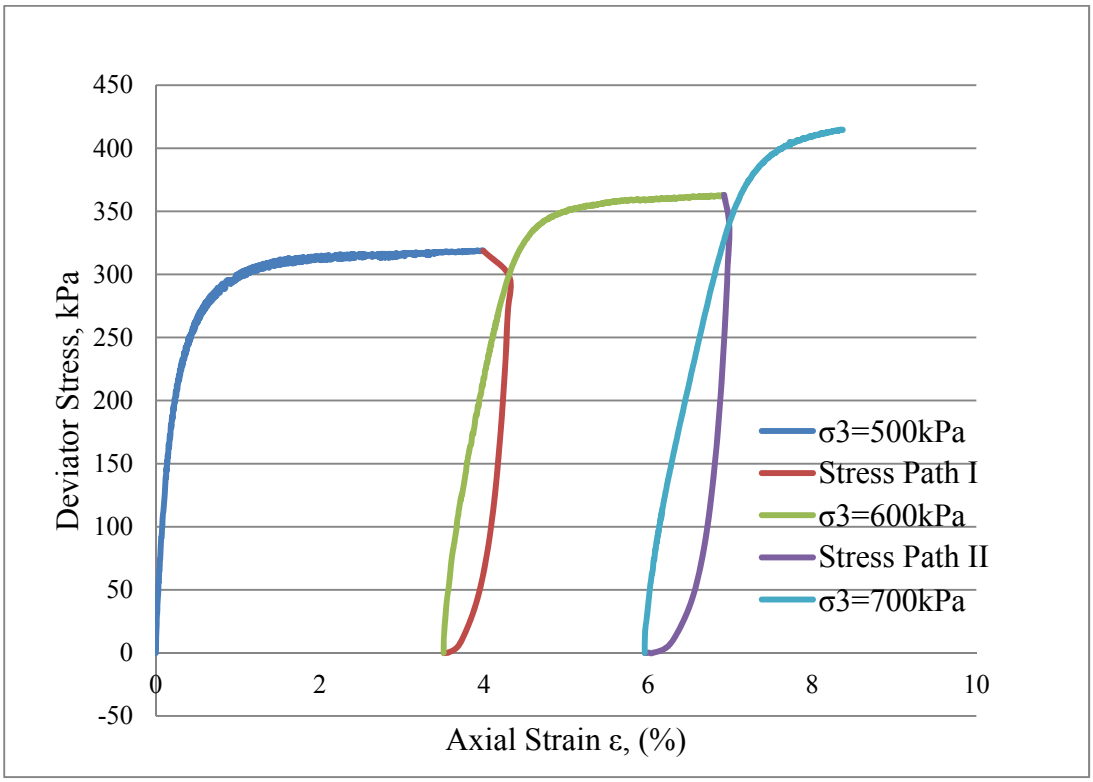


Figure 5.13 Variation of Deviator Stress versus axial strain for Spoil Sample 9

Figure 5.14 depicts the changes of excess pore pressure during shearing of the specimen (Sample 9) in all three stages under undrained conditions. It can be seen that the excess pore pressure increased as the sample is sheared under undrained conditions in each stage. In addition, the pore pressure graph provided an indirect check of experimental setup and membrane leakage which could affect the shearing strength parameters (Leroueil, Tavenas, La Rochelle, & Tremblay, 1990). Table 5.4 summarised deviator stress and pore pressure at the failure of each stage. The values tabulated in table 5.4 were obtained from Figure 5.13 and 5.15. Using these values and confining pressures for each stage, total and effective major principal stresses ($\sigma_1$ and $\sigma_1$') and total and effective minor principal stresses ($\sigma_3$ and $\sigma_3$') were computed.

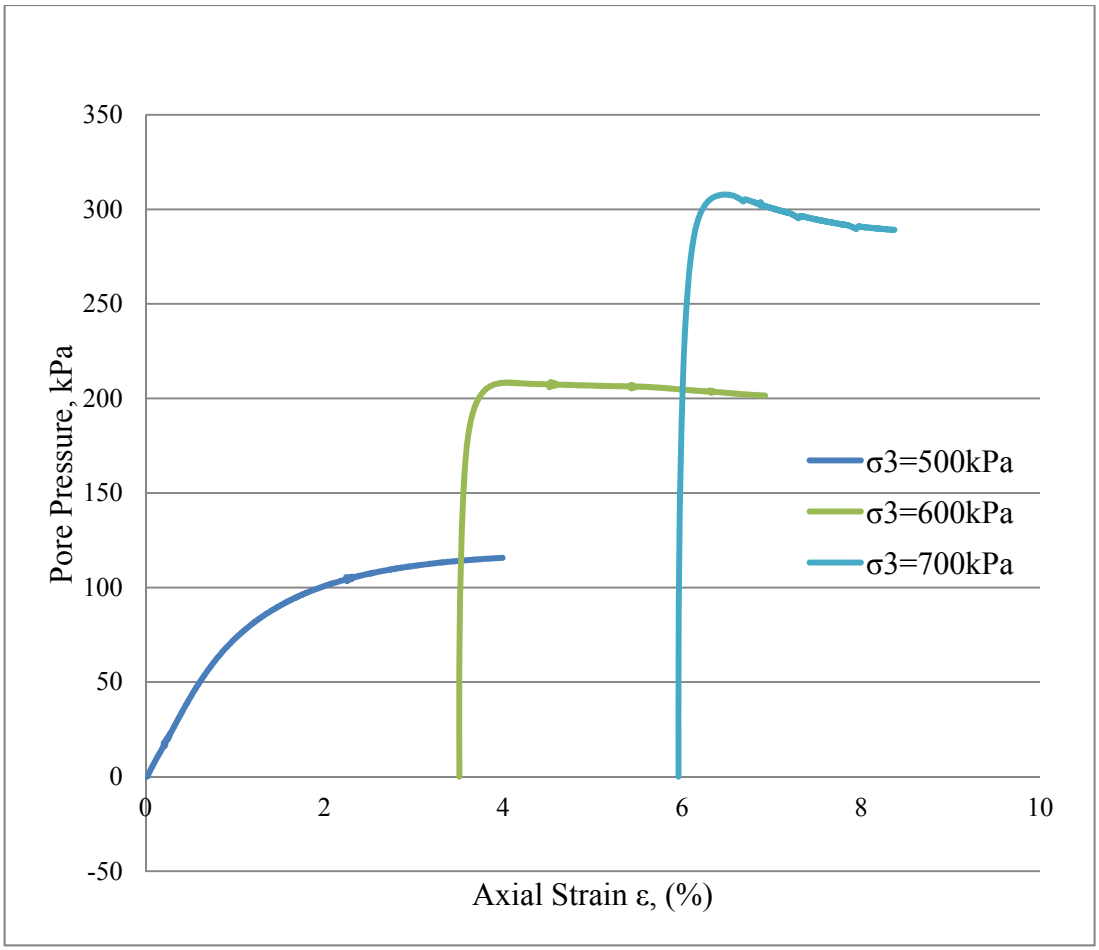


Figure 5.14 Variation of pore pressure versus axial strain for the specimen of spoil sample 9

Table 5.4 Stresses at failure of all stages of the specimen prepared using sample 9

| Stages | Con. Pressure, $\sigma_3$ | Deviator Stress, $\sigma_d$ | Pore Pressure | Excess Pore Pressure ($U_{ex}$) kPa | $\sigma_1$ | $\sigma_3'$ kPa | $\sigma_1'$ kPa | $(\sigma_1' + \sigma_3')/2$ kPa | $(\sigma_1' - \sigma_3')/2$ kPa |
|---|---|---|---|---|---|---|---|---|---|
| 1st | 500 | 313.64 | 401.92 | 101.93 | 813.64 | 98.08 | 411.73 | 254.90 | 156.82 |
| 2nd | 600 | 357.02 | 506.23 | 206.26 | 957.02 | 93.77 | 450.79 | 272.28 | 178.51 |
| 3rd | 700 | 409.28 | 590.75 | 290.76 | 1109.28 | 109.25 | 518.53 | 313.89 | 204.64 |

Using effective major (σ1') and minor (σ3') principal stresses at failures of all three stages tabulated in table 5.4, three Mohr-circles were drawn as shown in Figure 5.15. The Mohr-coulomb failure envelop was then drawn to obtain effective shear strength parameters: effective cohesion (c') and effective friction angle (ϕ').

The Mohr-circles for failure total principal stresses (σ1 and σ3) of each stage were plotted as shown in Figure 5.16 to obtain total (undrained) shear strength parameters (c and ϕ). To obtain these total stress Mohr-circles, the centre of corresponding effective stress Mohr-circle was moved away from the origin by the pressure value equal to the excess pore water pressure at the failure of the corresponding stage. Table 5.5 presents summarised multistage triaxial test data and stress calculations which were used in drawing Mohr-circles to obtain both effective and total shear strength parameters of soil samples. Table 5.6 summarises the shear strength properties of spoil samples obtained from multi-stage triaxial testing.

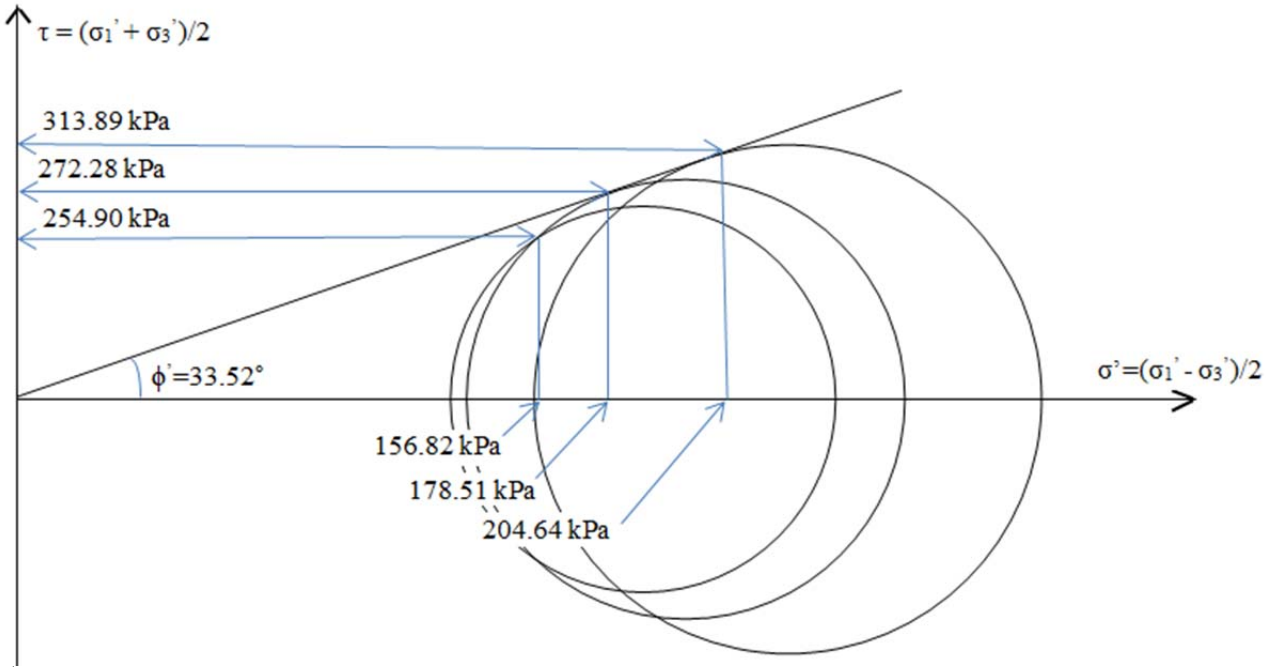


Figure 5.15 Effective Mhor's circle for sample 9

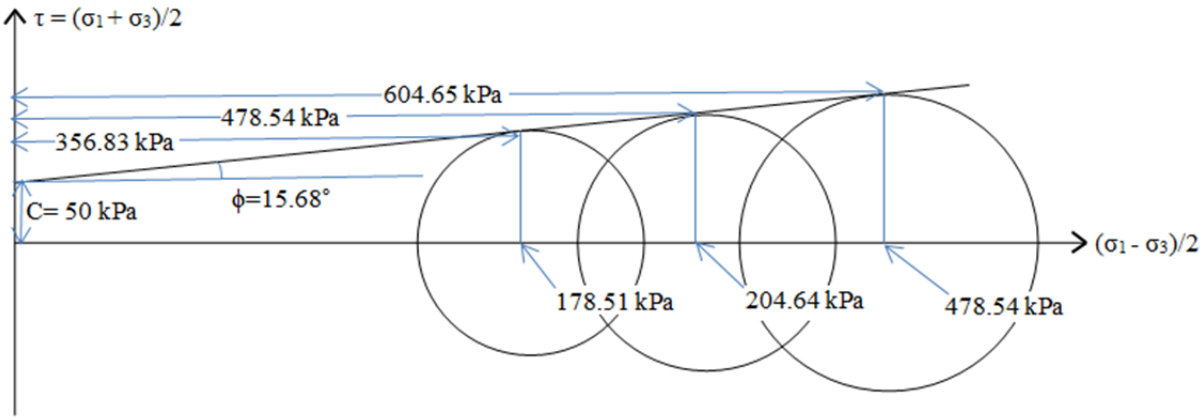


Figure 5.16 Mhor's circle for total stress of sample 9

Table 5.5 Summary of multistage triaxial test data at failure of all 10 specimens

| Samples | Con. Pressure, $\sigma_3$ | Deviator Stress, $\sigma_d$ | Back Pressure | Pore Pressure | Excess Pore Pressure ($U_{ex}$) kPa | $\sigma_1$ | $\sigma_3$', kPa | $\sigma_1$', kPa | $(\sigma_1' + \sigma_3')/2$ kPa | $(\sigma_1' - \sigma_3')/2$ kPa |
|---|---|---|---|---|---|---|---|---|---|---|
| Sample 1 | 350 | 141.52 | 295.00 | 311.00 | 16 | 491.52 | 40 | 181.52 | 110.76 | 70.76 |
| | 400 | 213.68 | 297.00 | 339.00 | 42 | 613.68 | 62 | 275.67 | 168.84 | 106.84 |
| | 450 | 295.40 | 301.00 | 362.00 | 61 | 745.40 | 88 | 383.41 | 235.7 | 147.7 |
| Sample 2 | 400 | 179.90 | 300.00 | 347.00 | 47 | 579.90 | 53 | 232.9 | 142.95 | 89.95 |
| | 500 | 257.18 | 303.00 | 418.00 | 115 | 757.18 | 83 | 340.18 | 211.59 | 128.59 |
| | 602 | 344.00 | 307.00 | 484.00 | 177 | 946.00 | 118 | 462 | 290 | 172 |
| Sample 3 | 695 | 282.22 | 298.00 | 574.00 | 276 | 977.22 | 121 | 403.23 | 262.11 | 141.11 |
| | 799 | 420.88 | 298.00 | 636.00 | 338 | 1219.88 | 163 | 583.89 | 373.44 | 210.44 |
| | 900 | 583.04 | 297.00 | 697.00 | 400 | 1483.04 | 203 | 786.04 | 494.52 | 291.52 |
| Sample 4 | 900 | 362.24 | 302.00 | 656.00 | 354 | 1262.24 | 244 | 606.25 | 425.12 | 181.12 |
| | 1000 | 736.34 | 300.00 | 735.00 | 435 | 1736.34 | 265 | 1001.33 | 633.17 | 368.17 |
| | 1100 | 1204.92 | 302.00 | 686.00 | 384 | 2304.92 | 414 | 1618.92 | 1016.46 | 602.46 |
| Sample 5 | 500 | 269.74 | 300.00 | 403.20 | 103.18 | 769.74 | 96.8 | 366.54 | 231.67 | 134.87 |
| | 600 | 329.58 | 300.00 | 496.97 | 196.86 | 929.58 | 103.03 | 432.61 | 267.82 | 164.79 |
| | 700 | 392.80 | 300.00 | 582.38 | 282.41 | 1092.80 | 117.63 | 510.42 | 314.03 | 196.40 |
| Sample 6 | 550 | 244.43 | 300.00 | 455.04 | 155.04 | 794.43 | 94.96 | 339.39 | 217.18 | 122.22 |
| | 600 | 306.20 | 300.00 | 503.85 | 203.85 | 906.20 | 96.15 | 402.35 | 249.25 | 153.10 |
| | 650 | 328.78 | 300.00 | 547.78 | 247.78 | 978.78 | 102.22 | 431.00 | 266.61 | 164.39 |
| Sample 7 | 500 | 304.56 | 300.00 | 388.51 | 88.51 | 804.56 | 111.49 | 416.05 | 263.77 | 152.28 |
| | 600 | 324.99 | 300.00 | 503.46 | 203.43 | 924.99 | 96.54 | 421.53 | 259.03 | 162.49 |
| | 700 | 345.43 | 300.00 | 603.50 | 303.5 | 1045.43 | 96.50 | 441.93 | 269.22 | 172.72 |
| Sample 8 | 500 | 279.18 | 300.00 | 403.06 | 103.03 | 779.18 | 96.94 | 376.11 | 236.53 | 139.59 |
| | 600 | 408.24 | 300.00 | 464.11 | 163.87 | 1008.24 | 135.89 | 544.13 | 340.01 | 204.12 |
| | 700 | 617.28 | 300.00 | 501.58 | 201.6 | 1317.28 | 198.42 | 815.69 | 507.06 | 308.64 |
| Sample 9 | 500 | 313.64 | 300.00 | 401.92 | 101.93 | 813.64 | 98.08 | 411.73 | 254.90 | 156.82 |
| | 600 | 357.02 | 300.00 | 506.23 | 206.26 | 957.02 | 93.77 | 450.79 | 272.28 | 178.51 |
| | 700 | 409.28 | 300.00 | 590.75 | 290.76 | 1109.28 | 109.25 | 518.53 | 313.89 | 204.64 |
| Sample 10 | 500 | 770.64 | 300.00 | 338.19 | 38.2 | 1270.64 | 161.81 | 932.46 | 547.13 | 385.32 |
| | 600 | 926.48 | 300.00 | 356.13 | 56.22 | 1526.48 | 243.87 | 1170.35 | 707.11 | 463.24 |
| | 700 | 1017.18 | 300.00 | 423.44 | 123.45 | 1717.18 | 276.56 | 1293.75 | 785.15 | 508.59 |

Table 5.6 Shear strength properties of spoil samples obtained from multi-stage triaxial tests

| Samples | Effective Cohesion, C' kPa | Effective friction angle, φ' (Degree) | Total Cohesion, C kPa | Total friction angle, φ (Degree) |
|---|---|---|---|---|
| Sample 1 | 1.00 | 38.62 | 12.00 | 26.98 |
| Sample 2 | 2.00 | 34.75 | 12.00 | 18.47 |
| Sample 3 | 2.00 | 33.29 | 10.00 | 15.83 |
| Sample 4 | 2.00 | 34.59 | 15.00 | 18.75 |
| Sample 5 | 2.00 | 34.74 | 20.00 | 17.05 |
| Sample 6 | 3.20 | 33.30 | 19.00 | 16.30 |
| Sample 7 | 4.00 | 33.83 | 30.00 | 16.90 |
| Sample 8 | 10.00 | 33.75 | 40.00 | 17.37 |
| Sample 9 | 20.00 | 33.52 | 50.00 | 15.68 |
| Sample 10 | 40.00 | 33.22 | 190.00 | 15.78 |

The effective shear strength parameter cohesion friction, varied from 1kPa to 40kPa and $38.62^0$ to $33.22^0$ due to slaking under different conditions (table 5.6). As can be seen from table 5.6, effective friction angle of spoil materials dropped due to slaking approximately $5.4^0$ from the initial fresh condition. Furthermore, effective cohesions were exhibited by gradual increment up to 90 days and after 180 days; it dramatically increased to 40kPa. For reduction of friction angle, both slaking time and overburden pressure played similar roles whereas for effective cohesion the increment slaking time played a dominate role. The undrained friction angle and cohesion presented in table 5.6 indicated a similar conclusion. Due to slaking, the

undrained friction angle for sample 2 was dropped to 18.47˚ from 26.98° (Sample 1). The friction angle gradually decreased with minor exemptions, with slaking time and overburden pressure which finally reached to 15.78° for spoil sample 10. The undrained cohesion gradually increased from 10kPa, sample 1 to 30kPa for sample 7. Then, it increased dramatically to 190kPa (sample 100). In fact, undrained cohesion was influenced dominantly by slaking duration. The result obtained from multistage triaxial tests are in a similar range obtained by others researchers with similar materials (Fityus, et al., 2008; Simmon & McManus, 2004; Ulusay, Arikan, & Yoleri, 1995).

### 5.5.2 Direct shear tests

In addition to triaxial tests, direct shear tests were performed on all 10 spoil samples to determine shear strength properties. The direct shear box which is a square (100 x 100 mm) with a depth of 47mm was employed in this study. Each spoil sample was sifted using a 6.7 mm sieve and tested as the maximum particle of testing material which should be 1/7 of the depth of the shear box according to Australian Standards (Standard, 1998). For each sample, four direct shear tests were conducted with vertical stresses of 100, 200, 300, 400 kPa. All samples were prepared by compacting spoil, with an initial water content of 10%, into the shear box to achieve the dry unit weight of 18kN/m$^3$. After saturation, each specimen was consolidated for about two hours under the specified vertical stress before shearing with the shear displacement rate of 0.002 mm/sec. Figure 5.17 presents the plots of shearing stress; shear displacement, vertical deformation, and shear displacement for all four specimens of each spoil sample. Considered was peak shear or shear stress at 12 mm shear displacement as the failure shear stress, failure shear stress versus normal stress were plotted for each spoil sample to obtain its drained (effective) shear strength parameter ($\phi$' and c'). In general, the failure shear stress increased and the specimen became more dilative with the increase in vertical stress. Shear strength parameters obtained for each spoil sample are tabulated in Table 5.7. As shown in Table 5.7, the effective friction angle ($\phi$') and effective cohesion (c') obtained from direct shear tests varied between 33.4° and 28.98° and 19.4kPa to 72.6kPa, respectively. The results obtained from direct shear tests were consistent but was slightly lower than the triaxial result (table 5.7). The particle size of direct shear test materials were smaller than triaxial test materials and that would be main reason for a difference

(Leonie Bradfield, 2013). The direct shear result was in the similar range obtained (Fityus, et al., 2008; Nakao & Fityus, 2008) by using direct shear apparatus on similar kinds of materials. From the shear strength parameters obtained from direct shear and triaxial testing (Table 5.6 and 5.7), it is clear that shearing strength reduces because of the slaking of spoils.

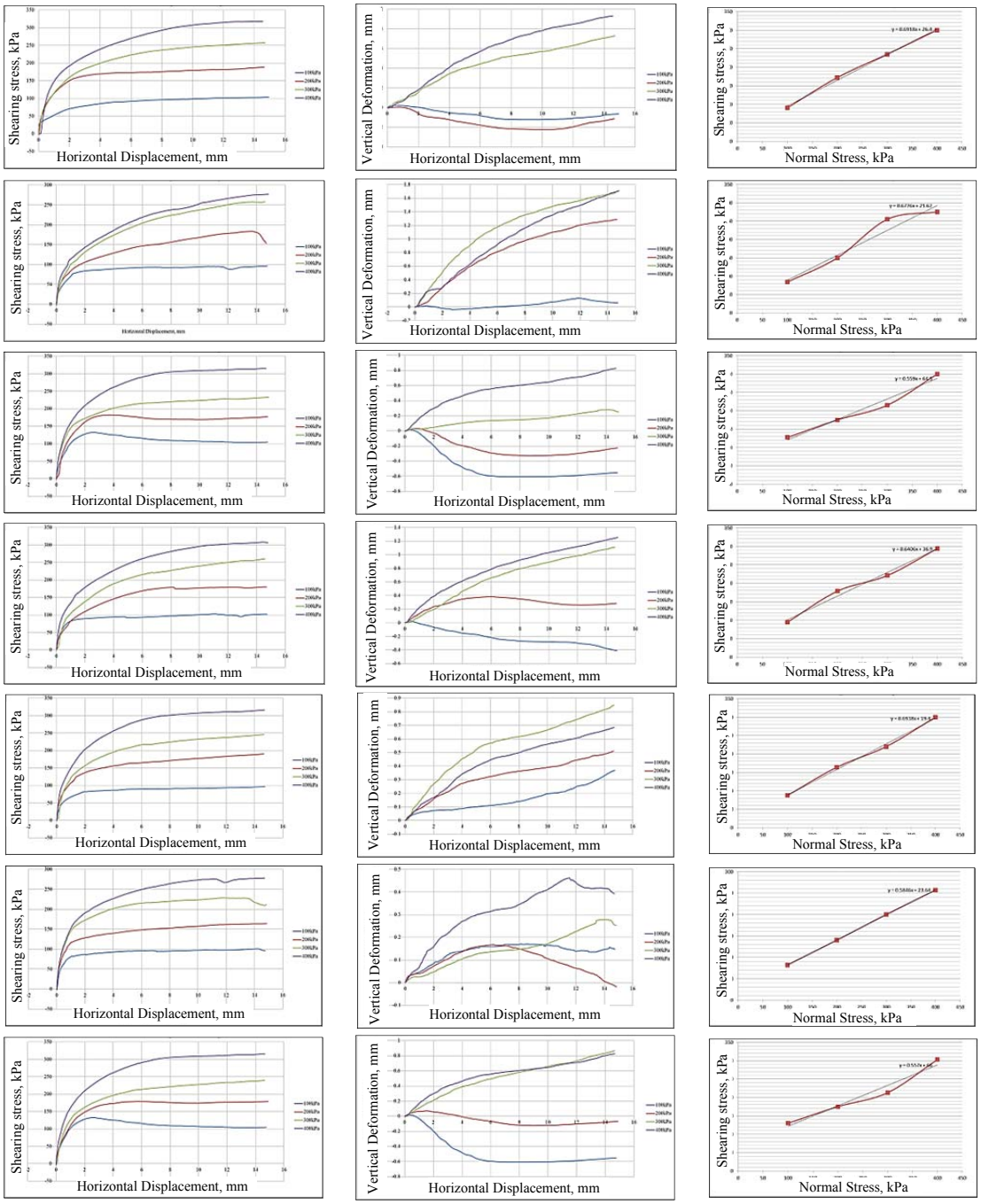

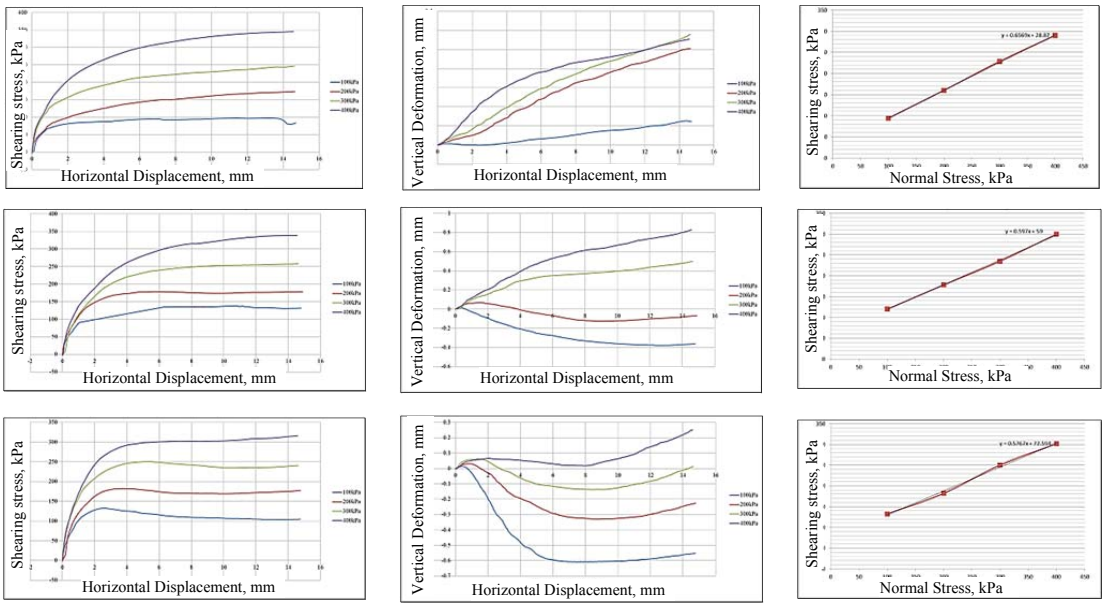


Figure 5.17 Graph plotted after direct shear test

Table 5.7 Summary of direct shear test results

| Sample | Normal Load (kPa) | Shearing Stress (kPa) | C´ kPa | φ´ deg |
|---|---|---|---|---|
| Sample 1 | 100 | 90.40 | 26.40 | 34.33 |
| | 200 | 172.00 | | |
| | 300 | 235.00 | | |
| | 400 | 300.00 | | |
| Sample 2 | 100 | 84.12 | 21.62 | 33.51 |
| | 200 | 150.00 | | |
| | 300 | 255.00 | | |
| | 400 | 275.00 | | |
| Sample 3 | 100 | 127.00 | 64.50 | 29.06 |
| | 200 | 175.00 | | |
| | 300 | 215.00 | | |
| | 400 | 300.00 | | |
| Sample 4 | 100 | 94.57 | 36.90 | 32.40 |
| | 200 | 178.66 | | |
| | 300 | 221.01 | | |
| | 400 | 294.00 | | |
| Sample 5 | 100 | 87.40 | 19.40 | 34.37 |
| | 200 | 164.00 | | |
| | 300 | 220.00 | | |
| | 400 | 300.00 | | |
| Sample 6 | 100 | 82.14 | 23.64 | 30.14 |
| | 200 | 140.00 | | |
| | 300 | 200.00 | | |
| | 400 | 257.00 | | |
| Sample 7 | 100 | 130.00 | 66.00 | 28.98 |
| | 200 | 175.00 | | |
| | 300 | 213.00 | | |
| | 400 | 303.00 | | |
| Sample 8 | 100 | 93.87 | 28.87 | 33.01 |
| | 200 | 160.00 | | |
| | 300 | 228.50 | | |
| | 400 | 290.00 | | |
| Sample 9 | 100 | 120.00 | 59.00 | 30.64 |
| | 200 | 178.00 | | |
| | 300 | 235.00 | | |
| | 400 | 300.00 | | |
| Sample 10 | 100 | 132.52 | 72.60 | 29.80 |
| | 200 | 182.14 | | |
| | 300 | 250.45 | | |
| | 400 | 302.00 | | |

## 5.6 EFFECTS OF SLAKING ON THE HYDRAULIC CONDUCTIVITY OF COAL MINE SPOIL

The influence of slaking on hydraulic conductivity was determined by the constant head permeability test. The graph (Figure 5.18) presents coefficient permeability of 10 spoil samples. It can be seen from the figure that permeability was higher for fresh spoil (sample one) which rapidly decreased to approximately $2.1\times10^{-06}$ m/sec for Sample two. Following, it decreased gradually (with some exemption) to $1.7\times10^{-08}$ m/sec for Sample 10.

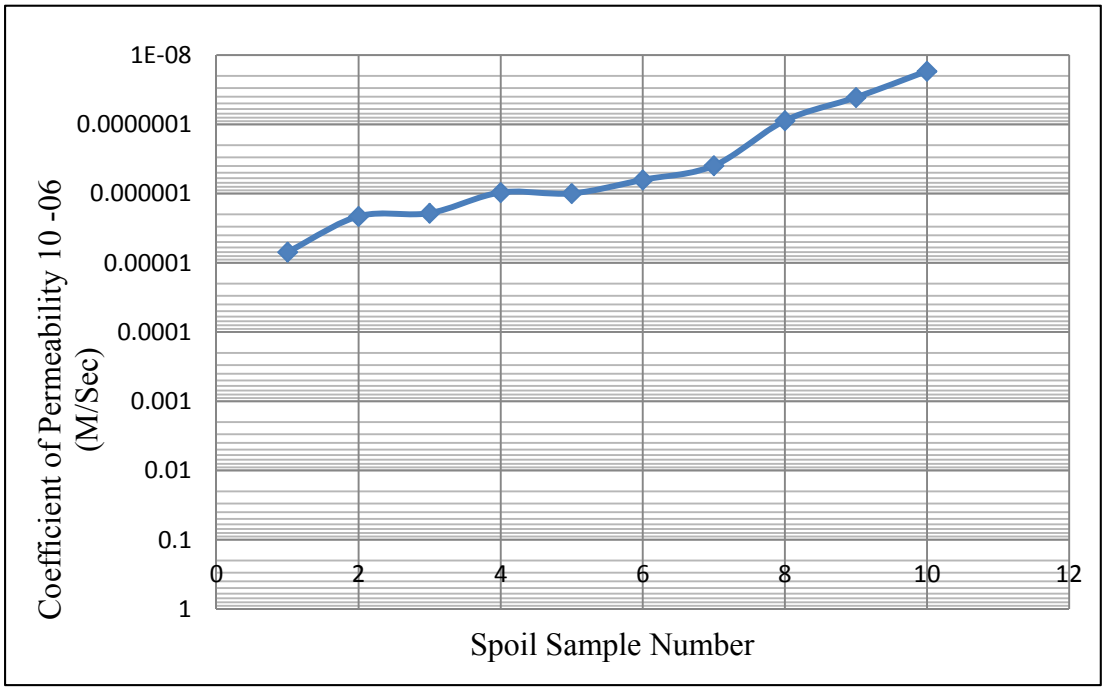


Figure 5.18 The variation coefficient of permeability (*k*) for slaked spoil samples

Figure 5.19 portrays the influence of overburden pressure and slaking time on permeability. It can be seen that the permeability decreases with an increase in overburden pressure as well as an increase in slaking time. Overburden pressure has a significant impact on permeability when it is slaked over a longer duration (e.g. 180 days). When the spoil is subjected to slaking over a long period for example, after 180 days of slaking, the permeability decreased from $0.884\times10^{-06}$ m/sec to $0.017\times10^{-06}$ m/sec (about 1/44), when the overburden pressure was increased from 300 to 900 kPa. For shorter slaking periods (e.g. two days), the permeability

decreases from 2.1 x $10^{-06}$ m/sec to 0.96 x $10^{-06}$ m/sec (about ½) when the overburden pressure increases from 300kPa to 900kPa.

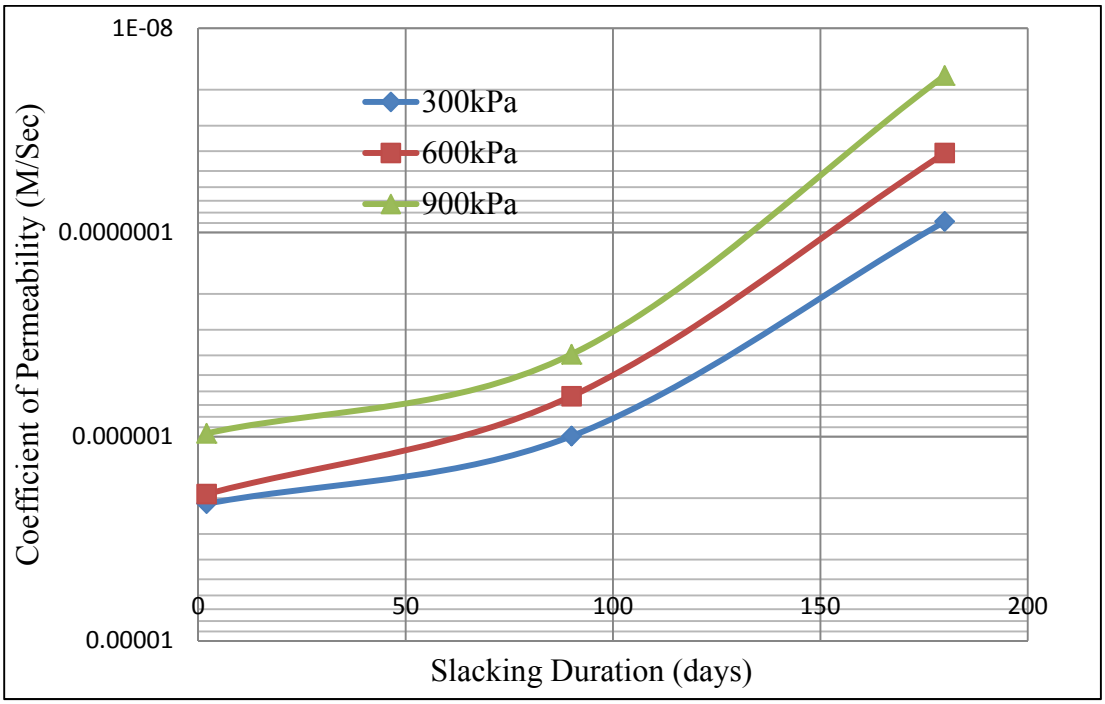


Figure 5.19 Influence of overburden pressure and time on spoil slaking

When the overburden pressure is increased, particles are crushed and compacted to decrease the volume of voids. The overburden pressure is maintained over a period of time. Spoil particles are further degraded by softened water and broken down in smaller fragments. As a result of the degradation of particle size the porosity decreased and the unit weight increased with time and overburden pressure. According to Kozeny-Carman, permeability or flow through of any sample is a function of unit weight, porosity and effective particle size (Taylor, 1948). Therefore, permeability decreases with increasing overburden pressure and slaking time. In brief, due to slaking over 180 days under different overburden pressures, spoil materials become low permeable gravel type materials from medium permeable (Terzaghi, Peck, & Mesri, 1996).

.

# Chapter 6: Conclusions and Recommendations

## 6.1 CONCLUSIONS

The extensive literature review revealed the consequences of the failure of spoil piles in open cut mining and suggested the slope failure of spoil pile base material as the main cause for the spoil pile failures. Further, it was observed that the spoil material was subjected to slaking over time when subjected to high pressure (overburden pressure) in saturated conditions. This highlighted the importance of using the mechanical properties (shear strength and hydraulic) of slaked spoil material when designing the spoil piles. The use of the properties of fresh spoil materials would overestimate the stability of the spoil pile and as a result, unexpected spoil pile failure would occur.

When measuring properties of slaked spoil, it is not feasible to take spoil samples which are subjected to different overburden pressures over different time periods. Therefore it is necessary to have a systematic method to slake spoil under controlled conditions in the laboratory. To fulfil this requirement, a pressure chamber was designed and manufactured for this study to slake spoil material under different pressures (up to 1000 kPa) over a period of time in saturated or unsaturated conditions. The pressure chamber consisted of an acrylic cylinder of 20 mm wall thickness with an internal diameter and height of 360 mm and 400 mm, respectively. The top and bottom plates (aluminium) were fastened by six bolts to seal the chamber. The chamber was able to accommodate approximately 60 kg of spoil allowing space for the piston plate.

To verify the applicability of the laboratory designed/manufactured pressure chambers to slake the mine spoil at the test site, coal mine spoil (Category 3) collected from a mine in the Bowen Basin in Queensland was subjected to different overburden pressures (300, 600, 900 kPa) and maintained over various time periods (two days, 90 days, and 180 days) under saturated conditions. This slaking program provided nine samples with different degrees of slaking. Each slaked spoil sample was tested for physical, chemical, and mechanical properties and the values were compared with those of fresh spoil samples and samples with different degrees of slaking. The results suggest the degradation of material properties as the degree of

slaking increases (increasing time and pressure). This verified the applicability of the pressure chambers developed in this study to slake the spoil under controlled parameters/conditions.

The LVDT attached to the vertical shaft of the piston in the pressure chamber measured the vertical deformation of the piston for each sample during the period when the pressure was sustained. The vertical downward movement was observed for all samples suggesting a volume decrease in all samples. The volume decrease (vertical settlement) could be caused by elastic deformation, consolidation settlement and particle breakdown (slaking). The elastic deformation is usually small and consolidated settlement should not be significant because the material is gravel. Therefore, the measured vertical deformation of the piston could be considered a good indication of spoil slaking. Sample 10 which was subjected to 900 kPa and maintained for 180 days gave the highest vertical deformation. The grainsize distribution curve of the samples confirmed that sample 10 had the greatest amount of particle breakage (slaking).

The physical properties (grain size distribution, Atterberg limits) of spoil samples (slaked samples) suggest that this category 3 soil material is not a highly slakable material. The amount of fines (particle smaller than 75μm in the fresh soil sample, sample 1) was about 8%. It increased to the maximum of 25% in sample 10 which was slaked over 180 days under 900 kPa overburden pressure. No significant increase in clay particles (particles smaller than 2μm) were observed in sample 10 compared to sample one (fresh spoil). As a result, no significant change in Atterberg limits was seen.

All 10 spoil samples were analysed (XRD) for minerals. Quartz, albite, kaolin, muscovite, mixed layer illite, anatase, siderite, ankerite, coal and other organic carbon with non-diffracting amorphous content, were identified as major minerals in this spoil material. From those minerals, only the amount of mixed layer illite, muscovite and non-diffracting amorphous were changed due to slaking of spoil material. Mixed layer illite was 21.7% in fresh spoil sample (sample one) which dropped to 11.6% in sample 10, slaked over 180 days maintaining an overburden pressure of 900 kPa. Whereas muscovite and amorphous contents increased by about 2.2% and 7.0%, respectively in sample 10 compared to fresh sample (sample 1).

The shear strength properties of spoil samples were obtained from consolidated undrained triaxial tests and direct shear tests. The undrained shear strength parameters from triaxial tests revealed that the material strength of spoil materials, category type 3 was medium to low with small cohesion, which were in similar range observed by other researchers (Simmon & McManus, 2004; Ulusay, Arikan, & Yoleri, 1995). Triaxial tests on fresh spoil gave effective friction angle of $38.6^0$, undrained friction angle of $27^0$, effective cohesion of 1 kPa, and undrained cohesion of 12 kPa. Due to slaking of spoil material over six months under 900 kPa overburden pressure, the effective friction and undrained friction angles decreased by 5.4˚ and 11.2°, respectively. The effective and total cohesion increased by 40 kPa and 170 kPa, respectively. Direct shear tests were conducted on each sample using particles passing through a 6.7 mm sieve. The results gave an effective friction angle and cohesion of fresh spoil as 34° and 26.4 kPa, respectively. The slaking caused a decrease effective friction angle by 4.5° and an increase in effective cohesion by 46.2 kPa.

The constant head permeability test results indicated a reduction in hydraulic conductivity due to slaking. The permeability property for fresh spoil was $6.99 \times 10^{-06}$ m/sec and dropped rapidly for short termed slaked spoil samples with pressure. After six months of slaking, the effect of overburden pressure became insignificant and the permeability coefficient dropped to approximately$1.70 \times 10^{-08}$ m/sec.

## 6.2 RECOMMENDATIONS

Based on the outcomes of this research, the following is recommended as future research studies that will enhance the practical applications of the outcomes of this study:

- It has been noticed that mine operations are sometimes stopped for a maximum period of one year or more before resuming operations. During this period, the saturated base spoil pile materials can slake under the overburden pressure applied by the self-weight of spoil pile. Therefore, it is recommended to extend this study to slake the spoil material for a period of one year or more under different overburden pressures and testing the slaked materials for chemical, physical, and mechanical properties.

- Further, it is recommended to perform similar studies on other types of spoil materials (category 1 and 2) and spoil materials from different mines in the same region to develop a database.
- In this research study, the spoil was subjected to slaking under saturated conditions throughout the whole period. However, in reality base spoil pile material can be subjected to drying (de-watering, draught) and wetting (ground water, rainfall) over the period under the same overburden pressure. Therefore, it is recommended to investigate the effects of cyclic drying-wetting of spoil on its slaking.
- It has been observed that most spoil piles fail due to the slippage of foundation spoil during filling and de-watering of the mine pit. Therefore, it is important to specify the spoil pile height, slope angle, and dewatering rate to make the spoil pile safe. This can be done by developing stability charts based on numerical stability analyses of spoil piles (e.g. using SLOPE/W and SEEP/W) by taking saturated /unsaturated shear strength and permeability properties of slaked spoil materials. It is recommended analysis occur to develop stability charts to help the mining geotechnical engineers to design safe spoil piles.
- When analysing stability of spoil pile stability during de-watering, the transient nature of the material condition (saturated to unsaturated) has to be considered. Therefore, it is important to conduct a study to measure the unsaturated properties such as shear strength, permeability function, and soil-water characteristic curve of slaked spoil materials.
- It is recommended to use a large direct shear apparatus (at least 150 mm x 150 mm x 150 mm shear box) when measuring shear strength of spoil materials to be used for the analysis for slope stability of spoil piles. Triaxial tests are more complicated and time consuming to perform. However, direct shear tests closely simulate the shear failure mechanism of a slope.

# References


Aksoy, C. O. (2005). Minimizing the economic unit cost of dragline-truck-shovel operations at Yatagan-Eskihisar open pit mine, Turkey. *CIM Bulletin, 98*(1088), 94. Retrieved from ProQuest Central.

Australian Coal. (2015). Retrieved from Australians for coal, http://www.australiansforcoal.com.au/coal-4-jobs.html

Bareither, C., Edil, T., Benson, C., & Mickelson, D. (2008). Geological and Physical Factors Affecting the Friction Angle of Compacted Sands. *Journal of Geotechnical and Geoenvironmental Engineering, 134*(10), 1476-1489.

Blight, G. E., & Fourie, A. B. (2005). Catastrophe revisited – disastrous flow failures of mine and municipal solid waste. *Geotechnical and Geological Engineering, 23*(3), 219-248.

BMA. Caval Ridge Coal Mine Project.

Bowen Basin Coal Mines and Coal Projects map with workforce (Quarter 2 2013). (2013).

Brandon, T., Duncan, J., & Gardner, W. (1990). Hydrocompression Settlement of Deep Fills. *Journal of Geotechnical Engineering, 116*(10), 1536-1548.

Bruno, G. (Singer-songwriter). (2015). Angular Unconformity at Telheiro Beach, Portugal. On. http://epod.usra.edu/blog/2015/01/angular-unconformity-at-telheiro-beach-portugal.html: Universities Space Research Association (USRA).

Cadierno, J., Romero, M., Valdés, A., del Pozo, J. M., González, J., Robles, D., & Espinosa, J. (2014). Characterization of Colliery Spoils in León: Potential Uses in Rural Infrastructures. *Geotechnical and Geological Engineering, 32*(2), 439-452.

Cai, F., Ugai, K., Wakai, A., & Li, Q. (1998). Effects of horizontal drains on slope stability under rainfall by three-dimensional finite element analysis. *Computers and Geotechnics, 23*(4), 255-275.

Camby, B. S., & Van Deventer, J. S. J. (1987). The use of TGA to estimate the loading of organics on activated carbon. *Thermochimica Acta, 113*(0), 341-350.

Campbell, G. D. (2005). *Cloud Break Deposit Geochemical Characterisation of Mine-waste Samples*

*(Static Testwork): Implications for Mine-Waste Management. Fortescue Metals Group Ltd.*

Cheeks, J. (1996). Settlement of Shallow Foundations on Uncontrolled Mine Spoil Fill. *Journal of Performance of Constructed Facilities, 10*(4), 143-151.

Chen, N.-s., Lu, Y., Deng, M.-f., Han, D.-w., Zhou, H.-b., & Yang, C.-l. (2013). Comparative study on debris flow initiation in limestone and sandstone spoil. *Journal of Mountain Science, 10*(2), 190-198. Retrieved from ProQuest Central.

Clarke, D., & Smethurst, J. A. (2010). Effects of climate change on cycles of wetting and drying in engineered clay slopes in England. *Quarterly Journal of Engineering Geology and Hydrogeology, 43*(4), 473-486.

Coffin, L. (2013). *Sedimentology, stratigraphy and petrography of the Permian-Triassic coal-bearing New Lenton deposit, Bowen Basin, Australia* MR86031(M.Sc.). University of Ottawa (Canada), Ann Arbor.

Coggan, J., Gao, F., Stead, D., & Elmo, D. (2012). Numerical modelling of the effects of weak immediate roof lithology on coal mine roadway stability. *International Journal of Coal Geology, 90–91*(0), 100-109.

Crespo Marquez, A. (2005). Modeling critical failures maintenance: a case study for mining. *Journal of Quality in Maintenance Engineering, 11*(4), 301-317.

de Rooij, G. H. (2004). Methods of Soil Analysis. *Vadose Zone Journal, 3*(2), 722.

Dehn, M., Bürger, G., Buma, J., & Gasparetto, P. (2000). Impact of climate change on slope stability using expanded downscaling. *Engineering Geology, 55*(3), 193-204.

Donzé, F. V., Bouchez, J., & Magnier, S. A. (1997). Modeling fractures in rock blasting. *International Journal of Rock Mechanics and Mining Sciences, 34*(8), 1153-1163.

Eckersley, J. D. (1985). Flowslides in stockpiled coal. *Engineering Geology, 22*(1), 13-22.

Effects of Particle Size Distribution on Shear Strength of Accumulation Soil. (2013). *Journal of Geotechnical and Geoenvironmental Engineering, 139*(11), 1994-1997.

Erguler, Z. A., & Shakoor, A. (2009). Quantification of Fragment Size Distribution of Clay-Bearing Rocks after Slake Durability Testing. *Environmental & Engineering Geoscience, XV*(2), 81-89.

Erguler, Z. A., & Ulusay, R. (2009). Assessment of physical disintegration characteristics of clay-bearing rocks: Disintegration index test and a new durability classification chart. *Engineering Geology, 105*(1–2), 11-19.

Fityus, S., Hancock, G., & Wells, T. (2008). Geotechnical characteristics of coal mine spoil. *Australian Geomechanics*.

Fu, W., & Liao, Y. (2010). Non-linear shear strength reduction technique in slope stability calculation. *Computers and Geotechnics, 37*(3), 288-298.

García Bastante, F., Alejano, L., & González-Cao, J. (2012). Predicting the extent of blast-induced damage in rock masses. *International Journal of Rock Mechanics and Mining Sciences, 56*(0), 44-53.

Gasmo, J. M., Rahardjo, H., & Leong, E. C. (2000). Infiltration effects on stability of a residual soil slope. *Computers and Geotechnics, 26*(2), 145-165.

Gautam, T. P., & Shakoor, A. (2013). Slaking behavior of clay-bearing rocks during a one-year exposure to natural climatic conditions. *Engineering Geology, 166*(0), 17-25.

Ghose, M. K., & Kundu, N. K. (2004). Deterioration of soil quality due to stockpiling in coal mining areas. *International Journal of Environmental Studies, 61*(3), 327-335.

Gökceoğlu, C., Ulusay, R., & Sönmez, H. (2000). Factors affecting the durability of selected weak and clay-bearing rocks from Turkey, with particular emphasis on the influence of the number of drying and wetting cycles. *Engineering Geology, 57*(3–4), 215-237.

Gotze, J. (2009). Chemistry, textures and physical properties of quartz - geological interpretation and technical application. *Mineralogical Magazine, 73*(4), 645-671.

Hamdi, E., Bouden Romdhane, N., du Mouza, J., & Le Cleac'h, J. (2008). Fragmentation Energy in Rock Blasting. *Geotechnical and Geological Engineering, 26*(2), 133-146.

Hem, P. (Singer-songwriter). (November 2012). Showing bench, ramp, overall slope and their respective angles. On: Norman B. Keevil Institute of Mining Engineering - University of British Columbia.

Hendrychová, M., Šálek, M., Tajovský, K., & Řehoř, M. (2012). Soil Properties and Species Richness of Invertebrates on Afforested Sites after Brown Coal Mining. *Restoration Ecology, 20*(5), 561-567.

Highland, L., Ellen, S. D., Christian, S. B., & Brown III, W. M. (1997). *Debris-flow hazards in the United States*: US Department of the Interior, US Geological Survey Denver, CO, USA.

Highter, W. H., & Tobin, R. F. (1980). Flow slides and the undrained brittleness index of some mine tailings. *Engineering Geology, 16*(1–2), 71-82.

Highter, W. H., & Vallee, R. P. (1980). The liquefaction of different mine tailings under stress-controlled loading. *Engineering Geology, 16*(1–2), 147-150.

Howladar, M. F. (2013). Coal mining impacts on water environs around the Barapukuria coal mining area, Dinajpur, Bangladesh. *Environmental Earth Sciences, 70*(1), 215-226.

Indraratna, B. (1994). The effect of normal stress-friction angle relationship on the stability analysis of a rockfill dam. *Geotechnical & Geological Engineering, 12*(2), 113-121.

Iverson, R. M. (1997). The physics of debris flows. *Reviews of Geophysics, 35*(3), 245.

Jhanwar, J. C., & Thote, N. R. (2011). Slope Failures in the Opencast Coal Mines of Wardha Valley Coalfield in Central India: A Study. *Rock Mechanics and Rock Engineering, 44*(5), 635-640.

Jiang, H., Wang, B., Inyang, H. I., Liu, J., Gu, K., & Shi, B. (2013). Role of expansive soil and topography on slope failure and its countermeasures, Yun County, China. *Engineering Geology, 152*(1), 155-161.

Kaiser, P. K., & Hewitt, K. J. (1983). Effect of groundwater flow on the stability and design of retained excavations : Can Geotech J, V19, N2, May 1982, P139–

153. *International Journal of Rock Mechanics and Mining Sciences & Geomechanics Abstracts, 20*(1), A22.

Kalinski, M. E., Karem, W. A., & Little, L. M. (2010). Estimating hydrocompression potential of mine spoils from a site in eastern Kentucky using dry unit weight and moisture content. *International Journal of Mining, Reclamation and Environment, 24*(4), 350-362.

Karem, W. A., Kalinski, M. E., & Hancher, D. E. (2007). Settlement of Mine Spoil Fill from Water Infiltration: Case Study in Eastern Kentucky. *Journal of Performance of Constructed Facilities, 21*(5), 345-350.

Karfakis, M. G., Bowman, C. H., & Topuz, E. (1996). Characterization of coal-mine refuse as backfilling material. *Geotechnical & Geological Engineering, 14*(2), 129-150.

Kayabasi, A., & Gokceoglu, C. (2012). Coal mining under difficult geological conditions: The Can lignite open pit (Canakkale, Turkey). *Engineering Geology, 135–136*(0), 66-82.

Kim, D., & Ha, S. (2014). Effects of Particle Size on the Shear Behavior of Coarse Grained Soils Reinforced with Geogrid. *Materials, 7*(2), 963-979.

Krinari, G. A., Khramchenkov, M. G., & Rakhmatulina, Y. S. (2014). Changes in the structures of mixed-layer illite-smectite during flooding of terrigenous oil reservoirs. *Russian Geology and Geophysics, 55*(7), 915.

Kusuma, G. J., Shimada, H., Sasaoka, T., Matsui, K., Nugraha, C., Gautama, R. S., . . . 松井紀久男. (2012). Physical and Geochemical Characteristics of Coal Mine Overburden Dump Related to Acid Mine Drainage Generation. *Memoirs of the Faculty of Engineering, Kyushu University, 72*(2), 23-38.

Lau, K. C., & Kenney, T. C. (1984). Horizontal drains to stabilize clay slopes. *Canadian Geotechnical Journal, 21*(2), 241-249.

Leonie Bradfield, J. S., Stephen Fityus. (2013). *Issues related to stability design of very high spoil dumps*. Paper presented at Coal Operators' Conference

Leroueil, S., Tavenas, R., La Rochelle, P., & Tremblay, M. (1990). Influence of filter paper and leakage on triaxial testing. *International Journal of Rock Mechanics and Mining Sciences and Geomechanics Abstracts, 27*(6), 334-334.

Li, S., Whitely, N., Xu, W., & Pan, W.-P. (2005). Characterization of Coal by Thermal Analysis Methods.

Li, Y. (2013). Effects of particle shape and size distribution on the shear strength behavior of composite soils. *Bulletin of Engineering Geology and the Environment, 72*(3), 371-381.

M Mohammadnejad, R. G., A Ramezanzadeh, ME Jalali. (2011). Prediction of blast-induced vibrations in limestone quarries using Support Vector Machine. *Journal of Vibration and Control, 18*(9), 1322–1329.

Mohamad Nor, O., Abbiss, C. P., Mohd. Raihan, T., & Khairul Anuar Mohd, N. (2011). Prediction of long-term settlement on soft clay using shear wave velocity and damping characteristics. *Engineering Geology, 123*(4), 259-270.

Mohammed, M. M. (1997). *Effects of groundwater on stability of rock and soil slopes* MQ37275(M.Eng.). McGill University (Canada), Ann Arbor. Retrieved from ProQuest Dissertations & Theses Global database.

Mokhov, A. V. (2011). Mine water drainage from flooded coal mines. *Doklady Earth Sciences, 438*(2), 733-735.

Molotilov, S. G., Cheskidov, V. I., Norri, V. K., Botvinnik, A. A., & Ils'buls'din, D. K. (2010). Methodical principles for planning the mining and loading equipment capacity for open cast mining with the use of dumpers. Part III: Service capacity determination. *Journal of Mining Science, 46*(1), 38-49.

Monjezi, M., Amiri, H., Farrokhi, A., & Goshtasbi, K. (2010). Prediction of Rock Fragmentation Due to Blasting in Sarcheshmeh Copper Mine Using Artificial Neural Networks. *Geotechnical and Geological Engineering, 28*(4), 423-430.

Murray, H. H. (1999). Applied clay mineralogy today and tomorrow. *Clay Minerals, 34*(1), 39-39.

Murray, H. H. (2006). *Applied clay mineralogy: occurrences, processing and applications of kaolins, bentonites, palygorskite-sepiolite, and common clays* (Vol. 2): Elsevier Science.

Nakao, T., & Fityus, S. (2008). Direct Shear Testing of a Marginal Material Using a Large Shear Box. *Geotechnical Testing Journal, 31*(5), 1-11.

Nguyen, V. U., & Chowdhury, R. N. (1984). Probabilistic study of spoil pile stability in strip coal mines—Two techniques compared. *International Journal of*

*Rock Mechanics and Mining Sciences & Geomechanics Abstracts, 21*(6), 303-312.

Okagbue, C. O. (1984). The geotechnical characteristics and stability of a spoil heap at a southwestern pennsylvania coal mine, U.S.A. *Engineering Geology, 20*(4), 325-341.

Okagbue, C. O. (1986). An investigation of landslide problems in spoil piles in a strip coal mining area, West Virginia (U.S.A.). *Engineering Geology, 22*(4), 317-333.

Paranunzio, R., Laio, F., Nigrelli, G., & Chiarle, M. (2015). A method to reveal climatic variables triggering slope failures at high elevation. *Natural Hazards, 76*(2), 1039-1061.

Pernichele, A. D., & Kahle, M. B. (1971). Stability of Waste Dumps at Kennecott's Binghani Canyon Mine. *AIME Transactions, 250*.

Poulsen, B., Khanal, M., Rao, A. M., Adhikary, D., & Balusu, R. (2014). Mine Overburden Dump Failure: A Case Study. *Geotechnical and Geological Engineering, 32*(2), 297-309.

Prakash, B. B. (2009). *Design of stable slopes for opencast mines* Bachelor of Technology in Mining Engineering. National Institute of Technology Rourkela.

Rahardjo, H., Hritzuk, K. J., Leong, E. C., & Rezaur, R. B. (2003). Effectiveness of horizontal drains for slope stability. *Engineering Geology, 69*(3–4), 295-308.

Richards, B. G. ( 1998). Slope stability in the Bowen Basin Part 1. *Australian Geomechanics*, 20-32.

Rizkalla, M. F. A. (1983). *Stability of open pit mine spoil piles* Masters in civil engineering. The university of Alberta, Edmonton, Alberta.

Rouainia, M., Davies, O., O'Brien, T., & Glendinning, S. (2009). Numerical modelling of climate effects on slope stability. *Proceedings of the ICE - Engineering Sustainability, 162*, 81-89.

Sadisun, I. A., Shimada, H., Ichinose, M., & Matsui, K. (2005). Study on the physical disintegration characteristics of Subang claystone subjected to a modified slaking index test. *Geotechnical & Geological Engineering, 23*(3), 199-218.

Santi, P. M. (2006). Field Methods for Characterizing Weak Rock for Engineering. *Environmental & Engineering Geoscience, XII*(1), 1–11.

Schmidt, J., & Dikau, R. (2004). Modeling historical climate variability and slope stability. *Geomorphology, 60*(3–4), 433-447.

Seedsman, R. W., & Emerson, W. W. (1985a). The formation of planes of weakness in the highwall at Goonyella Mine, Queensland, Australia. *Engineering Geology, 22*(2), 157-173.

Seedsman, R. W., & Emerson, W. W. (1985b). The role of clay-rich rocks in spoil pile failures at Goonyella Mine, Queensland, Australia. *International Journal of Rock Mechanics and Mining Sciences & Geomechanics Abstracts, 22*(2), 113-118.

Seedsman, R. W., Richards, B. G., & Williams, D. J. (1988). The Possibility of Undrained Failure in Bowen Basin Spoil Piles. In (pp. 404-409): Institution of Engineers, Australia.

ShearTrac-II (Singer-songwriter). (2015). Direct Shear Apparatus. On.

Shrestha, R. K., & Lal, R. (2011). Changes in physical and chemical properties of soil after surface mining and reclamation. *Geoderma, 161*(3–4), 168-176.

Simmon, J., & McManus, D. (2004). Shear strength framework for design of dumped spoil slopes for open pit coal mines. *Proceedings Advances in Geotechnical Engineering, 2*, 981-991.

Simpson, T. A., & Walker, R. A. (1975). Slope stability and groundwater control in Eufaula bauxite district, Alabama : Abstract of paper for Soc. Min. Engrs, 1975, AIME, Ann. Meeting, New York. MIN. ENGNG, AIME, V26, N12, DEC. 1974, P68. *International Journal of Rock Mechanics and Mining Sciences & Geomechanics Abstracts, 12*(4), 66.

Smith, C. C., Cripps, J. C., & Wymer, M. J. (1999). Permeability of compacted colliery spoil — a parametric study. *Engineering Geology, 53*(2), 187-193.

Spears, D. A., & Taylor, R. K. (1972). The influence of weathering on the composition and engineering properties of in situ coal measures rocks. *International Journal of Rock Mechanics and Mining Sciences & Geomechanics Abstracts, 9*(6), 729-730.

Standard, A. (13 April 1993). *Geotechnical site investigations (AS 1726—1993)*: Council of Standards Australia.

Standard, A. (1998). *Methods of testing soils for engineering purposes. Method 6.2.2: Soil strength and consolidation tests—Determination of the shear strength of a soil—Direct shear test using a shear box*: Australian Standard.

Standard, A. (2001, AS 1289.6.7.1—2001). *Methods of testing soils for engineering purposes. Method 6.7.1: Soil strength and consolidation tests—Determination of permeability of a soil—Constant head method for a remoulded specimen (AS 1289.6.7.1—2001)*. Sydney, NSW 2001, Australia: Standards Australia International Ltd.

Standard, A. (2006, 7 June 2006 ). *Methods of testing soils for engineering purposes. Method 3.9.2: Soil classification tests— Determination of the cone liquid limit of soil— One-point method (AS 1289.3.9.2—2006)*. Sydney, NSW 2001: Standards Australia Limited.

Standard, A. (2008, 19 November 2008.). *Methods of testing soils for engineering purposes. Method 3.4.1: Soil classification tests— Determination of the linear shrinkage of a soil— Standard method (AS 1289.3.4.1—2008)*: Standards Australia Limited.

Standard, A. (2009a, 6 February 2009). *Methods of testing soils for engineering purposes. Method 3.2.1: Soil classification tests— Determination of the plastic limit of a soil—Standard method (AS 1289.3.2.1—2009)*. Sydney, NSW 2001, Australia: Standards Australia Limited.

Standard, A. (2009b, 3 April 2009). *Methods of testing soils for engineering purposes. Method 3.6.1: Soil classification tests— Determination of the particle size distribution of a soil—Standard method of analysis by sieving (AS 1289.3.6.1—2009)*: Standards Australia Limited.

Stavridakis, E. I. (1999). Influence of Liquid Limit and Slaking on Cement Stabilized Clayey Admixtures. *Geotechnical & Geological Engineering, 17*(2), 145-154.

System, U. C. T. (Singer-songwriter). (2015). Universal Cyclic Triaxial System. On. 4 Wadhurst Drive, Boronia, Victoria 3155, Australia.

Taylor, D. W. (1948). *Fundamentals of soil mechanics*. New York

Taylor, R. K. (1975). English and Welsh colliery spoil heaps - mineralogical and mechanical interrelationships. *Engineering Geology, 9*(1), 39-52.

Terzaghi, K., Peck, R. B., & Mesri, G. (1996). *Soil mechanics in engineering practice*. New York: Wiley.

Tordesillas, A., Shi, J., & Tshaikiwsky, T. (2011). Stress–dilatancy and force chain evolution. *International Journal for Numerical and Analytical Methods in Geomechanics, 35*(2), 264-292.

Ulusay, R., & Aksoy, H. (1994). Assessment of the failure mechanism of a highwall slope under spoil pile loadings at a coal mine. *Engineering Geology, 38*(1–2), 117-134.

Ulusay, R., Arikan, F., & Yoleri, M. F. (1995). Engineering geological characterization of coal mine waste material and an evaluation in the context of back-analysis of spoil pile instabilities in a strip mine, SW Turkey. *Engineering Geology, 40*(1–2), 77-101.

Ulusay, R., Arikan, F., Yoleri, M. F., & Çağlan, D. (1995). Engineering geological characterization of coal mine waste material and an evaluation in the context of back-analysis of spoil pile instabilities in a strip mine, SW Turkey. *Engineering Geology, 40*(1–2), 77-101.

Ulusay, R., Çağlan, D., Arikan, F., & Yoleri, M. F. (1996). Characteristics of biplanar wedge spoil pile instabilities and methods to improve stability. *Canadian Geotechnical Journal, 33*(1), 58-79.

Upadhyay, O. P., Sharma, D. K., & Singh, D. P. (1990). Factors affecting stability of waste dumps in mines. *International Journal of Surface Mining, Reclamation and Environment, 4*(3), 95-99.

Ward, C. R., Corcoran, J. F., Saxby, J. D., & Read, H. W. (1996). Occurrence of phosphorus minerals in Australian coal seams. *International Journal of Coal Geology, 30*(3), 185-210.

Ward, C. R., Nunt-jaruwong, S., & Swanson, J. (2005). Use of mineralogical analysis in geotechnical assessment of rock strata for coal mining. *International Journal of Coal Geology, 64*(1–2), 156-171.

Wilkins, J. K. (1970). A theory for the shear strength of rockfill. *Rock Mechanics, 2*, 205-222.

Wunsch, D. R., Dinger, J. S., Taylor, P. B., Carey, D. I., & Graham, C. D. R. (1996). *Hydrogeology, hydrogeochemistry, and spoil settlement at a large mine-spoil area in Eastern Kentucky: Star Fire Tract*.

X'Pert³Powder (Singer-songwriter). (2015). X'Pert³ Powder-Key specifications and options. On: PANalytical B.V.

Zhang, Y., Chen, G., Zheng, L., Li, Y., & Zhuang, X. (2013). Effects of geometries on three-dimensional slope stability. *Canadian Geotechnical Journal, 50*(3), 233.

Zuo, J., Wang, Z., Zhou, H., Pei, J., & Liu, J. (2013). Failure behavior of a rock-coal-rock combined body with a weak coal interlayer. *International Journal of Mining Science and Technology, 23*(6), 907-912.